The Triangle Sky

Triangle centers lifted to a ranked geometry of tetrahedral apices

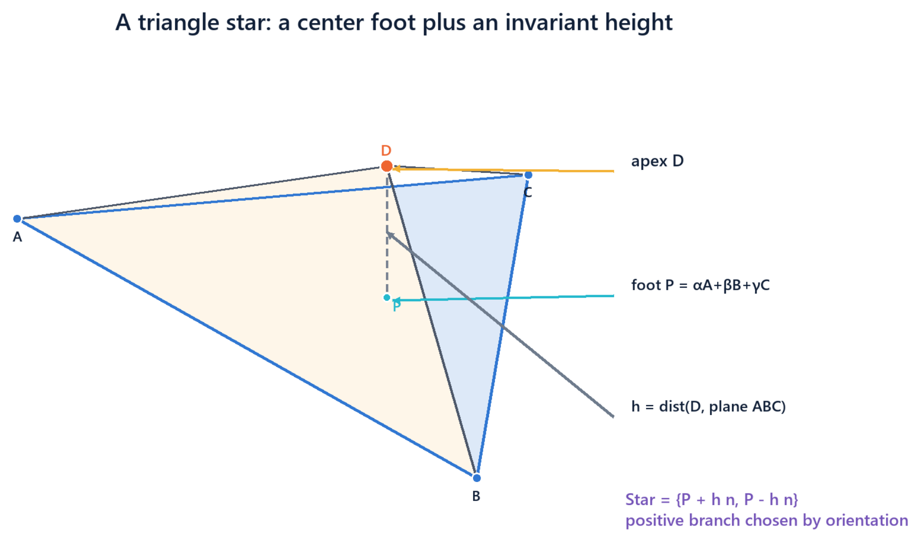

Ismail Hammoudeh

Living research report, version 0.2

30 August 2026

Public working paper; not peer reviewed.

Suggested citation: I. Hammoudeh, *The Triangle Sky*, living research report, v0.2 (2026).

Abstract

The *Triangle Sky* assigns to a reference triangle ABC not merely a point in its plane, but a geometrically natural apex D in space. The perpendicular projection P of D is a triangle center and the altitude h supplies an additional symmetric homogeneous invariant. This living research report defines the construction, distinguishes three uses of variance, introduces a provisional cost-and-coincidence ranking called the Stars Cascade, and proves a closure theorem for expressions that satisfy an exact permutation certificate. It presents thirty catalogue entries, three optimization constructions with exact stationary solutions, and three further optimization candidates supported numerically. Data for the 6–9–13 and 13–20–21 triangles include directed trilinear distances, heights and a numerical audit against a dated snapshot of the Encyclopedia of Triangle Centers (ETC). A later chapter extends the construction to twin apices in $\mathbb{R}^4$ and proves that a natural orthocentric hyperstar has both feet at $X(4)$. Proved statements, exact computer-algebra identities, numerical evidence, conjectures and database observations are explicitly distinguished. Complexified entries are retained as algebraic continuations, but are not identified with real Euclidean tetrahedra outside their stated real domains.

Contents

List of Figures

Reader's guide and claim-status legend

This document reports an ongoing project rather than a completed classification. Readers interested in the central idea and established mathematics may begin with Chapters 1–4 and the exact Orthocentric Hyperstar theorem in the hyperstar chapter. The thirty-entry catalogue and the ETC reproduction chapter are reference sections: their raw implementation expressions are included for auditability and may be skipped on a first reading.

The following labels specify the epistemic status of claims throughout the report.

PROVED	A mathematical proof is given in this report or follows directly from a cited theorem.
EXACT CAS	An exact symbolic identity was verified by computer algebra; this is stronger than a numerical fit but is not a substitute for a conceptual proof.
NUMERICAL	A reproducible numerical calculation supports the statement on stated controls; global validity is not claimed.
CONJECTURE	A proposed general statement or uniqueness/global-optimality claim remains open.
DATABASE AUDIT	A match or non-match relative to a named ETC snapshot, normalization and tolerance; this is not timeless mathematical membership.

Current claim map

The certified-cascade theorem and the exact OHS results are **PROVED**. Stored algebraic catalogue expressions and the reduced EVS/CVS/IVS stationary formulas are **EXACT CAS**. ERS, DGS and NFIS minimizers, projected centers derived from them, the Euler-line census and ETC non-matches are **NUMERICAL** or **DATABASE AUDIT**. Global existence and uniqueness of all six optimization constructions, and completeness of the cascade, remain **CONJECTURE**.

Terminology used in the catalogue

The *foot* of an apex is its orthogonal projection to the plane ABC. A *trace* of two stars is the intersection with the base plane of the spatial line joining selected apices; a *cross-conjugate trace* joins one apex to the reflected apex of the other star. The report's historical phrase "absolute trilinears" means the normalized *directed perpendicular distances* to the three sidelines; negative values are therefore meaningful. Section 4.2 translates the implementation operators used in the catalogue cards.

Chapter 1

From the plane to the sky

1.1 Notation

The side lengths opposite A, B, C are $a = BC$, $b = CA$, $c = AB$; $p = a + b + c$ is the *perimeter*, $s = p/2$ the semiperimeter, Δ the area, r the inradius and R the circumradius. A unit normal to the oriented plane ABC is denoted by $\mathbf{n}$. Barycentrics are normalized when $\alpha + \beta + \gamma = 1$.

For the numerical tests we place $A = (0, 0)$, $B = (c, 0)$ and

$$C = \left(\frac{b^2 + c^2 - a^2}{2c}, \; \frac{2\Delta}{c} \right).$$

The two reference triangles deliberately have different character: 6–9–13 is obtuse, while 13–20–21 is acute. This makes domain failures visible.

1.2 Triangle centers

Definition 1.1 (Triangle center)**.** A triangle center is a point-valued rule $F(A, B, C)$ that is equivariant under Euclidean similarities and independent of the labelling of the same geometric triangle. Algebraically, a homogeneous center function $f(a, b, c)$ that is symmetric in its last two arguments gives trilinears

$$f(a, b, c) : f(b, c, a) : f(c, a, b),$$

and barycentrics

$$af(a, b, c) : bf(b, c, a) : cf(c, a, b).$$

This is the convention used by Kimberling's ETC [1, 2]. Familiar examples are the incenter $X(1)$ with barycentrics $a : b : c$, the centroid $X(2)$ with $1 : 1 : 1$, the circumcenter $X(3)$, and the orthocenter $X(4)$.

1.3 Triangle stars

Definition 1.2 (Triangle star)**.** A triangle star is an unordered pair of mirror apices

$$\mathcal{S}(ABC) = \{P + h\mathbf{n}, \; P - h\mathbf{n}\},$$

where P is a triangle center and h^2 is a symmetric homogeneous function of degree two in (a, b, c). On an oriented triangle the positive branch $D = P + h\mathbf{n}$ may be selected.

Thus a star is completely specified by its *foot* P and invariant height h. Reflection changes the sign of $h\mathbf{n}$ but not the unordered star.

Definition 1.3 (Real domain and complexified star)**.** The *real domain* of a triangle-star formula is the set of nondegenerate real triangles on which its foot and $h^2 \geq 0$ are real and every construction used in its definition is nondegenerate. Outside this domain, an expression that continues algebraically and retains the certified permutation law is called a *complexified star*. It is an algebraic continuation, not the apex of a real Euclidean tetrahedron.

Every catalogue entry should therefore be read together with its reality data and branch convention. The two numerical control triangles expose, but do not completely characterize, these domains.

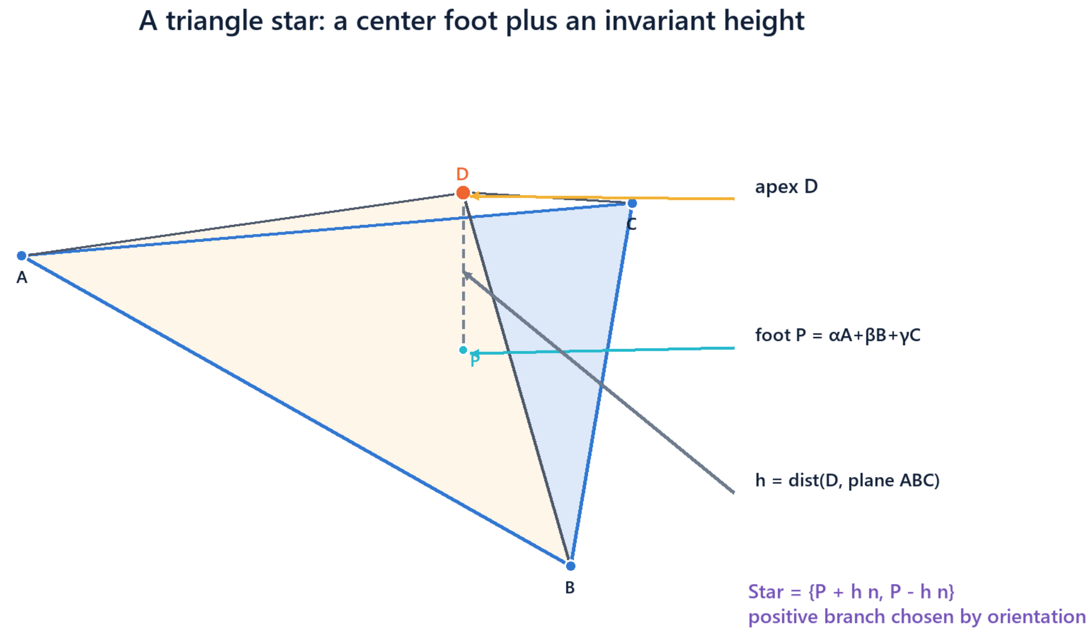

Figure 1.1: A star is a spatial apex with a label-independent foot and height. The supplied Mathematica source reproduces this geometric scene.

1.4 Three meanings of variance

The word "variance" appears in three logically separate places.

1. A **center certificate**. Evaluate a labelled construction on all six permutations $\pi \in S_3$. After mapping every result back to the same physical triangle, define
$$V_{\text{center}} = \frac{1}{6} \sum_{\pi \in S_3} \|F_\pi - \overline{F}\|^2.$$
A triangle center has $V_{\text{center}} = 0$ (exactly, not merely numerically).
2. A **star certificate**. For candidate apices D_π, let P_π be their perpendicular feet and $u_\pi = h_\pi^2$. The required conditions are
$$V_{\text{foot}} = \frac{1}{6} \sum \|P_\pi - \overline{P}\|^2 = 0, \qquad V_{\text{height}} = \frac{1}{6} \sum (u_\pi - \overline{u})^2 = 0.$$
Odd permutations may exchange the two mirror apices; squaring the height removes that harmless sign.
3. An **optimization objective**. The Edge-Variance Star (EVS), for example, minimizes the ordinary statistical variance of the six tetrahedral edge lengths. This objective need not vanish.

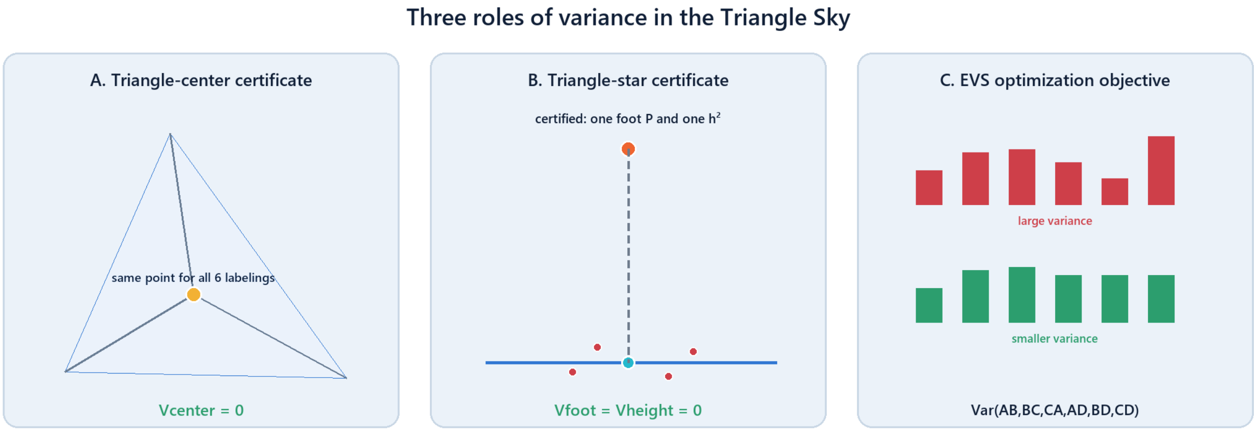

Figure 1.2: Center variance, star variance and objective variance answer different questions.

Chapter 2

The principal stars

Define

$$q = \sqrt{\frac{p^2}{4} - (r + 2R)^2}.$$

For an acute triangle q is real in the primitive constructions below; for an obtuse triangle it may be imaginary, correctly recording nonexistence of the corresponding real tetrahedron.

Star	Geometric definition	Foot	Height	Role
ES	equifacial/disphenoid apex: all four faces congruent	$X(20)$	$2q$	primitive equal-face star
OS	DA, DB, DC are mutually perpendicular	$X(4)$	q	primitive orthogonal star
CS1	centroid of A, B, C, and ES; also 12 other independent constructions	$X(3)$	$q/2$	first circumstar
Rank 1	centroid of A, B, C, and OS; five independent definitions	$X(5)$	$q/4$	best-ranked cascade star

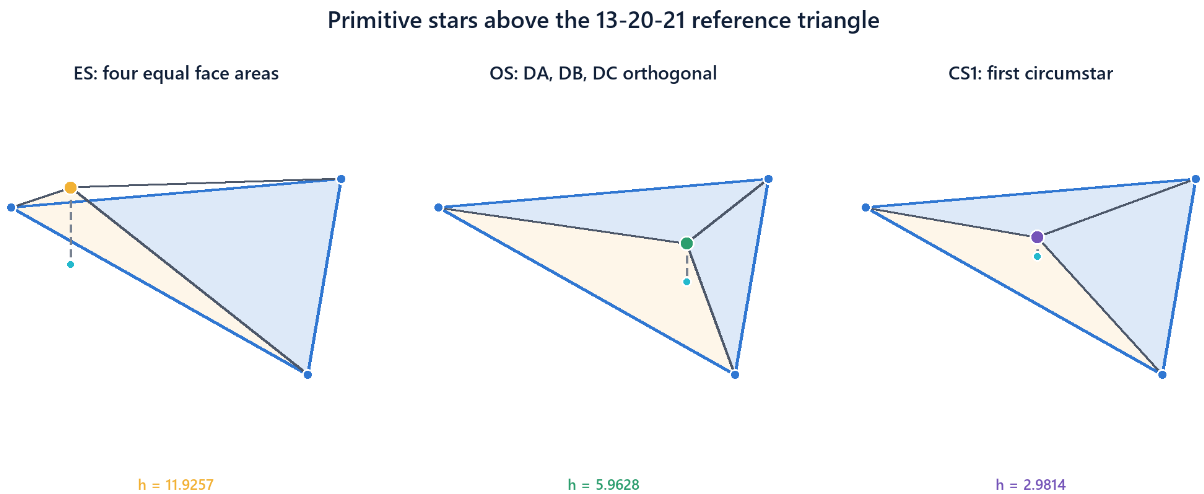

Figure 2.1: Three primitive stars on the acute 13–20–21 triangle.

The ES is a disphenoid: opposite edges are equal, so its four faces are congruent. The OS is the trirectangular tetrahedron whose three edges incident with D are orthogonal. The high multiplicity of CS1 is mathematically significant: thirteen geometrically different operations land on the same apex. Those coincidences are theorems, not duplicate spellings.

2.1 Six optimization constructions: exact stationary solutions and numerical candidates

Let $\delta_e \in (0, \pi)$ be the six internal dihedral angles of $ABCD$, R_T, r_T, V_T its circumradius, inradius and volume, and $\mathbf{n}_i$ the four outward unit face normals. The adopted objectives are:

$$\begin{aligned}
\text{EVS}: &\quad \min_D \operatorname{Var}(AB, BC, CA, AD, BD, CD),\\
\text{CVS}: &\quad \min_D \frac{(4\pi/3)R_T^3}{V_T},\\
\text{IVS}: &\quad \max_D \frac{(4\pi/3)r_T^3}{V_T},\\
\text{ERS}: &\quad \min_D \frac{R_T}{r_T},\\
\text{DGS}: &\quad \min_D \sum_e \left(\cos\delta_e - \frac{1}{3}\right)^2,\\
\text{NFIS}: &\quad \min_D \left\| \sum_{i=1}^{4} \mathbf{n}_i\mathbf{n}_i^{\mathsf{T}} - \frac{4}{3}I_3 \right\|_F^2.
\end{aligned}$$

For a fixed nondegenerate base, the admissible set used in the numerical work is

$$\mathcal{A}(ABC) = \{D = P + h\mathbf{n} : P \in \operatorname{aff}(ABC),\ h > 0,\ ABCD \text{ nondegenerate, and the objective is finite}\}.$$

The two mirror components $h > 0$ and $h < 0$ are identified. Boundary configurations with $h = 0$, infinite circumradius or zero inradius are excluded; a global theorem must nevertheless analyze whether a minimizing sequence can approach such a boundary or escape to infinity.

The regular tetrahedral angle is $\arccos(1/3)$. Among the viable dihedral objectives studied, the cosine target is the cleanest algebraically and is close to NFIS because both are quadratic Gram-matrix defects. Direct angle range minimization is a useful robust comparator but is nonsmooth when the active maximum or minimum changes. Dihedral quality measures are standard in tetrahedral meshing [14, 13, 12]; DGS makes that principle a canonical fixed-base star.

The reduced stationary equations for the first three BSA objectives simplify strikingly (**EXACT CAS**):

	foot	height
EVS	$X(3)$	$\sqrt{(p/3)^2 - R^2}$
CVS	$X(3)$	$\sqrt{2}R$
IVS	$X(1)$	$2\sqrt{2}r$

These identities specify exact stationary candidates, but the present report does not yet supply a complete global existence-and-uniqueness proof on $\mathcal{A}(ABC)$. ERS, DGS and NFIS are defined here by numerical minimization of their stationary/optimality systems (**NUMERICAL**); their numerical feet produced no match in the audited ETC snapshot (**DATABASE AUDIT**). Until coercivity, boundary behavior, global minimality, uniqueness up to reflection and a symbolic permutation certificate are proved, all six should be understood as *optimization-star candidates*; EVS, CVS and IVS have the stronger exact closed forms displayed above.

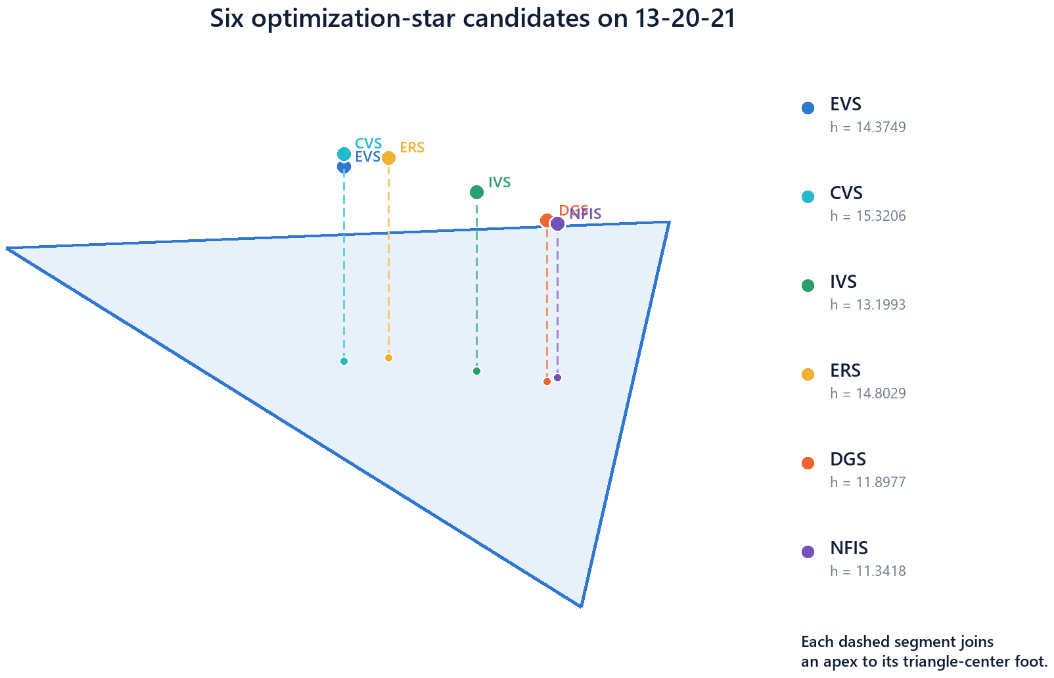

Figure 2.2: The six optimization-star candidates on the acute control triangle. The exact stationary EVS/CVS pair shares the circumcenter foot but has different height.

2.1.1 Suggested catalogue costs

Costs measure conceptual construction effort, not numerical difficulty. The adopted rational values are all strictly between 1 and 3:

Star	EVS	CVS	IVS	ERS	DGS	NFIS
Cost	2	9/4	3/2	7/4	2	5/2

IVS receives the lowest cost because its optimal foot and height reduce to the incenter and $2\sqrt{2}r$. NFIS receives the highest because it requires four normalized face normals, a frame operator and a Frobenius-norm minimization.

2.2 What normal isotropy means

For every closed tetrahedron the vector-area identity is $\sum_i A_i \mathbf{n}_i = 0$. In an equifacial tetrahedron all A_i are equal, hence $\sum_i \mathbf{n}_i = 0$: this is a *first-moment* balance. NFIS instead tries to make the *second moment* $\sum_i \mathbf{n}_i \mathbf{n}_i^{\mathsf{T}}$ a scalar matrix. Tight-frame theory identifies this as isotropy [10, 11].

The distinction is concrete on 13–20–21. The equifacial star has normal sum essentially zero, but frame eigenvalues

$$(0.4233,\ 1.3545,\ 2.2222),$$

which are far from equal. NFIS has eigenvalues

$$(1.1028,\ 1.4053,\ 1.4919),$$

much closer to 4/3, but its normal sum is not zero. A regular tetrahedron alone realizes both ideals exactly.

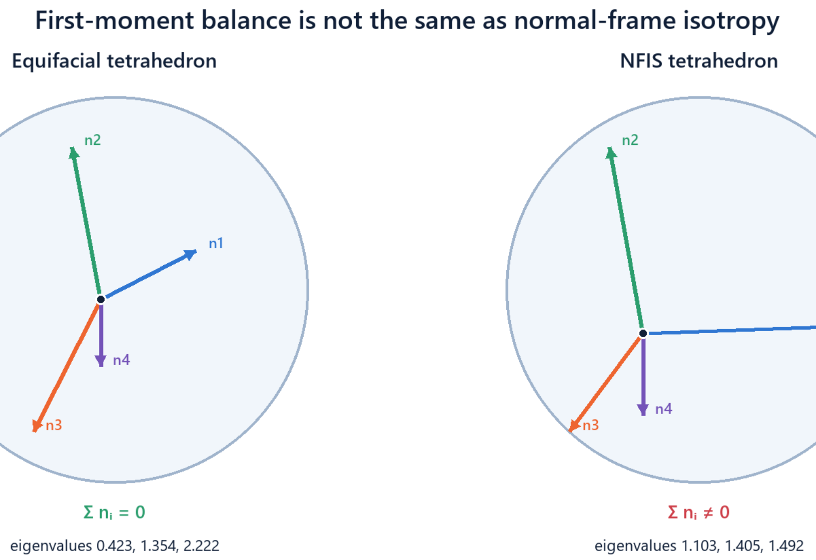

Figure 2.3: Equifacial centering of normals versus NFIS second-moment isotropy.

Chapter 3

Why the Triangle Sky matters

Classical center theory organizes point-valued natural constructions in a triangle [1, 2, 3]. The Triangle Sky adds one invariant scalar degree of freedom and thereby connects planar center geometry to fixed-face tetrahedra. This creates several kinds of value:

- **A discovery engine.** Different spatial constructions can coincide even when their planar descriptions look unrelated. Each coincidence suggests a theorem.
- **A bridge between invariants.** Heights simplify to expressions in p, r, R; feet often collapse to ETC centers. Tetrahedral statements therefore feed back into triangle geometry.
- **A controlled domain laboratory.** Acute/obtuse transitions appear as the sign of a radicand. Complex stars retain algebraic continuity and show exactly where a real construction fails.
- **Optimization geometry.** Mesh-quality, circumsphere, insphere, dihedral and frame objectives become comparable on the same fixed base.
- **A ranked catalogue rather than a list.** The index rewards simple definitions and independently meaningful coincidences, allowing the most explanatory stars to rise.

The Grace–Danielsson inequality and its refinements show how triangle and tetrahedral radius inequalities already interact [8, 9]. The Triangle Sky makes that interaction constructive and cataloguable.

3.1 Related work and boundary of novelty

Triangle-center functions and the ETC supply the planar language and identification problem [1, 2]; classical Euclidean and polytope geometry supply the background on triangle and simplex constructions [3, 4, 5]. Work on simplex centers and orthocentric simplices gives especially relevant higher-dimensional context [20, 21]. Radius inequalities connect a tetrahedron to one of its faces [8, 9]. The DGS objective belongs to the broader tradition of tetrahedral mesh-quality measures [14, 15, 16, 12], while NFIS uses the language of finite tight frames [10, 19, 11].

The contribution claimed here is narrower than the totality of those subjects: the report proposes the term *triangle star* for the foot–height pair, a typed cascade for producing such objects, a provisional coincidence-sensitive ranking, and a computational programme for comparing their descendants with the ETC. Individual tetrahedra, centers, identities or optimization principles may be classical or overlap earlier work. No claim of exhaustive novelty is made without a specific literature comparison, and the catalogue is not asserted to be complete.

Chapter 4

The Stars Cascade

4.1 Primitive objects and allowable functions

The cascade starts with the reference vertices A, B, C, the basic triangle centers $X(1), \ldots, X(4)$, and primitive stars $Z(1) = \mathrm{ES}$, $Z(2) = \mathrm{OS}$ and $Z(3) = \mathrm{CS1}$. It then closes under typed geometric operations. The current grammar is summarized below.

Operation	Meaning	construction cost
A, B, C	reference vertices	0
$X(1), \ldots, X(4)$	basic planar centers embedded in the base plane	1
$Z(1), Z(2), Z(3)$	primitive stars ES, OS, CS1	1
$Y_i(Q_1, \ldots, Q_k)$	named tetrahedral center/construction applied to arguments	$1 + \sum c(Q_j)$
Conjugate(Q)	mirror in the base plane	$1 + c(Q)$
line, plane, intersection, trace	the indicated incidence construction	$1 + \sum c(Q_j)$
axis or perpendicular foot	natural projection/axis construction	$1 + c(Q)$

The implementation also enforces types, definedness and nondegeneracy: an intersection must be unique; a normalized vector must be nonzero; an optimization must have a specified admissible domain and selected minimizer.

4.2 Operator dictionary

The detailed cards preserve Mathematica-style expressions so that the catalogue can be audited against the data export. Their principal symbols have the following geometric meanings.

Implementation symbol	Reader-facing meaning
`TSA`, `TSB`, `TSC`	the three embedded vertices A, B, C of the reference triangle
`TSX[i]`	the planar Kimberling center $X(i)$ embedded in the base plane
`TSZ[i]`	the ith primitive or previously certified triangle star
`TSY[1,...]`	the tetrahedral incenter of the four supplied points

Implementation symbol	Reader-facing meaning
`TSY[2,...]`	the tetrahedral centroid of the four supplied points
`TSY[3,...]`	the tetrahedral circumcenter of the four supplied points
`TSConjugate[Q]`	reflection of Q in the base plane
`TSPlane[...]`	the plane through the supplied noncollinear points
`TSFoot[Q,plane]`	the orthogonal projection of Q onto the named plane

An internal expression is a reproducibility record, not the preferred geometric definition. The simplest geometric description is stated first whenever one is presently known; raw expressions are retained in the catalogue reference section rather than in the conceptual development.

4.3 Independent definitions

Two formulas are counted as independent only when their *geometric operations* are genuinely different. Reordering arguments, rescaling homogeneous coordinates, simplifying an identity, or replacing an object by its already-proved equal object does not create a new definition. Nor may a proof use the desired coincidence as an input. By contrast, “tetrahedral centroid”, “intersection of an axis with a plane”, and “circumcenter of four specified points” may count independently when a nontrivial theorem proves that they coincide. Rank 4 (CS1) has thirteen such definitions; this is why its catalogue entry is much stronger than a formula with thirteen syntactic spellings.

Independence is a mathematical classification judgment, not a property that follows from expression inequality alone. The public catalogue therefore distinguishes the raw number of coinciding expressions from the smaller number of claimed geometric definitions. A definitive count requires an equivalence record for every pair, identifying whether the reduction is syntactic, algebraic, a consequence of a previously known coincidence, or a genuinely independent theorem. Counts in this version are provisional wherever that dependency record is not yet supplied.

4.4 Cost and index

If a star has independent definitions of costs $c_1, \ldots, c_m$, its effective index is the parallel-resistance score

$$I = \left(\sum_{j=1}^{m} \frac{1}{c_j} \right)^{-1}.$$

One simple definition lowers the index; several independent definitions lower it further. Thus smaller means conceptually better. Exact rational arithmetic is used. A documented primitive normalization is retained for CS1 so that the primitive has index 1 while its thirteen definitions are still recorded.

The index is a *provisional heuristic complexity score*, not a canonical invariant. Its ordering depends on the selected primitive costs and on judgments of independence. Consequently, “best ranked” always means best under this declared scoring policy. The exceptional CS1 normalization is reported rather than hidden, but it also shows why alternative cost schedules and sensitivity calculations are needed before interpreting small rank differences.

4.4.1 A small sensitivity audit

As a first robustness check, the thirty displayed entries were reranked from their stored definition-function counts c_j under three policies: the unnormalized harmonic score $(\sum c_j^{-1})^{-1}$, a one-unit overhead $(\sum (c_j + 1)^{-1})^{-1}$, and a quadratic penalty $(\sum c_j^{-2})^{-1}$. The first nine entries under each policy are:

Policy	original rank labels, in the new order
Unnormalized harmonic	$4, 1, 2, 3, 5, 6, 7, 8, 9$
One-unit overhead	$4, 1, 5, 2, 3, 6, 7, 8, 9$
Quadratic penalty	$4, 2, 3, 1, 6, 8, 9, 5, 7$

The same nine entries occupy these leading positions, but their order changes substantially. In particular, removing the special primitive normalization moves CS1 (original rank 4) to the front. The audit supports a stable leading cluster, not a canonical fine ordering within that cluster.

4.5 A guarantee theorem

It would be false to claim that every arbitrary expression in the grammar is automatically a star: a construction can remember the label A, or an intersection can be undefined. The correct theorem concerns the *certified cascade*.

Theorem 4.1 (Certified-cascade theorem)**.** *Let $E(A, B, C)$ be a well-defined spatial expression assembled from similarity-natural primitives and the allowable operations above. Suppose its six relabelled evaluations satisfy the exact orbit condition: even permutations produce the same oriented apex, while odd permutations produce either the same apex or its conjugate in the plane ABC. Then E determines a triangle star. Consequently, every expression admitted to the certified Stars Cascade is a guaranteed triangle star.*

Proof. Every primitive is homogeneous and commutes with similarities. Lines, planes, perpendicular projection, unique intersection, centroids, circumcenters, incenters and the other natural tetrahedral constructions also commute with similarities; conjugation commutes with similarities and reverses the selected normal. Structural induction on the expression tree therefore shows that E is similarity-equivariant.

Write $D_\pi = E(\pi(A, B, C))$, transported back to the original physical triangle. By the orbit hypothesis, all perpendicular feet P_π coincide: conjugate points have the same foot. Their signed heights agree for even permutations and may reverse sign for odd permutations, so all h_π^2 coincide. The common foot is consequently label-independent and similarity-equivariant, hence a triangle center; the common h^2 is symmetric and homogeneous of degree two. Therefore $\{P + h\mathbf{n}, P - h\mathbf{n}\}$ is a triangle star by definition. The generator admits an expression only after this exact certificate and definedness checks, proving the final assertion. □

Remark 4.2 (Symbolic proof versus numerical audit)*.* The theorem is exact. Numerical evaluation on scalene test triangles is a valuable bug detector and ETC search key, but it is not the proof of permutation invariance. Exact coordinate simplification or a separately verified symbolic identity supplies that proof.

Remark 4.3 (Scope of the certificate)*.* The theorem is a closure statement: its exact orbit hypothesis already encodes the required label behavior. It does not prove that the grammar is complete, that the heuristic ranking is canonical, or that every recorded coincidence is geometrically independent. A machine-checkable entry should record its expression tree, exact orbit identities, nonvanishing assumptions, branch choices, real domain and hash of the source expression. The present JSON export records catalogue data; a complete certificate manifest remains a reproducibility target.

Chapter 5

Computational conventions and ETC audit

5.1 Barycentrics and directed trilinear distances

For normalized barycentrics (α, β, γ) the report uses the signed perpendicular distances to the three sidelines,

$$(x : y : z)_{\text{abs}} = \left(\frac{2\Delta\alpha}{a}, \frac{2\Delta\beta}{b}, \frac{2\Delta\gamma}{c}\right).$$

Earlier project files call these quantities *absolute trilinears*; the less ambiguous term *normalized directed trilinear distances* is used here. Negative components denote a point outside the corresponding sideline. Complex values are printed as $u + vi$.

5.2 ETC matching protocol

The ETC was audited using a local copy of its searchable trilinear tables and their cyclic permutations, with projective numerical normalization [2]. The snapshot contained 72,486 searchable entries and was checked in July 2026. The matching tolerance was 10^{-9} after normalization; finite real candidates were screened on the 6–9–13 triangle and checked independently on the acute 13–20–21 control whenever the formula was available there. Complex entries were compared by projective ratios, including the argument of the first trilinear as explained in the reproduction chapter.

A positive database identification in this report is a numerical fingerprint unless an explicit symbolic projective identity is also cited. "No match" means only that no entry in this dated snapshot survived the stated screen: it is not a proof of absence from a later ETC version, of absence under an unparsed representation, or of mathematical novelty. Before an ETC submission, the center axioms and projective identity should be verified symbolically on a generic triangle and the audit repeated on several independent generic controls. The audit scripts, input description and snapshot metadata belong to the reproducibility package; where the ETC source itself cannot be redistributed, a dated checksum and acquisition note should replace it.

5.3 Reality and branch policy

Square roots use the principal algebraic branch in the machine tables. A complex foot or height on 6–9–13 is not converted into an unrelated real construction. Ranks 8, 9 and 30 illustrate this issue especially strongly. The acute 13–20–21 triangle acts as a real-domain control.

5.4 Status of the principal data sets

Data or result	Status	Interpretation
Certified-cascade theorem	PROVED	Conditional closure theorem under an exact orbit and definedness certificate.
Ranked symbolic records	EXACT CAS	Exact stored expressions; geometric independence and domain certification are not complete for every card.
EVS/CVS/IVS formulas	EXACT CAS	Exact solutions of reduced stationary equations; full global optimization proofs remain open here.
ERS/DGS/NFIS	NUMERICAL	Numerically selected candidate minimizers on the stated controls.
ETC identifications and non-matches	DATABASE AUDIT	Dated numerical fingerprint audit at tolerance 10^{-9} unless explicitly promoted by symbolic identity.
OHS and CPOH identities	PROVED	Exact results proved in the hyperstar chapter, subject to their stated nondegeneracy domains.

Chapter 6

Catalogue reference: the first thirty ranked stars

6.1 Landscape table

The next landscape table gives every requested field in compact form. “Defs” is the current, partly judgment-based count of geometrically independent definitions. A blank ETC entry means that no numerical match survived the dated audit. The displayed order is induced by the provisional scoring policy, not by an intrinsic mathematical ordering. Detailed cards are retained as an audit supplement; readers may skip them on a first pass.

Rank	index	defs	ETC foot	abs. trilin. 6–9–13	abs. trilin. 13–20–21	$h_{6,9,13}$	$h_{13,20,21}$
1	10/13	5	X(5)	0.552872 : -0.318107 : 3.605721	5.358974 : 4.216667 : 4.666667	0.000000+2.193767i	1.490712
2	1	1	X(20)	19.241345 : 18.321066 : -17.923771	15.282051 : 4.066667 : -1.333333	0.000000+17.550132i	11.925696
3	1	1	X(4)	-5.676619 : -6.531164 : 10.782218	2.051282 : 4.266667 : 6.666667	0.000000+8.775066i	5.962848
4	1	13	X(3)	6.782363 : 5.894951 : -3.570777	8.666667 : 4.166667 : 2.666667	0.000000+4.387533i	2.981424
5	5/4	4	X(631)	4.290566 : 3.409728 : -0.700178	7.343590 : 4.186667 : 3.466667	0.000000+1.755013i	1.192570
6	10/7	2	X(140)	3.667617 : 2.788422 : 0.017472	7.012821 : 4.191667 : 3.666667	0.000000+1.096883i	0.745356
7	5/3	3	X(3091)	-0.693026 : -1.560718 : 5.041020	4.697436 : 4.226667 : 5.066667	0.000000+3.510026i	2.385139
8	2	1	—	-0.205378+2.607461i : -0.556875+2.555568i : 4.120983-2.972683i	3.150566 : 4.372660 : 5.885212	1.530160+2.121237i	2.247951
9	2	1	—	4.583215-1.334908i : 3.769486-1.097901i : -1.084310+1.376196i	8.058618 : 4.198434 : 3.012823	0.489941+1.682142i	1.347376
10	5/2	2	X(5)	0.552872 : -0.318107 : 3.605721	5.358974 : 4.216667 : 4.666667	0.000000+4.387533i	2.981424
11	5/2	2	X(3)	6.782363 : 5.894951 : -3.570777	8.666667 : 4.166667 : 2.666667	0.000000+2.193767i	1.490712
12	5/2	2	X(548)	9.897108 : 9.001480 : -7.159025	10.320513 : 4.141667 : 1.666667	0.000000+1.096883i	0.745356
13	5/2	2	X(1125)	2.394604 : 1.737262 : 1.332743	6.012821 : 4.316667 : 4.166667	0.000000+2.193767i	1.490712
14	5/2	2	X(2)	2.629369 : 1.752913 : 1.213555	6.461538 : 4.200000 : 4.000000	0.000000+2.193767i	1.490712
15	5/2	2	X(140)	3.667617 : 2.788422 : 0.017472	7.012821 : 4.191667 : 3.666667	0.000000+2.193767i	1.490712
16	5/2	2	X(140)	3.667617 : 2.788422 : 0.017472	7.012821 : 4.191667 : 3.666667	0.000000+3.290650i	2.236068
17	5/2	2	X(13624)	5.509349 : 4.843790 : -2.255505	7.666667 : 4.291667 : 3.166667	0.000000+3.290650i	2.236068
18	5/2	2	X(9955)	-0.720142 : -1.369267 : 4.920992	4.358974 : 4.341667 : 5.166667	0.000000+1.096883i	0.745356
19	5/2	2	X(12100)	5.744114 : 4.859441 : -2.374694	8.115385 : 4.175000 : 3.000000	0.000000+3.290650i	2.236068
20	5/2	2	X(5066)	-0.485377 : -1.353616 : 4.801803	4.807692 : 4.225000 : 5.000000	0.000000+1.096883i	0.745356
21	5/2	2	X(3)	6.782363 : 5.894951 : -3.570777	8.666667 : 4.166667 : 2.666667	0.000000+3.290650i	2.236068
22	5/2	2	X(5)	0.552872 : -0.318107 : 3.605721	5.358974 : 4.216667 : 4.666667	0.000000+1.096883i	0.745356
23	5/2	2	X(140)	3.667617 : 2.788422 : 0.017472	7.012821 : 4.191667 : 3.666667	0.000000+5.484416i	3.726780
24	5/2	2	—	1.356355 : 0.701752 : 2.528826	5.461538 : 4.325000 : 4.500000	0.000000+1.096883i	0.745356

Rank	index	defs	ETC foot	abs. trilin. 6–9–13	abs. trilin. 13–20–21	$h_{6,9,13}$	$h_{13,20,21}$
25	5/2	2	X(1125)	2.394604 : 1.737262 : 1.332743	6.012821 : 4.316667 : 4.166667	0.000000+1.096883i	0.745356
26	5/2	2	X(13624)	5.509349 : 4.843790 : -2.255505	7.666667 : 4.291667 : 3.166667	0.000000+5.484416i	3.726780
27	5/2	2	X(2)	2.629369 : 1.752913 : 1.213555	6.461538 : 4.200000 : 4.000000	0.000000+1.096883i	0.745356
28	5/2	2	X(12100)	5.744114 : 4.859441 : -2.374694	8.115385 : 4.175000 : 3.000000	0.000000+5.484416i	3.726780
29	5/2	2	X(3)	6.782363 : 5.894951 : -3.570777	8.666667 : 4.166667 : 2.666667	0.000000+5.484416i	3.726780
30	3	1	—	0.599005+2.531270i : 0.315935+2.472117i : 3.145477-2.879744i	3.319781 : 4.392393 : 5.761666	0.798085+0.871730i	1.062930

6.2 Detailed catalogue cards

This section is a machine-oriented reference supplement. The center function is printed in normalized barycentric form in Mathematica syntax and the height line reproduces the stored exact algebraic expression. These formulas do not by themselves prove global definedness or reality. ETC labels inherit **DATABASE AUDIT** status unless a symbolic projective identity is stated separately. For ranks 8, 9 and 30, no reduction to a function of p, r, R alone was found; their full side-length expression is retained rather than overstated.

Rank 1 — index 10/13

Independent definitions: 5 (raw coinciding expressions: 34).
ETC foot: X(5).

All independent definitions D1.

```
TSY[2, TSA, TSB, TSC, TSZ[2]]
```

D2.

```
TSY[1, TSConjugate[TSZ[1]], TSX[4], TSZ[2], TSZ[3]]
```

D3.

```
TSY[1, TSConjugate[TSZ[3]], TSX[4], TSZ[2], TSZ[3]]
```

D4.

```
TSY[1, TSX[2], TSX[4], TSZ[2], TSZ[3]]
```

D5.

```
TSY[2, TSConjugate[TSZ[3]], TSX[4], TSZ[2], TSZ[3]]
```

Normalized barycentric center function

```
{((b^2 - c^2)^2 - a^2*(b^2 + c^2))/(2*(a^4 + (b^2 - c^2)^2 - 2*a^2*(b^2 + c^2))), (4 + b*((a - b - c)^(-
1) - (a + b - c)^(-1) + (a - b + c)^(-1) - (a + b + c)^(-1)))/8, (a^4 + b^4 - b^2*c^2 - a^2*(2*b^2 +
 c^2))/(2*(a^4 + (b^2 - c^2)^2 - 2*a^2*(b^2 + c^2)))}
```

Invariant height

```
Sqrt[p^2 - 4*(r + 2*R)^2]/8
```

6-9-13: barycentrics `0.07008929 : -0.06049107 : 0.99040179`; absolute trilinears `0.552872 : -0.318107 : 3.605721`; $h =$`0.000000+2.193767i`.
13-20-21: barycentrics `0.27645503 : 0.33465608 : 0.38888889`; absolute trilinears `5.358974 : 4.216667 : 4.666667`; $h =$`1.490712`.

Rank 2 — index 1

Independent definitions: 1 (raw coinciding expressions: 73).
ETC foot: X(20).

All independent definitions D1.

```
TSZ[1]
```

Normalized barycentric center function

```
{-1 + a*((a - b - c)^(-1) + (a + b - c)^(-1) + (a - b + c)^(-1) + (a + b + c)^(-1)), -1 + b*((a + b - c)
^(-1) - (a - b + c)^(-1) + (-a + b + c)^(-1) + (a + b + c)^(-1)), 3 - (a + b)/(a + b - c) + (-a + b)/(
a - b + c) + (a - b)/(-a + b + c) - (a + b)/(a + b + c)}
```

Invariant height

```
2*Sqrt[p^2/4 - (r + 2*R)^2]
```

6-9-13: barycentrics 2.43928571 : 3.48392857 : -4.92321429; absolute trilinears 19.241345 : 18.321066 : -17.923771; h =0.000000+17.550132i.
13-20-21: barycentrics 0.78835979 : 0.32275132 : -0.11111111; absolute trilinears 15.282051 : 4.066667 : -1.333333; h =11.925696.

Rank 3 — index 1

Independent definitions: 1 (raw coinciding expressions: 73).
ETC foot: X(4).

All independent definitions D1.

```
TSZ[2]
```

Normalized barycentric center function

```
{(-a^4 + (b^2 - c^2)^2)/(a^4 + (b^2 - c^2)^2 - 2*a^2*(b^2 + c^2)), (a^4 - b^4 - 2*a^2*c^2 + c^4)/(a^4 +
 (b^2 - c^2)^2 - 2*a^2*(b^2 + c^2)), (a^4 - 2*a^2*b^2 + b^4 - c^4)/(a^4 + (b^2 - c^2)^2 - 2*a^2*(b^2 +
 c^2))}
```

Invariant height

```
Sqrt[p^2/4 - (r + 2*R)^2]
```

6-9-13: barycentrics -0.71964286 : -1.24196429 : 2.96160714; absolute trilinears -5.676619 : -6.531164 : 10.782218; h =0.000000+8.775066i.
13-20-21: barycentrics 0.10582011 : 0.33862434 : 0.55555556; absolute trilinears 2.051282 : 4.266667 : 6.666667; h =5.962848.

Rank 4 — index 1

Independent definitions: 13 (raw coinciding expressions: 189).
ETC foot: X(3).

All independent definitions D1.

```
TSZ[3]
```

D2.

```
TSY[1, TSA, TSB, TSC, TSZ[1]]
```

D3.

```
TSY[2, TSA, TSB, TSC, TSZ[1]]
```

D4.

```
TSY[3, TSA, TSB, TSC, TSConjugate[TSZ[2]]]
```

D5.

```
TSY[3, TSA, TSB, TSC, TSZ[1]]
```

D6.

```
TSY[3, TSA, TSB, TSConjugate[TSZ[2]], TSZ[1]]
```

D7.

```
TSY[3, TSA, TSC, TSConjugate[TSZ[2]], TSZ[1]]
```

D8.

```
TSY[3, TSA, TSB, TSC, TSFoot[TSConjugate[TSZ[2]], TSPlane[TSA, TSB, TSZ[1]]]]
```

D9.

```
TSY[3, TSA, TSB, TSC, TSFoot[TSConjugate[TSZ[2]], TSPlane[TSA, TSC, TSZ[1]]]]
```

D10.

```
TSY[3, TSA, TSB, TSC, TSFoot[TSConjugate[TSZ[2]], TSPlane[TSB, TSC, TSZ[1]]]]
```

D11.

```
TSY[3, TSA, TSB, TSC, TSFoot[TSZ[1], TSPlane[TSA, TSB, TSConjugate[TSZ[2]]]]]
```

D12.

```
TSY[3, TSA, TSB, TSC, TSFoot[TSZ[1], TSPlane[TSA, TSC, TSConjugate[TSZ[2]]]]]
```

D13.

```
TSY[3, TSA, TSB, TSC, TSFoot[TSZ[1], TSPlane[TSB, TSC, TSConjugate[TSZ[2]]]]]
```

Normalized barycentric center function

```
{(a^2*(a^2 - b^2 - c^2))/(a^4 + (b^2 - c^2)^2 - 2*a^2*(b^2 + c^2)), (b^2*(-a^2 + b^2 - c^2))/(a^4 + (
b^2 - c^2)^2 - 2*a^2*(b^2 + c^2)), (c^2*(-a^2 - b^2 + c^2))/(a^4 + (b^2 - c^2)^2 - 2*a^2*(b^2 + c^2))}
```

Invariant height

```
Sqrt[p^2 - 4*(r + 2*R)^2]/4
```

6-9-13: barycentrics 0.85982143 : 1.12098214 : -0.98080357; absolute trilinears 6.782363 : 5.894951 : -3.570777; h =0.000000+4.387533i.
13-20-21: barycentrics 0.44708995 : 0.33068783 : 0.22222222; absolute trilinears 8.666667 : 4.166667 : 2.666667; h =2.981424.

Rank 5 — index $5/4$

Independent definitions: 4 (raw coinciding expressions: 8).
ETC foot: X(631).

All independent definitions D1.

```
TSY[1, TSConjugate[TSZ[2]], TSX[3], TSZ[1], TSZ[2]]
```

D2.

```
TSY[1, TSConjugate[TSZ[2]], TSX[3], TSZ[2], TSZ[3]]
```

D3.

```
TSY[1, TSX[2], TSX[3], TSZ[1], TSZ[2]]
```

D4.

```
TSY[1, TSX[2], TSX[3], TSZ[2], TSZ[3]]
```

Normalized barycentric center function

```
{(3*a^4 + (b^2 - c^2)^2 - 4*a^2*(b^2 + c^2))/(5*(a^4 + (b^2 - c^2)^2 - 2*a^2*(b^2 + c^2))), (2 + b*((a +
 b - c)^(-1) - (a - b + c)^(-1) + (-a + b + c)^(-1) + (a + b + c)^(-1)))/10, (a^4 + b^4 - 4*b^2*c^2 + 3*
c^4 - 2*a^2*(b^2 + 2*c^2))/(5*(a^4 + (b^2 - c^2)^2 - 2*a^2*(b^2 + c^2)))}
```

Invariant height

```
Sqrt[p^2 - 4*(r + 2*R)^2]/10
```

6-9-13: barycentrics 0.54392857 : 0.64839286 : -0.19232143; absolute trilinears 4.290566 : 3.409728 : -0.700178; h =0.000000+1.755013i.
13-20-21: barycentrics 0.37883598 : 0.33227513 : 0.28888889; absolute trilinears 7.343590 : 4.186667 : 3.466667; h =1.192570.

Rank 6 — index $10/7$

Independent definitions: 2 (raw coinciding expressions: 28).
ETC foot: X(140).

All independent definitions D1.

```
TSY[2, TSA, TSB, TSC, TSZ[3]]
```

D2.

```
TSY[2, TSConjugate[TSZ[2]], TSConjugate[TSZ[3]], TSX[4], TSZ[1]]
```

Normalized barycentric center function

```
{(2*a^4 + (b^2 - c^2)^2 - 3*a^2*(b^2 + c^2))/(4*(a^4 + (b^2 - c^2)^2 - 2*a^2*(b^2 + c^2))), (4 + b*((a +
 b - c)^(-1) - (a - b + c)^(-1) + (-a + b + c)^(-1) + (a + b + c)^(-1)))/16, (a^4 + b^4 - 3*b^2*c^2 + 2*
c^4 - a^2*(2*b^2 + 3*c^2))/(4*(a^4 + (b^2 - c^2)^2 - 2*a^2*(b^2 + c^2)))}
```

Invariant height

```
Sqrt[p^2 - 4*(r + 2*R)^2]/16
```

6-9-13: barycentrics 0.46495536 : 0.53024554 : 0.00479911; absolute trilinears 3.667617 : 2.788422 : 0.017472; h =0.000000+1.096883i.
13-20-21: barycentrics 0.36177249 : 0.33267196 : 0.30555556; absolute trilinears 7.012821 : 4.191667 : 3.666667; h =0.745356.

Rank 7 — index $5/3$

Independent definitions: 3 (raw coinciding expressions: 6).
ETC foot: X(3091).

All independent definitions D1.

```
TSY[1, TSConjugate[TSZ[1]], TSX[4], TSZ[1], TSZ[2]]
```

D2.

```
TSY[1, TSConjugate[TSZ[3]], TSX[4], TSZ[1], TSZ[2]]
```

D3.

```
TSY[1, TSX[2], TSX[4], TSZ[1], TSZ[2]]
```

Normalized barycentric center function

```
{(3 + a*(-(a + b - c)^(-1) - (a - b + c)^(-1) + (-a + b + c)^(-1) - (a + b + c)^(-1)))/5, (3 + b*((a -
 b - c)^(-1) - (a + b - c)^(-1) + (a - b + c)^(-1) - (a + b + c)^(-1)))/5, -1/5*(-3*a^4 - 3*b^4 + 2*b^2*
c^2 + c^4 + 2*a^2*(3*b^2 + c^2))/(a^4 + (b^2 - c^2)^2 - 2*a^2*(b^2 + c^2))}
```

Invariant height

```
Sqrt[p^2 - 4*(r + 2*R)^2]/5
```

6-9-13: barycentrics -0.08785714 : -0.29678571 : 1.38464286; absolute trilinears -0.693026 : -1.560718 : 5.041020; h =0.000000+3.510026i.
13-20-21: barycentrics 0.24232804 : 0.33544974 : 0.42222222; absolute trilinears 4.697436 : 4.226667 : 5.066667; h =2.385139.

Rank 8 — index 2

Independent definitions: 1 (raw coinciding expressions: 2).
ETC foot: no accepted ETC match.

All independent definitions D1.

```
TSY[1, TSA, TSB, TSC, TSZ[2]]
```

Normalized barycentric center function

```
{(-2*a^2*(b^2 + c^2)*Sqrt[a^4 - (b^2 - c^2)^2] + a^4*(-Sqrt[-((a - b - c)*(a + b - c)*(a - b + c)*(a +
 b + c))] + Sqrt[a^4 - (b^2 - c^2)^2]) + (b - c)^2*(b + c)^2*(Sqrt[-((a - b - c)*(a + b - c)*(a - b + c)
*(a + b + c))] + Sqrt[a^4 - (b^2 - c^2)^2]))/((a - b - c)*(a + b - c)*(a - b + c)*(a + b + c)*(Sqrt[-(
a^2 - b^2)^2 + c^4] + Sqrt[b^4 - (a^2 - c^2)^2] + Sqrt[a^4 - (b^2 - c^2)^2] + 2*Sqrt[b^2*c^2 - (-a^2 +
 b^2 + c^2)^2/4])), (a^4*(Sqrt[-((a - b - c)*(a + b - c)*(a - b + c)*(a + b + c))] + Sqrt[b^4 - (a^2 -
 c^2)^2]) + (b - c)*(b + c)*(b^2*(-Sqrt[-((a - b - c)*(a + b - c)*(a - b + c)*(a + b + c))] + Sqrt[b^4 -
 (a^2 - c^2)^2]) - c^2*(Sqrt[-((a - b - c)*(a + b - c)*(a - b + c)*(a + b + c))] + Sqrt[b^4 - (a^2 -
 c^2)^2])) - 2*a^2*(b^2*Sqrt[b^4 - (a^2 - c^2)^2] + c^2*(Sqrt[-((a - b - c)*(a + b - c)*(a - b + c)*(a +
 b + c))] + Sqrt[b^4 - (a^2 - c^2)^2])))/((a - b - c)*(a + b - c)*(a - b + c)*(a + b + c)*(Sqrt[-(a^2 -
 b^2)^2 + c^4] + Sqrt[b^4 - (a^2 - c^2)^2] + Sqrt[a^4 - (b^2 - c^2)^2] + 2*Sqrt[b^2*c^2 - (-a^2 + b^2 +
 c^2)^2/4])), (a^4*(Sqrt[-((a - b - c)*(a + b - c)*(a - b + c)*(a + b + c))] + Sqrt[-(a^2 - b^2)^2 +
 c^4]) - 2*a^2*(c^2*Sqrt[-(a^2 - b^2)^2 + c^4] + b^2*(Sqrt[-((a - b - c)*(a + b - c)*(a - b + c)*(a +
 b + c))] + Sqrt[-(a^2 - b^2)^2 + c^4])) + (b - c)*(b + c)*(c^2*(Sqrt[-((a - b - c)*(a + b - c)*(a - b +
 c)*(a + b + c))] - Sqrt[-(a^2 - b^2)^2 + c^4]) + b^2*(Sqrt[-((a - b - c)*(a + b - c)*(a - b + c)*(a +
 b + c))] + Sqrt[-(a^2 - b^2)^2 + c^4])))/((a - b - c)*(a + b - c)*(a - b + c)*(a + b + c)*(Sqrt[-(a^2 -
 b^2)^2 + c^4] + Sqrt[b^4 - (a^2 - c^2)^2] + Sqrt[a^4 - (b^2 - c^2)^2] + 2*Sqrt[b^2*c^2 - (-a^2 + b^2 +
 c^2)^2/4]))}
```

Invariant height

```
Sqrt[(a + b - c)*(a - b + c)*(-a + b + c)*(a + b + c)*(p + 2*r + 4*R)*(p - 2*(r + 2*R))]/(2*(Sqrt[-(
a^2 - b^2)^2 + c^4] + Sqrt[b^4 - (a^2 - c^2)^2] + Sqrt[a^4 - (b^2 - c^2)^2] + 2*Sqrt[b^2*c^2 - (-a^2 +
 b^2 + c^2)^2/4]))
```

6-9-13: barycentrics `-0.02603637+0.33055607i : -0.10589514+0.48596599i : 1.13193152-0.81652206i`; absolute trilinears `-0.205378+2.607461i : -0.556875+2.555568i : 4.120983-2.972683i`; h =`1.530160+2.121237i`.

13-20-21: barycentrics `0.16252919 : 0.34703649 : 0.49043432`; absolute trilinears `3.150566 : 4.372660 : 5.885212`; h =`2.247951`.

Rank 9 — index 2

Independent definitions: 1 (raw coinciding expressions: 2).
ETC foot: no accepted ETC match.

All independent definitions D1.

```
TSY[1, TSA, TSB, TSC, TSZ[3]]
```

Normalized barycentric center function

```
{(a*(Sqrt[2]*a^4*Sqrt[-a^2 + b^2 + c^2] + Sqrt[2]*(b^2 - c^2)^2*Sqrt[-a^2 + b^2 + c^2] - 2*Sqrt[2]*a^2*(
b^2 + c^2)*Sqrt[-a^2 + b^2 + c^2] + 2*a^3*Sqrt[-a^4 - (b^2 - c^2)^2 + 2*a^2*(b^2 + c^2)] - 2*a*(b^2 +
 c^2)*Sqrt[-a^4 - (b^2 - c^2)^2 + 2*a^2*(b^2 + c^2)]))/((a^4 + (b^2 - c^2)^2 - 2*a^2*(b^2 + c^2))*(
Sqrt[2]*c*Sqrt[a^2 + b^2 - c^2] + Sqrt[2]*b*Sqrt[a^2 - b^2 + c^2] + Sqrt[2]*a*Sqrt[-a^2 + b^2 + c^2] +
 4*Sqrt[b^2*c^2 - (-a^2 + b^2 + c^2)^2/4])), (b*(Sqrt[2]*a^4*Sqrt[a^2 - b^2 + c^2] - 2*a^2*(Sqrt[2]*b^2*
Sqrt[a^2 - b^2 + c^2] + Sqrt[2]*c^2*Sqrt[a^2 - b^2 + c^2] + b*Sqrt[-a^4 - (b^2 - c^2)^2 + 2*a^2*(b^2 +
 c^2)]) + (b^2 - c^2)*(Sqrt[2]*b^2*Sqrt[a^2 - b^2 + c^2] - Sqrt[2]*c^2*Sqrt[a^2 - b^2 + c^2] + 2*b*
Sqrt[-a^4 - (b^2 - c^2)^2 + 2*a^2*(b^2 + c^2)])))/((a^4 + (b^2 - c^2)^2 - 2*a^2*(b^2 + c^2))*(Sqrt[2]*c*
Sqrt[a^2 + b^2 - c^2] + Sqrt[2]*b*Sqrt[a^2 - b^2 + c^2] + Sqrt[2]*a*Sqrt[-a^2 + b^2 + c^2] + 4*Sqrt[b^2*
c^2 - (-a^2 + b^2 + c^2)^2/4])), (c*(Sqrt[2]*a^4*Sqrt[a^2 + b^2 - c^2] - 2*a^2*(Sqrt[2]*b^2*Sqrt[a^2 +
 b^2 - c^2] + c*(Sqrt[2]*c*Sqrt[a^2 + b^2 - c^2] + Sqrt[-a^4 - (b^2 - c^2)^2 + 2*a^2*(b^2 + c^2)])) + (
b^2 - c^2)*(Sqrt[2]*b^2*Sqrt[a^2 + b^2 - c^2] - c*(Sqrt[2]*c*Sqrt[a^2 + b^2 - c^2] + 2*Sqrt[-a^4 - (
b^2 - c^2)^2 + 2*a^2*(b^2 + c^2)]))))/((a^4 + (b^2 - c^2)^2 - 2*a^2*(b^2 + c^2))*(Sqrt[2]*c*Sqrt[a^2 +
 b^2 - c^2] + Sqrt[2]*b*Sqrt[a^2 - b^2 + c^2] + Sqrt[2]*a*Sqrt[-a^2 + b^2 + c^2] + 4*Sqrt[b^2*c^2 - (-
a^2 + b^2 + c^2)^2/4]))}
```

Invariant height

```
Sqrt[(a + b - c)*(a - b + c)*(-a + b + c)*(a + b + c)*(p + 2*r + 4*R)*(p - 2*(r + 2*R))]/(2*(2*Sqrt[(a +
 b - c)*(a - b + c)*(-a + b + c)*(a + b + c)] + Sqrt[2]*c*Sqrt[a^2 + b^2 - c^2] + Sqrt[2]*b*Sqrt[a^2 -
 b^2 + c^2] + Sqrt[2]*a*Sqrt[-a^2 + b^2 + c^2]))
```

6-9-13: barycentrics `0.58102851-0.16923042i : 0.71680443-0.20877653i : -0.29783294+0.37800695i`; absolute trilinears `4.583215-1.334908i : 3.769486-1.097901i : -1.084310+1.376196i`; h =`0.489941+1.682142i`.

13-20-21: barycentrics `0.41572236 : 0.33320902 : 0.25106862`; absolute trilinears `8.058618 : 4.198434 : 3.012823`; h =`1.347376`.

Rank 10 — index $5/2$

Independent definitions: 2 (raw coinciding expressions: 4).
ETC foot: X(5).

All independent definitions D1.

```
TSY[1, TSX[3], TSX[4], TSZ[1], TSZ[2]]
```

D2.

```
TSY[2, TSConjugate[TSZ[2]], TSX[4], TSZ[1], TSZ[2]]
```

Normalized barycentric center function

```
{((b^2 - c^2)^2 - a^2*(b^2 + c^2))/(2*(a^4 + (b^2 - c^2)^2 - 2*a^2*(b^2 + c^2))), (4 + b*((a - b - c)^(-
1) - (a + b - c)^(-1) + (a - b + c)^(-1) - (a + b + c)^(-1)))/8, (a^4 + b^4 - b^2*c^2 - a^2*(2*b^2 +
 c^2))/(2*(a^4 + (b^2 - c^2)^2 - 2*a^2*(b^2 + c^2)))}
```

Invariant height

```
Sqrt[p^2 - 4*(r + 2*R)^2]/4
```

6-9-13: barycentrics `0.07008929 : -0.06049107 : 0.99040179`; absolute trilinears `0.552872 : -0.318107 : 3.605721`; h =`0.000000+4.387533i`.
13-20-21: barycentrics `0.27645503 : 0.33465608 : 0.38888889`; absolute trilinears `5.358974 : 4.216667 : 4.666667`; h =`2.981424`.

Rank 11 — index $5/2$

Independent definitions: 2 (raw coinciding expressions: 4).
ETC foot: X(3).

All independent definitions D1.

```
TSY[2, TSConjugate[TSZ[1]], TSX[4], TSZ[1], TSZ[2]]
```

D2.

```
TSY[2, TSConjugate[TSZ[2]], TSConjugate[TSZ[3]], TSZ[1], TSZ[3]]
```

Normalized barycentric center function

```
{(a^2*(a^2 - b^2 - c^2))/(a^4 + (b^2 - c^2)^2 - 2*a^2*(b^2 + c^2)), (b^2*(-a^2 + b^2 - c^2))/(a^4 + (
b^2 - c^2)^2 - 2*a^2*(b^2 + c^2)), (c^2*(-a^2 - b^2 + c^2))/(a^4 + (b^2 - c^2)^2 - 2*a^2*(b^2 + c^2))}
```

Invariant height

```
Sqrt[p^2 - 4*(r + 2*R)^2]/8
```

6-9-13: barycentrics `0.85982143 : 1.12098214 : -0.98080357`; absolute trilinears `6.782363 : 5.894951 : -3.570777`; h =`0.000000+2.193767i`.
13-20-21: barycentrics `0.44708995 : 0.33068783 : 0.22222222`; absolute trilinears `8.666667 : 4.166667 : 2.666667`; h =`1.490712`.

Rank 12 — index $5/2$

Independent definitions: 2 (raw coinciding expressions: 4).
ETC foot: X(548).

All independent definitions D1.

```
TSY[2, TSConjugate[TSZ[1]], TSConjugate[TSZ[3]], TSZ[1], TSZ[2]]
```

D2.

```
TSY[2, TSConjugate[TSZ[1]], TSX[4], TSZ[1], TSZ[3]]
```

Normalized barycentric center function

```
{-1/4*(-6*a^4 + (b^2 - c^2)^2 + 5*a^2*(b^2 + c^2))/(a^4 + (b^2 - c^2)^2 - 2*a^2*(b^2 + c^2)), (-4 + 7*b*
((a + b - c)^(-1) - (a - b + c)^(-1) + (-a + b + c)^(-1) + (a + b + c)^(-1)))/16, -1/4*(a^4 + b^4 + 5*
b^2*c^2 - 6*c^4 + a^2*(-2*b^2 + 5*c^2))/(a^4 + (b^2 - c^2)^2 - 2*a^2*(b^2 + c^2))}
```

Invariant height

```
Sqrt[p^2 - 4*(r + 2*R)^2]/16
```

6-9-13: barycentrics `1.25468750 : 1.71171875 : -1.96640625`; absolute trilinears `9.897108 : 9.001480 : -7.159025`; h =`0.000000+1.096883i`.
13-20-21: barycentrics `0.53240741 : 0.32870370 : 0.13888889`; absolute trilinears `10.320513 : 4.141667 : 1.666667`; h =`0.745356`.

Rank 13 — index $5/2$

Independent definitions: 2 (raw coinciding expressions: 4).
ETC foot: X(1125).

All independent definitions D1.

```
TSY[2, TSConjugate[TSZ[2]], TSX[1], TSX[4], TSZ[1]]
```

D2.

```
TSY[2, TSConjugate[TSZ[3]], TSX[1], TSZ[2], TSZ[3]]
```

Normalized barycentric center function

```
{(1 + a/(a + b + c))/4, (1 + b/(a + b + c))/4, (a + b + 2*c)/(4*(a + b + c))}
```

Invariant height

```
Sqrt[p^2 - 4*(r + 2*R)^2]/8
```

6-9-13: barycentrics `0.30357143 : 0.33035714 : 0.36607143`; absolute trilinears `2.394604 : 1.737262 : 1.332743`; h =`0.000000+2.193767i`.
13-20-21: barycentrics `0.31018519 : 0.34259259 : 0.34722222`; absolute trilinears `6.012821 : 4.316667 : 4.166667`; h =`1.490712`.

Rank 14 — index $5/2$

Independent definitions: 2 (raw coinciding expressions: 4).
ETC foot: X(2).

All independent definitions D1.

```
TSY[2, TSConjugate[TSZ[2]], TSX[2], TSX[4], TSZ[1]]
```

D2.

```
TSY[2, TSConjugate[TSZ[3]], TSX[2], TSZ[2], TSZ[3]]
```

Normalized barycentric center function

```
{1/3, 1/3, 1/3}
```

Invariant height

```
Sqrt[p^2 - 4*(r + 2*R)^2]/8
```

6-9-13: barycentrics 0.33333333 : 0.33333333 : 0.33333333; absolute trilinears 2.629369 : 1.752913 : 1.213555; h =0.000000+2.193767i.
13-20-21: barycentrics 0.33333333 : 0.33333333 : 0.33333333; absolute trilinears 6.461538 : 4.200000 : 4.000000; h =1.490712.

Rank 15 — index $5/2$

Independent definitions: 2 (raw coinciding expressions: 4).
ETC foot: X(140).

All independent definitions D1.

```
TSY[2, TSConjugate[TSZ[2]], TSX[3], TSX[4], TSZ[1]]
```

D2.

```
TSY[2, TSConjugate[TSZ[3]], TSX[3], TSZ[2], TSZ[3]]
```

Normalized barycentric center function

```
{(2*a^4 + (b^2 - c^2)^2 - 3*a^2*(b^2 + c^2))/(4*(a^4 + (b^2 - c^2)^2 - 2*a^2*(b^2 + c^2))), (4 + b*((a +
 b - c)^(-1) - (a - b + c)^(-1) + (-a + b + c)^(-1) + (a + b + c)^(-1)))/16, (a^4 + b^4 - 3*b^2*c^2 + 2*
c^4 - a^2*(2*b^2 + 3*c^2))/(4*(a^4 + (b^2 - c^2)^2 - 2*a^2*(b^2 + c^2)))}
```

Invariant height

```
Sqrt[p^2 - 4*(r + 2*R)^2]/8
```

6-9-13: barycentrics 0.46495536 : 0.53024554 : 0.00479911; absolute trilinears 3.667617 : 2.788422 : 0.017472; h =0.000000+2.193767i.
13-20-21: barycentrics 0.36177249 : 0.33267196 : 0.30555556; absolute trilinears 7.012821 : 4.191667 : 3.666667; h =1.490712.

Rank 16 — index $5/2$

Independent definitions: 2 (raw coinciding expressions: 4).
ETC foot: X(140).

All independent definitions D1.

```
TSY[2, TSConjugate[TSZ[2]], TSConjugate[TSZ[3]], TSZ[1], TSZ[2]]
```

D2.

```
TSY[2, TSConjugate[TSZ[2]], TSX[4], TSZ[1], TSZ[3]]
```

Normalized barycentric center function

```
{(2*a^4 + (b^2 - c^2)^2 - 3*a^2*(b^2 + c^2))/(4*(a^4 + (b^2 - c^2)^2 - 2*a^2*(b^2 + c^2))), (4 + b*((a +
 b - c)^(-1) - (a - b + c)^(-1) + (-a + b + c)^(-1) + (a + b + c)^(-1)))/16, (a^4 + b^4 - 3*b^2*c^2 + 2*
c^4 - a^2*(2*b^2 + 3*c^2))/(4*(a^4 + (b^2 - c^2)^2 - 2*a^2*(b^2 + c^2)))}
```

Invariant height

```
(3*Sqrt[p^2 - 4*(r + 2*R)^2])/16
```

6-9-13: barycentrics 0.46495536 : 0.53024554 : 0.00479911; absolute trilinears 3.667617 : 2.788422 : 0.017472; h =0.000000+3.290650i.
13-20-21: barycentrics 0.36177249 : 0.33267196 : 0.30555556; absolute trilinears 7.012821 : 4.191667 : 3.666667; h =2.236068.

Rank 17 — index $5/2$

Independent definitions: 2 (raw coinciding expressions: 4).
ETC foot: X(13624).

All independent definitions D1.

```
TSY[2, TSConjugate[TSZ[2]], TSX[1], TSZ[1], TSZ[3]]
```

D2.

```
TSY[2, TSConjugate[TSZ[3]], TSX[1], TSX[4], TSZ[1]]
```

Normalized barycentric center function

```
{(a*(3/(a + b - c) + 3/(a - b + c) - 3/(-a + b + c) + 7/(a + b + c)))/16, (b*(3/(a + b - c) - 3/(a - b +
 c) + 3/(-a + b + c) + 7/(a + b + c)))/16, (16 - (3*(a + b))/(a + b - c) - (3*(a - b))/(a - b + c) + (3*
(a - b))/(-a + b + c) - (7*(a + b))/(a + b + c))/16}
```

Invariant height

```
(3*Sqrt[p^2 - 4*(r + 2*R)^2])/16
```

6-9-13: barycentrics `0.69843750 : 0.92109375 : -0.61953125`; absolute trilinears `5.509349 : 4.843790 : -2.255505`; h =`0.000000+3.290650i`.
13-20-21: barycentrics `0.39550265 : 0.34060847 : 0.26388889`; absolute trilinears `7.666667 : 4.291667 : 3.166667`; h =`2.236068`.

Rank 18 — index $5/2$

Independent definitions: 2 (raw coinciding expressions: 4).
ETC foot: X(9955).

All independent definitions D1.

```
TSY[2, TSConjugate[TSZ[2]], TSX[1], TSZ[2], TSZ[3]]
```

D2.

```
TSY[2, TSConjugate[TSZ[3]], TSX[1], TSX[4], TSZ[2]]
```

Normalized barycentric center function

```
{(8 + a*(-3/(a + b - c) - 3/(a - b + c) + 3/(-a + b + c) + (a + b + c)^(-1)))/16, (8 + b*(-3/(a + b - c)
 + 3/(a - b + c) - 3/(-a + b + c) + (a + b + c)^(-1)))/16, ((3*(a + b))/(a + b - c) + (3*(a - b))/(a -
 b + c) - (3*(a - b))/(-a + b + c) - (a + b)/(a + b + c))/16}
```

Invariant height

```
Sqrt[p^2 - 4*(r + 2*R)^2]/16
```

6-9-13: barycentrics `-0.09129464 : -0.26037946 : 1.35167411`; absolute trilinears `-0.720142 : -1.369267 : 4.920992`; h =`0.000000+1.096883i`.
13-20-21: barycentrics `0.22486772 : 0.34457672 : 0.43055556`; absolute trilinears `4.358974 : 4.341667 : 5.166667`; h =`0.745356`.

Rank 19 — index $5/2$

Independent definitions: 2 (raw coinciding expressions: 4).
ETC foot: X(12100).

All independent definitions D1.

```
TSY[2, TSConjugate[TSZ[2]], TSX[2], TSZ[1], TSZ[3]]
```

D2.

```
TSY[2, TSConjugate[TSZ[3]], TSX[2], TSX[4], TSZ[1]]
```

Normalized barycentric center function

```
{(10*a^4 + (b^2 - c^2)^2 - 11*a^2*(b^2 + c^2))/(12*(a^4 + (b^2 - c^2)^2 - 2*a^2*(b^2 + c^2))), (4 + 9*b*
((a + b - c)^(-1) - (a - b + c)^(-1) + (-a + b + c)^(-1) + (a + b + c)^(-1)))/48, ((a^2 - b^2)^2 - 11*(
a^2 + b^2)*c^2 + 10*c^4)/(12*(a - b - c)*(a + b - c)*(a - b + c)*(a + b + c))}
```

Invariant height

```
(3*Sqrt[p^2 - 4*(r + 2*R)^2])/16
```

6-9-13: barycentrics 0.72819940 : 0.92406994 : -0.65226935; absolute trilinears 5.744114 : 4.859441 : -2.374694; h =0.000000+3.290650i.
13-20-21: barycentrics 0.41865079 : 0.33134921 : 0.25000000; absolute trilinears 8.115385 : 4.175000 : 3.000000; h =2.236068.

Rank 20 — index $5/2$

Independent definitions: 2 (raw coinciding expressions: 4).
ETC foot: X(5066).

All independent definitions D1.

```
TSY[2, TSConjugate[TSZ[2]], TSX[2], TSZ[2], TSZ[3]]
```

D2.

```
TSY[2, TSConjugate[TSZ[3]], TSX[2], TSX[4], TSZ[2]]
```

Normalized barycentric center function

```
{(-2*a^4 + 7*(b^2 - c^2)^2 - 5*a^2*(b^2 + c^2))/(12*(a^4 + (b^2 - c^2)^2 - 2*a^2*(b^2 + c^2))), (28 + 9*
b*((a - b - c)^(-1) - (a + b - c)^(-1) + (a - b + c)^(-1) - (a + b + c)^(-1)))/48, (7*(a^2 - b^2)^2 - 5*
(a^2 + b^2)*c^2 - 2*c^4)/(12*(a - b - c)*(a + b - c)*(a - b + c)*(a + b + c))}
```

Invariant height

```
Sqrt[p^2 - 4*(r + 2*R)^2]/16
```

6-9-13: barycentrics -0.06153274 : -0.25740327 : 1.31893601; absolute trilinears -0.485377 : -1.353616 : 4.801803; h =0.000000+1.096883i.
13-20-21: barycentrics 0.24801587 : 0.33531746 : 0.41666667; absolute trilinears 4.807692 : 4.225000 : 5.000000; h =0.745356.

Rank 21 — index $5/2$

Independent definitions: 2 (raw coinciding expressions: 4).
ETC foot: X(3).

All independent definitions D1.

```
TSY[2, TSConjugate[TSZ[2]], TSX[3], TSZ[1], TSZ[3]]
```

D2.

```
TSY[2, TSConjugate[TSZ[3]], TSX[3], TSX[4], TSZ[1]]
```

Normalized barycentric center function

```
{(a^2*(a^2 - b^2 - c^2))/(a^4 + (b^2 - c^2)^2 - 2*a^2*(b^2 + c^2)), (b^2*(-a^2 + b^2 - c^2))/(a^4 + (
b^2 - c^2)^2 - 2*a^2*(b^2 + c^2)), (c^2*(-a^2 - b^2 + c^2))/(a^4 + (b^2 - c^2)^2 - 2*a^2*(b^2 + c^2))}
```

Invariant height

```
(3*Sqrt[p^2 - 4*(r + 2*R)^2])/16
```

6-9-13: barycentrics 0.85982143 : 1.12098214 : -0.98080357; absolute trilinears 6.782363 : 5.894951 : -3.570777; h =0.000000+3.290650i.
13-20-21: barycentrics 0.44708995 : 0.33068783 : 0.22222222; absolute trilinears 8.666667 : 4.166667 : 2.666667; h =2.236068.

Rank 22 — index $5/2$

Independent definitions: 2 (raw coinciding expressions: 4).
ETC foot: X(5).

All independent definitions D1.

```
TSY[2, TSConjugate[TSZ[2]], TSX[3], TSZ[2], TSZ[3]]
```

D2.

```
TSY[2, TSConjugate[TSZ[3]], TSX[3], TSX[4], TSZ[2]]
```

Normalized barycentric center function

```
{((b^2 - c^2)^2 - a^2*(b^2 + c^2))/(2*(a^4 + (b^2 - c^2)^2 - 2*a^2*(b^2 + c^2))), (4 + b*((a - b - c)^(-1) - (a + b - c)^(-1) + (a - b + c)^(-1) - (a + b + c)^(-1)))/8, (a^4 + b^4 - b^2*c^2 - a^2*(2*b^2 + c^2))/(2*(a^4 + (b^2 - c^2)^2 - 2*a^2*(b^2 + c^2)))}
```

Invariant height

```
Sqrt[p^2 - 4*(r + 2*R)^2]/16
```

6-9-13: barycentrics 0.07008929 : -0.06049107 : 0.99040179; absolute trilinears 0.552872 : -0.318107 : 3.605721; h =0.000000+1.096883i.
13-20-21: barycentrics 0.27645503 : 0.33465608 : 0.38888889; absolute trilinears 5.358974 : 4.216667 : 4.666667; h =0.745356.

Rank 23 — index $5/2$

Independent definitions: 2 (raw coinciding expressions: 4).
ETC foot: X(140).

All independent definitions D1.

```
TSY[2, TSConjugate[TSZ[2]], TSZ[1], TSZ[2], TSZ[3]]
```

D2.

```
TSY[2, TSConjugate[TSZ[3]], TSX[4], TSZ[1], TSZ[2]]
```

Normalized barycentric center function

```
{(2*a^4 + (b^2 - c^2)^2 - 3*a^2*(b^2 + c^2))/(4*(a^4 + (b^2 - c^2)^2 - 2*a^2*(b^2 + c^2))), (4 + b*((a + b - c)^(-1) - (a - b + c)^(-1) + (-a + b + c)^(-1) + (a + b + c)^(-1)))/16, (a^4 + b^4 - 3*b^2*c^2 + 2*c^4 - a^2*(2*b^2 + 3*c^2))/(4*(a^4 + (b^2 - c^2)^2 - 2*a^2*(b^2 + c^2)))}
```

Invariant height

```
(5*Sqrt[p^2 - 4*(r + 2*R)^2])/16
```

6-9-13: barycentrics 0.46495536 : 0.53024554 : 0.00479911; absolute trilinears 3.667617 : 2.788422 : 0.017472; h =0.000000+5.484416i.
13-20-21: barycentrics 0.36177249 : 0.33267196 : 0.30555556; absolute trilinears 7.012821 : 4.191667 : 3.666667; h =3.726780.

Rank 24 — index $5/2$

Independent definitions: 2 (raw coinciding expressions: 4).
ETC foot: no accepted ETC match.

All independent definitions D1.

```
TSY[2, TSConjugate[TSZ[3]], TSX[1], TSX[2], TSZ[2]]
```

D2.

```
TSY[2, TSX[1], TSX[2], TSX[4], TSZ[3]]
```

Normalized barycentric center function

```
{1/3 + (a*(-(a + b - c)^(-1) - (a - b + c)^(-1) + (-a + b + c)^(-1) + 3/(a + b + c)))/16, 1/3 + (b*((a -
 b - c)^(-1) - (a + b - c)^(-1) + (a - b + c)^(-1) + 3/(a + b + c)))/16, (16 + (3*(a + b))/(a + b - c) +
 (3*(a - b))/(a - b + c) - (3*(a - b))/(-a + b + c) - (9*(a + b))/(a + b + c))/48}
```

Invariant height

```
Sqrt[p^2 - 4*(r + 2*R)^2]/16
```

6-9-13: barycentrics 0.17194940 : 0.13344494 : 0.69460565; absolute trilinears 1.356355 : 0.701752 : 2.528826; h =0.000000+1.096883i.
13-20-21: barycentrics 0.28174603 : 0.34325397 : 0.37500000; absolute trilinears 5.461538 : 4.325000 : 4.500000; h =0.745356.

Rank 25 — index $5/2$

Independent definitions: 2 (raw coinciding expressions: 4).
ETC foot: X(1125).

All independent definitions D1.

```
TSY[2, TSConjugate[TSZ[3]], TSX[1], TSX[3], TSZ[2]]
```

D2.

```
TSY[2, TSX[1], TSX[3], TSX[4], TSZ[3]]
```

Normalized barycentric center function

```
{(1 + a/(a + b + c))/4, (1 + b/(a + b + c))/4, (a + b + 2*c)/(4*(a + b + c))}
```

Invariant height

```
Sqrt[p^2 - 4*(r + 2*R)^2]/16
```

6-9-13: barycentrics 0.30357143 : 0.33035714 : 0.36607143; absolute trilinears 2.394604 : 1.737262 : 1.332743; h =0.000000+1.096883i.
13-20-21: barycentrics 0.31018519 : 0.34259259 : 0.34722222; absolute trilinears 6.012821 : 4.316667 : 4.166667; h =0.745356.

Rank 26 — index $5/2$

Independent definitions: 2 (raw coinciding expressions: 4).
ETC foot: X(13624).

All independent definitions D1.

```
TSY[2, TSConjugate[TSZ[3]], TSX[1], TSZ[1], TSZ[2]]
```

D2.

```
TSY[2, TSX[1], TSX[4], TSZ[1], TSZ[3]]
```

Normalized barycentric center function

```
{(a*(3/(a + b - c) + 3/(a - b + c) - 3/(-a + b + c) + 7/(a + b + c)))/16, (b*(3/(a + b - c) - 3/(a - b + c) + 3/(-a + b + c) + 7/(a + b + c)))/16, (16 - (3*(a + b))/(a + b - c) - (3*(a - b))/(a - b + c) + (3*(a - b))/(-a + b + c) - (7*(a + b))/(a + b + c))/16}
```

Invariant height

```
(5*Sqrt[p^2 - 4*(r + 2*R)^2])/16
```

6-9-13: barycentrics `0.69843750 : 0.92109375 : -0.61953125`; absolute trilinears `5.509349 : 4.843790 : -2.255505`; h =`0.000000+5.484416i`.
13-20-21: barycentrics `0.39550265 : 0.34060847 : 0.26388889`; absolute trilinears `7.666667 : 4.291667 : 3.166667`; h =`3.726780`.

Rank 27 — index $5/2$

Independent definitions: 2 (raw coinciding expressions: 4).
ETC foot: X(2).

All independent definitions D1.

```
TSY[2, TSConjugate[TSZ[3]], TSX[2], TSX[3], TSZ[2]]
```

D2.

```
TSY[2, TSX[2], TSX[3], TSX[4], TSZ[3]]
```

Normalized barycentric center function

```
{1/3, 1/3, 1/3}
```

Invariant height

```
Sqrt[p^2 - 4*(r + 2*R)^2]/16
```

6-9-13: barycentrics `0.33333333 : 0.33333333 : 0.33333333`; absolute trilinears `2.629369 : 1.752913 : 1.213555`; h =`0.000000+1.096883i`.
13-20-21: barycentrics `0.33333333 : 0.33333333 : 0.33333333`; absolute trilinears `6.461538 : 4.200000 : 4.000000`; h =`0.745356`.

Rank 28 — index $5/2$

Independent definitions: 2 (raw coinciding expressions: 4).
ETC foot: X(12100).

All independent definitions D1.

```
TSY[2, TSConjugate[TSZ[3]], TSX[2], TSZ[1], TSZ[2]]
```

D2.

```
TSY[2, TSX[2], TSX[4], TSZ[1], TSZ[3]]
```

Normalized barycentric center function

```
{(10*a^4 + (b^2 - c^2)^2 - 11*a^2*(b^2 + c^2))/(12*(a^4 + (b^2 - c^2)^2 - 2*a^2*(b^2 + c^2))), (4 + 9*b*((a + b - c)^(-1) - (a - b + c)^(-1) + (-a + b + c)^(-1) + (a + b + c)^(-1)))/48, ((a^2 - b^2)^2 - 11*(a^2 + b^2)*c^2 + 10*c^4)/(12*(a - b - c)*(a + b - c)*(a - b + c)*(a + b + c))}
```

Invariant height

```
(5*Sqrt[p^2 - 4*(r + 2*R)^2])/16
```

6-9-13: barycentrics `0.72819940 : 0.92406994 : -0.65226935`; absolute trilinears `5.744114 : 4.859441 : -2.374694`; h =`0.000000+5.484416i`.
13-20-21: barycentrics `0.41865079 : 0.33134921 : 0.25000000`; absolute trilinears `8.115385 : 4.175000 : 3.000000`; h =`3.726780`.

Rank 29 — index 5/2

Independent definitions: 2 (raw coinciding expressions: 4).
ETC foot: X(3).

All independent definitions D1.

```
TSY[2, TSConjugate[TSZ[3]], TSX[3], TSZ[1], TSZ[2]]
```

D2.

```
TSY[2, TSX[3], TSX[4], TSZ[1], TSZ[3]]
```

Normalized barycentric center function

```
{(a^2*(a^2 - b^2 - c^2))/(a^4 + (b^2 - c^2)^2 - 2*a^2*(b^2 + c^2)), (b^2*(-a^2 + b^2 - c^2))/(a^4 + (
b^2 - c^2)^2 - 2*a^2*(b^2 + c^2)), (c^2*(-a^2 - b^2 + c^2))/(a^4 + (b^2 - c^2)^2 - 2*a^2*(b^2 + c^2))}
```

Invariant height

```
(5*Sqrt[p^2 - 4*(r + 2*R)^2])/16
```

6-9-13: barycentrics `0.85982143 : 1.12098214 : -0.98080357`; absolute trilinears `6.782363 : 5.894951 : -3.570777`; h =`0.000000+5.484416i`.
13-20-21: barycentrics `0.44708995 : 0.33068783 : 0.22222222`; absolute trilinears `8.666667 : 4.166667 : 2.666667`; h =`3.726780`.

Rank 30 — index 3

Independent definitions: 1 (raw coinciding expressions: 2).
ETC foot: no accepted ETC match.

All independent definitions D1.

```
TSY[1, TSA, TSB, TSC, TSY[1, TSA, TSB, TSC, TSZ[2]]]
```

Normalized barycentric center function

```
{(a^4 - b^4 + 2*b^2*c^2 - c^4 + 2*Sqrt[a^4 - b^4 + 2*b^2*c^2 - c^4]*Sqrt[b^2*c^2 - (-a^2 + b^2 + c^2)^2/
4] + Sqrt[2]*Sqrt[-a^4 + b^4 + 2*a^2*c^2 - c^4]*Sqrt[((a^4 - b^4 + 2*b^2*c^2 - c^4)*(-a^4 + 2*a^2*b^2 -
 b^4 + 2*a^2*c^2 + 2*b^2*c^2 - c^4 + 2*Sqrt[a^4 - b^4 + 2*b^2*c^2 - c^4]*Sqrt[b^2*c^2 - (-a^2 + b^2 +
 c^2)^2/4]))/(Sqrt[-a^4 + b^4 + 2*a^2*c^2 - c^4] + Sqrt[a^4 - b^4 + 2*b^2*c^2 - c^4] + Sqrt[-a^4 + 2*
a^2*b^2 - b^4 + c^4] + 2*Sqrt[b^2*c^2 - (-a^2 + b^2 + c^2)^2/4])^2] + Sqrt[2]*Sqrt[a^4 - b^4 + 2*b^2*
c^2 - c^4]*Sqrt[((a^4 - b^4 + 2*b^2*c^2 - c^4)*(-a^4 + 2*a^2*b^2 - b^4 + 2*a^2*c^2 + 2*b^2*c^2 - c^4 +
 2*Sqrt[a^4 - b^4 + 2*b^2*c^2 - c^4]*Sqrt[b^2*c^2 - (-a^2 + b^2 + c^2)^2/4]))/(Sqrt[-a^4 + b^4 + 2*a^2*
c^2 - c^4] + Sqrt[a^4 - b^4 + 2*b^2*c^2 - c^4] + Sqrt[-a^4 + 2*a^2*b^2 - b^4 + c^4] + 2*Sqrt[b^2*c^2 - (
-a^2 + b^2 + c^2)^2/4])^2] + Sqrt[2]*Sqrt[-a^4 + 2*a^2*b^2 - b^4 + c^4]*Sqrt[((a^4 - b^4 + 2*b^2*c^2 -
 c^4)*(-a^4 + 2*a^2*b^2 - b^4 + 2*a^2*c^2 + 2*b^2*c^2 - c^4 + 2*Sqrt[a^4 - b^4 + 2*b^2*c^2 - c^4]*
Sqrt[b^2*c^2 - (-a^2 + b^2 + c^2)^2/4]))/(Sqrt[-a^4 + b^4 + 2*a^2*c^2 - c^4] + Sqrt[a^4 - b^4 + 2*b^2*
c^2 - c^4] + Sqrt[-a^4 + 2*a^2*b^2 - b^4 + c^4] + 2*Sqrt[b^2*c^2 - (-a^2 + b^2 + c^2)^2/4])^2] + 2*
Sqrt[2]*Sqrt[b^2*c^2 - (-a^2 + b^2 + c^2)^2/4]*Sqrt[((a^4 - b^4 + 2*b^2*c^2 - c^4)*(-a^4 + 2*a^2*b^2 -
 b^4 + 2*a^2*c^2 + 2*b^2*c^2 - c^4 + 2*Sqrt[a^4 - b^4 + 2*b^2*c^2 - c^4]*Sqrt[b^2*c^2 - (-a^2 + b^2 +
 c^2)^2/4]))/(Sqrt[-a^4 + b^4 + 2*a^2*c^2 - c^4] + Sqrt[a^4 - b^4 + 2*b^2*c^2 - c^4] + Sqrt[-a^4 + 2*
a^2*b^2 - b^4 + c^4] + 2*Sqrt[b^2*c^2 - (-a^2 + b^2 + c^2)^2/4])^2])/((Sqrt[-a^4 + b^4 + 2*a^2*c^2 -
 c^4] + Sqrt[a^4 - b^4 + 2*b^2*c^2 - c^4] + Sqrt[-a^4 + 2*a^2*b^2 - b^4 + c^4] + 2*Sqrt[b^2*c^2 - (-
a^2 + b^2 + c^2)^2/4])*(2*Sqrt[b^2*c^2 - (-a^2 + b^2 + c^2)^2/4] + Sqrt[2]*Sqrt[-(((a^4 - b^4 - 2*a^2*
c^2 + c^4)*(-a^4 + 2*a^2*b^2 - b^4 + 2*a^2*c^2 + 2*b^2*c^2 - c^4 + 2*Sqrt[-a^4 + b^4 + 2*a^2*c^2 - c^4]*
Sqrt[b^2*c^2 - (-a^2 + b^2 + c^2)^2/4]))/(Sqrt[-a^4 + b^4 + 2*a^2*c^2 - c^4] + Sqrt[a^4 - b^4 + 2*b^2*
c^2 - c^4] + Sqrt[-a^4 + 2*a^2*b^2 - b^4 + c^4] + 2*Sqrt[b^2*c^2 - (-a^2 + b^2 + c^2)^2/4])^2)] +
 Sqrt[2]*Sqrt[((a^4 - b^4 + 2*b^2*c^2 - c^4)*(-a^4 + 2*a^2*b^2 - b^4 + 2*a^2*c^2 + 2*b^2*c^2 - c^4 + 2*
Sqrt[a^4 - b^4 + 2*b^2*c^2 - c^4]*Sqrt[b^2*c^2 - (-a^2 + b^2 + c^2)^2/4]))/(Sqrt[-a^4 + b^4 + 2*a^2*
c^2 - c^4] + Sqrt[a^4 - b^4 + 2*b^2*c^2 - c^4] + Sqrt[-a^4 + 2*a^2*b^2 - b^4 + c^4] + 2*Sqrt[b^2*c^2 - (
-a^2 + b^2 + c^2)^2/4])^2] + Sqrt[2]*Sqrt[-(((a^4 - 2*a^2*b^2 + b^4 - c^4)*(-a^4 + 2*a^2*b^2 - b^4 + 2*
a^2*c^2 + 2*b^2*c^2 - c^4 + 2*Sqrt[-a^4 + 2*a^2*b^2 - b^4 + c^4]*Sqrt[b^2*c^2 - (-a^2 + b^2 + c^2)^2/4])
)/(Sqrt[-a^4 + b^4 + 2*a^2*c^2 - c^4] + Sqrt[a^4 - b^4 + 2*b^2*c^2 - c^4] + Sqrt[-a^4 + 2*a^2*b^2 -
 b^4 + c^4] + 2*Sqrt[b^2*c^2 - (-a^2 + b^2 + c^2)^2/4])^2)])), (-a^4 + b^4 + 2*a^2*c^2 - c^4 + 2*Sqrt[-
a^4 + b^4 + 2*a^2*c^2 - c^4]*Sqrt[b^2*c^2 - (-a^2 + b^2 + c^2)^2/4] + Sqrt[2]*Sqrt[-a^4 + b^4 + 2*a^2*
c^2 - c^4]*Sqrt[-(((a^4 - b^4 - 2*a^2*c^2 + c^4)*(-a^4 + 2*a^2*b^2 - b^4 + 2*a^2*c^2 + 2*b^2*c^2 - c^4 +
 2*Sqrt[-a^4 + b^4 + 2*a^2*c^2 - c^4]*Sqrt[b^2*c^2 - (-a^2 + b^2 + c^2)^2/4]))/(Sqrt[-a^4 + b^4 + 2*a^2*
```

```
c^2 - c^4] + Sqrt[a^4 - b^4 + 2*b^2*c^2 - c^4] + Sqrt[-a^4 + 2*a^2*b^2 - b^4 + c^4] + 2*Sqrt[b^2*c^2 - (
-a^2 + b^2 + c^2)^2/4])^2)] + Sqrt[2]*Sqrt[a^4 - b^4 + 2*b^2*c^2 - c^4]*Sqrt[-(((a^4 - b^4 - 2*a^2*c^2 +
 c^4)*(-a^4 + 2*a^2*b^2 - b^4 + 2*a^2*c^2 + 2*b^2*c^2 - c^4 + 2*Sqrt[-a^4 + b^4 + 2*a^2*c^2 - c^4]*
Sqrt[b^2*c^2 - (-a^2 + b^2 + c^2)^2/4]))/(Sqrt[-a^4 + b^4 + 2*a^2*c^2 - c^4] + Sqrt[a^4 - b^4 + 2*b^2*
c^2 - c^4] + Sqrt[-a^4 + 2*a^2*b^2 - b^4 + c^4] + 2*Sqrt[b^2*c^2 - (-a^2 + b^2 + c^2)^2/4])^2)] +
 Sqrt[2]*Sqrt[-a^4 + 2*a^2*b^2 - b^4 + c^4]*Sqrt[-(((a^4 - b^4 - 2*a^2*c^2 + c^4)*(-a^4 + 2*a^2*b^2 -
 b^4 + 2*a^2*c^2 + 2*b^2*c^2 - c^4 + 2*Sqrt[-a^4 + b^4 + 2*a^2*c^2 - c^4]*Sqrt[b^2*c^2 - (-a^2 + b^2 +
 c^2)^2/4]))/(Sqrt[-a^4 + b^4 + 2*a^2*c^2 - c^4] + Sqrt[a^4 - b^4 + 2*b^2*c^2 - c^4] + Sqrt[-a^4 + 2*
a^2*b^2 - b^4 + c^4] + 2*Sqrt[b^2*c^2 - (-a^2 + b^2 + c^2)^2/4])^2)] + 2*Sqrt[2]*Sqrt[b^2*c^2 - (-a^2 +
 b^2 + c^2)^2/4]*Sqrt[-(((a^4 - b^4 - 2*a^2*c^2 + c^4)*(-a^4 + 2*a^2*b^2 - b^4 + 2*a^2*c^2 + 2*b^2*c^2 -
 c^4 + 2*Sqrt[-a^4 + b^4 + 2*a^2*c^2 - c^4]*Sqrt[b^2*c^2 - (-a^2 + b^2 + c^2)^2/4]))/(Sqrt[-a^4 + b^4 +
 2*a^2*c^2 - c^4] + Sqrt[a^4 - b^4 + 2*b^2*c^2 - c^4] + Sqrt[-a^4 + 2*a^2*b^2 - b^4 + c^4] + 2*Sqrt[b^2*
c^2 - (-a^2 + b^2 + c^2)^2/4])^2)])/((Sqrt[-a^4 + b^4 + 2*a^2*c^2 - c^4] + Sqrt[a^4 - b^4 + 2*b^2*c^2 -
 c^4] + Sqrt[-a^4 + 2*a^2*b^2 - b^4 + c^4] + 2*Sqrt[b^2*c^2 - (-a^2 + b^2 + c^2)^2/4])*(2*Sqrt[b^2*c^2 -
 (-a^2 + b^2 + c^2)^2/4] + Sqrt[2]*Sqrt[-(((a^4 - b^4 - 2*a^2*c^2 + c^4)*(-a^4 + 2*a^2*b^2 - b^4 + 2*
a^2*c^2 + 2*b^2*c^2 - c^4 + 2*Sqrt[-a^4 + b^4 + 2*a^2*c^2 - c^4]*Sqrt[b^2*c^2 - (-a^2 + b^2 + c^2)^2/4])
)/(Sqrt[-a^4 + b^4 + 2*a^2*c^2 - c^4] + Sqrt[a^4 - b^4 + 2*b^2*c^2 - c^4] + Sqrt[-a^4 + 2*a^2*b^2 -
 b^4 + c^4] + 2*Sqrt[b^2*c^2 - (-a^2 + b^2 + c^2)^2/4])^2)] + Sqrt[2]*Sqrt[((a^4 - b^4 + 2*b^2*c^2 -
 c^4)*(-a^4 + 2*a^2*b^2 - b^4 + 2*a^2*c^2 + 2*b^2*c^2 - c^4 + 2*Sqrt[a^4 - b^4 + 2*b^2*c^2 - c^4]*
Sqrt[b^2*c^2 - (-a^2 + b^2 + c^2)^2/4]))/(Sqrt[-a^4 + b^4 + 2*a^2*c^2 - c^4] + Sqrt[a^4 - b^4 + 2*b^2*
c^2 - c^4] + Sqrt[-a^4 + 2*a^2*b^2 - b^4 + c^4] + 2*Sqrt[b^2*c^2 - (-a^2 + b^2 + c^2)^2/4])^2] +
 Sqrt[2]*Sqrt[-(((a^4 - 2*a^2*b^2 + b^4 - c^4)*(-a^4 + 2*a^2*b^2 - b^4 + 2*a^2*c^2 + 2*b^2*c^2 - c^4 +
 2*Sqrt[-a^4 + 2*a^2*b^2 - b^4 + c^4]*Sqrt[b^2*c^2 - (-a^2 + b^2 + c^2)^2/4]))/(Sqrt[-a^4 + b^4 + 2*a^2*
c^2 - c^4] + Sqrt[a^4 - b^4 + 2*b^2*c^2 - c^4] + Sqrt[-a^4 + 2*a^2*b^2 - b^4 + c^4] + 2*Sqrt[b^2*c^2 - (
-a^2 + b^2 + c^2)^2/4])^2)])), (-a^4 + 2*a^2*b^2 - b^4 + c^4 + 2*Sqrt[-a^4 + 2*a^2*b^2 - b^4 + c^4]*
Sqrt[b^2*c^2 - (-a^2 + b^2 + c^2)^2/4] + Sqrt[2]*Sqrt[-a^4 + b^4 + 2*a^2*c^2 - c^4]*Sqrt[-(((a^4 - 2*
a^2*b^2 + b^4 - c^4)*(-a^4 + 2*a^2*b^2 - b^4 + 2*a^2*c^2 + 2*b^2*c^2 - c^4 + 2*Sqrt[-a^4 + 2*a^2*b^2 -
 b^4 + c^4]*Sqrt[b^2*c^2 - (-a^2 + b^2 + c^2)^2/4]))/(Sqrt[-a^4 + b^4 + 2*a^2*c^2 - c^4] + Sqrt[a^4 -
 b^4 + 2*b^2*c^2 - c^4] + Sqrt[-a^4 + 2*a^2*b^2 - b^4 + c^4] + 2*Sqrt[b^2*c^2 - (-a^2 + b^2 + c^2)^2/4])
^2)] + Sqrt[2]*Sqrt[a^4 - b^4 + 2*b^2*c^2 - c^4]*Sqrt[-(((a^4 - 2*a^2*b^2 + b^4 - c^4)*(-a^4 + 2*a^2*
b^2 - b^4 + 2*a^2*c^2 + 2*b^2*c^2 - c^4 + 2*Sqrt[-a^4 + 2*a^2*b^2 - b^4 + c^4]*Sqrt[b^2*c^2 - (-a^2 +
 b^2 + c^2)^2/4]))/(Sqrt[-a^4 + b^4 + 2*a^2*c^2 - c^4] + Sqrt[a^4 - b^4 + 2*b^2*c^2 - c^4] + Sqrt[-a^4 +
 2*a^2*b^2 - b^4 + c^4] + 2*Sqrt[b^2*c^2 - (-a^2 + b^2 + c^2)^2/4])^2)] + Sqrt[2]*Sqrt[-a^4 + 2*a^2*
b^2 - b^4 + c^4]*Sqrt[-(((a^4 - 2*a^2*b^2 + b^4 - c^4)*(-a^4 + 2*a^2*b^2 - b^4 + 2*a^2*c^2 + 2*b^2*c^2 -
 c^4 + 2*Sqrt[-a^4 + 2*a^2*b^2 - b^4 + c^4]*Sqrt[b^2*c^2 - (-a^2 + b^2 + c^2)^2/4]))/(Sqrt[-a^4 + b^4 +
 2*a^2*c^2 - c^4] + Sqrt[a^4 - b^4 + 2*b^2*c^2 - c^4] + Sqrt[-a^4 + 2*a^2*b^2 - b^4 + c^4] + 2*Sqrt[b^2*
c^2 - (-a^2 + b^2 + c^2)^2/4])^2)] + 2*Sqrt[2]*Sqrt[b^2*c^2 - (-a^2 + b^2 + c^2)^2/4]*Sqrt[-(((a^4 - 2*
a^2*b^2 + b^4 - c^4)*(-a^4 + 2*a^2*b^2 - b^4 + 2*a^2*c^2 + 2*b^2*c^2 - c^4 + 2*Sqrt[-a^4 + 2*a^2*b^2 -
 b^4 + c^4]*Sqrt[b^2*c^2 - (-a^2 + b^2 + c^2)^2/4]))/(Sqrt[-a^4 + b^4 + 2*a^2*c^2 - c^4] + Sqrt[a^4 -
 b^4 + 2*b^2*c^2 - c^4] + Sqrt[-a^4 + 2*a^2*b^2 - b^4 + c^4] + 2*Sqrt[b^2*c^2 - (-a^2 + b^2 + c^2)^2/4])
^2)])/((Sqrt[-a^4 + b^4 + 2*a^2*c^2 - c^4] + Sqrt[a^4 - b^4 + 2*b^2*c^2 - c^4] + Sqrt[-a^4 + 2*a^2*b^2 -
 b^4 + c^4] + 2*Sqrt[b^2*c^2 - (-a^2 + b^2 + c^2)^2/4])*(2*Sqrt[b^2*c^2 - (-a^2 + b^2 + c^2)^2/4] +
 Sqrt[2]*Sqrt[-(((a^4 - b^4 - 2*a^2*c^2 + c^4)*(-a^4 + 2*a^2*b^2 - b^4 + 2*a^2*c^2 + 2*b^2*c^2 - c^4 +
 2*Sqrt[-a^4 + b^4 + 2*a^2*c^2 - c^4]*Sqrt[b^2*c^2 - (-a^2 + b^2 + c^2)^2/4]))/(Sqrt[-a^4 + b^4 + 2*a^2*
c^2 - c^4] + Sqrt[a^4 - b^4 + 2*b^2*c^2 - c^4] + Sqrt[-a^4 + 2*a^2*b^2 - b^4 + c^4] + 2*Sqrt[b^2*c^2 - (
-a^2 + b^2 + c^2)^2/4])^2)] + Sqrt[2]*Sqrt[((a^4 - b^4 + 2*b^2*c^2 - c^4)*(-a^4 + 2*a^2*b^2 - b^4 + 2*
a^2*c^2 + 2*b^2*c^2 - c^4 + 2*Sqrt[a^4 - b^4 + 2*b^2*c^2 - c^4]*Sqrt[b^2*c^2 - (-a^2 + b^2 + c^2)^2/4]))
/(Sqrt[-a^4 + b^4 + 2*a^2*c^2 - c^4] + Sqrt[a^4 - b^4 + 2*b^2*c^2 - c^4] + Sqrt[-a^4 + 2*a^2*b^2 - b^4 +
 c^4] + 2*Sqrt[b^2*c^2 - (-a^2 + b^2 + c^2)^2/4])^2] + Sqrt[2]*Sqrt[-(((a^4 - 2*a^2*b^2 + b^4 - c^4)*(-
a^4 + 2*a^2*b^2 - b^4 + 2*a^2*c^2 + 2*b^2*c^2 - c^4 + 2*Sqrt[-a^4 + 2*a^2*b^2 - b^4 + c^4]*Sqrt[b^2*
c^2 - (-a^2 + b^2 + c^2)^2/4]))/(Sqrt[-a^4 + b^4 + 2*a^2*c^2 - c^4] + Sqrt[a^4 - b^4 + 2*b^2*c^2 -
 c^4] + Sqrt[-a^4 + 2*a^2*b^2 - b^4 + c^4] + 2*Sqrt[b^2*c^2 - (-a^2 + b^2 + c^2)^2/4])^2)]))}
```

Invariant height

```
((-a^4 + 2*a^2*b^2 - b^4 + 2*a^2*c^2 + 2*b^2*c^2 - c^4)*Sqrt[p^2/4 - (r + 2*R)^2])/((Sqrt[-a^4 + b^4 +
 2*a^2*c^2 - c^4] + Sqrt[a^4 - b^4 + 2*b^2*c^2 - c^4] + Sqrt[-a^4 + 2*a^2*b^2 - b^4 + c^4] + 2*Sqrt[b^2*
c^2 - (-a^2 + b^2 + c^2)^2/4])*(2*Sqrt[b^2*c^2 - (-a^2 + b^2 + c^2)^2/4] + Sqrt[2]*Sqrt[-(((a^4 - b^4 -
 2*a^2*c^2 + c^4)*(-a^4 + 2*a^2*b^2 - b^4 + 2*a^2*c^2 + 2*b^2*c^2 - c^4 + 2*Sqrt[-a^4 + b^4 + 2*a^2*
c^2 - c^4]*Sqrt[b^2*c^2 - (-a^2 + b^2 + c^2)^2/4]))/(Sqrt[-a^4 + b^4 + 2*a^2*c^2 - c^4] + Sqrt[a^4 -
 b^4 + 2*b^2*c^2 - c^4] + Sqrt[-a^4 + 2*a^2*b^2 - b^4 + c^4] + 2*Sqrt[b^2*c^2 - (-a^2 + b^2 + c^2)^2/4])
^2)] + Sqrt[2]*Sqrt[((a^4 - b^4 + 2*b^2*c^2 - c^4)*(-a^4 + 2*a^2*b^2 - b^4 + 2*a^2*c^2 + 2*b^2*c^2 -
 c^4 + 2*Sqrt[a^4 - b^4 + 2*b^2*c^2 - c^4]*Sqrt[b^2*c^2 - (-a^2 + b^2 + c^2)^2/4]))/(Sqrt[-a^4 + b^4 +
 2*a^2*c^2 - c^4] + Sqrt[a^4 - b^4 + 2*b^2*c^2 - c^4] + Sqrt[-a^4 + 2*a^2*b^2 - b^4 + c^4] + 2*Sqrt[b^2*
c^2 - (-a^2 + b^2 + c^2)^2/4])^2] + Sqrt[2]*Sqrt[-(((a^4 - 2*a^2*b^2 + b^4 - c^4)*(-a^4 + 2*a^2*b^2 -
 b^4 + 2*a^2*c^2 + 2*b^2*c^2 - c^4 + 2*Sqrt[-a^4 + 2*a^2*b^2 - b^4 + c^4]*Sqrt[b^2*c^2 - (-a^2 + b^2 +
 c^2)^2/4]))/(Sqrt[-a^4 + b^4 + 2*a^2*c^2 - c^4] + Sqrt[a^4 - b^4 + 2*b^2*c^2 - c^4] + Sqrt[-a^4 + 2*
a^2*b^2 - b^4 + c^4] + 2*Sqrt[b^2*c^2 - (-a^2 + b^2 + c^2)^2/4])^2)]))
```

6-9-13: barycentrics 0.07593768+0.32089707i : 0.06007805+0.47009699i : 0.86398426-0.79099406i; absolute trilinears 0.599005+2.531270i : 0.315935+2.472117i : 3.145477-2.879744i; h =0.798085+0.871730i.
13-20-21: barycentrics 0.17125857 : 0.34860262 : 0.48013881; absolute trilinears 3.319781 : 4.392393 : 5.761666; h =1.062930.

Chapter 7

Optimization-candidate numerical table

The optimization entries are computed independently of the cascade ranking. Barycentrics are normalized; heights use the same length unit as the base sides. EVS, CVS and IVS use their exact stationary formulas (**EXACT CAS**); ERS, DGS and NFIS are numerical minimizers (**NUMERICAL**). This table does not certify global uniqueness.

Star	triangle	foot barycentrics	height
EVS	6-9-13	`0.859821429 : 1.120982143 : -0.980803571`	5.666627276
CVS	6-9-13	`0.859821429 : 1.120982143 : -0.980803571`	10.488131047
IVS	6-9-13	`0.214285729 : 0.321428587 : 0.464285684`	4.780914472
ERS	6-9-13	`0.461423004 : 0.500868966 : 0.037708030`	8.549117039
DGS	6-9-13	`0.054388683 : 0.359105998 : 0.586505319`	3.246163192
NFIS	6-9-13	`0.046456601 : 0.097068207 : 0.856475191`	2.040352593
EVS	13-20-21	`0.447089947 : 0.330687831 : 0.222222222`	14.374939613
CVS	13-20-21	`0.447089947 : 0.330687831 : 0.222222222`	15.320646926
IVS	13-20-21	`0.240740739 : 0.370370381 : 0.388888879`	13.199326336
ERS	13-20-21	`0.379786801 : 0.327752527 : 0.292460672`	14.802912945
DGS	13-20-21	`0.130131268 : 0.405277486 : 0.464591247`	11.897723960
NFIS	13-20-21	`0.115502606 : 0.395527312 : 0.488970082`	11.341753314

For any apex with normalized foot barycentrics λ_i and lateral face areas F_a, F_b, F_c, the projected tetrahedral centers used in the audit are

$$g_i = \frac{1+\lambda_i}{4}, \qquad \iota_i = \frac{F_i + \Delta\lambda_i}{F_a + F_b + F_c + \Delta}.$$

Here g is the foot of the tetrahedral centroid and ι the foot of the tetrahedral incenter. The foot of the tetrahedral circumcenter is always the base circumcenter $X(3)$, because subtracting the equations $|O - A|^2 = |O - D|^2$ etc. leaves the planar circumcenter equations.

Chapter 8

Reproduction of ETC centers by the Star Cascade

This chapter asks how much of Kimberling's *Encyclopedia of Triangle Centers* (ETC) is recovered by the low-index Triangle Sky. A star contributes planar centers in two fundamentally different ways: directly through its orthogonal foot, and relationally through the trace of a line joining two apices. The second mechanism is much richer. It turns the Triangle Sky into an incidence geometry above the reference triangle rather than merely a list of spatial lifts of already-known centers.

The numerical audit uses the searchable July 2026 ETC snapshot containing 72,486 entries [2]. All statements called *matches* below are projective numerical fingerprints on the generic scalene 6–9–13 triangle, using the three cyclic ETC search tables and tolerance

$$\varepsilon = 10^{-9}.$$

They are strong discovery evidence, but a single-triangle numerical match is not a symbolic identity. Where a candidate formula is available, the 13–20–21 triangle is used as an independent control; several additional generic controls and a symbolic projective identity are still required before an ETC submission. The distinction is especially important for complex coordinates and for the Euler-line census. Every match and non-match in this chapter therefore has **DATABASE AUDIT** status unless explicitly promoted by an exact identity.

8.1 Catalogue universe and counting conventions

The audit contains every consolidated star of effective index at most 5:

$$\text{167 constructive cascade stars} \quad + \quad \text{6 optimization-star candidates} \quad = \quad \text{173 stars.}$$

The optimization candidates are IVS, DGS, ERS, EVS, NFIS and CVS. They are included as computational entries without asserting global uniqueness. A consolidated star is counted once regardless of how many geometrically independent definitions lead to it. Thus the number of unordered pairs of distinct stars is

$$\binom{173}{2} = 14{,}878.$$

For a star S_i with selected apex D_i, let

$$F_i = \operatorname{foot}(D_i)$$

be its orthogonal projection to the plane $\Pi = \operatorname{plane}(ABC)$. Two trace families are studied.

Definition 8.1 (Ordinary and cross-conjugate traces)**.** For distinct stars S_i, S_j, define

$$T_{ij} = \operatorname{Tr}(S_i, S_j) = D_iD_j \cap \Pi,$$
$$T_{i\bar{j}} = \operatorname{Tr}(S_i, \overline{S_j}) = D_i\overline{D_j} \cap \Pi,$$

whenever the indicated line has a unique finite intersection with Π. The bar denotes the opposite/conjugate branch of the star.

If Π is represented by $z = 0$, $D_i = (x_i, y_i, z_i)$ and $D_j = (x_j, y_j, z_j)$, then

$$T_{ij} = D_i - \frac{z_i}{z_j - z_i}(D_j - D_i), \qquad z_i \neq z_j.$$

8.2 ETC matching protocol

For a finite point with trilinears $x : y : z$, the ETC search normalization is

$$k = \frac{2\Delta}{ax + by + cz}, \qquad (x : y : z) \longmapsto (kx, ky, kz).$$

These are the signed perpendicular distances from the point to the three sidelines. A real candidate is accepted in the numerical audit when its normalized triple agrees with the same ETC index in the three cyclic tables for $(6, 9, 13)$, $(9, 13, 6)$ and $(13, 6, 9)$.

The ETC convention for a nonreal first trilinear is different: the Search table stores its principal argument. Accordingly, a complex candidate is screened first by $\arg x$ and then checked cyclically through

$$\boxed{(\arg x, \arg y, \arg z) = (T_{6,9,13}(n), T_{9,13,6}(n), T_{13,6,9}(n)).}$$

Comparing only the phase differences $\arg y - \arg x$ and $\arg z - \arg x$ is invariant under an arbitrary common complex phase, but is too permissive for the representative convention used by the ETC tables. Phase-difference matches are therefore retained only as provisional diagnostics; they are not counted in the real ETC frequencies.

8.3 ETC centers occurring as star feet

The *foot frequency* of $X(n)$ is the number of consolidated stars whose foot is identified with $X(n)$. Among the 173 stars, 77 have ETC-matched feet, representing 25 distinct ETC centers. Thus

$$\frac{77}{173} \approx 44.5\%$$

of the audited stars have an ETC-recognized foot.

Table 8.1: Complete ETC foot-frequency list for the index-≤ 5 catalogue.

ETC center	frequency
$X(3)$	9
$X(2)$	7
$X(140)$	7
$X(12100)$	7
$X(13624)$	7
$X(1125)$	5
$X(5)$	4
$X(548)$	4
$X(8703)$	4
$X(50828)$	4
$X(5066)$	3
$X(9955)$	3

ETC center	frequency
$X(1)$	1
$X(4)$	1
$X(20)$	1
$X(546)$	1
$X(550)$	1
$X(631)$	1
$X(3091)$	1
$X(3628)$	1
$X(10304)$	1
$X(15690)$	1
$X(16239)$	1
$X(50802)$	1
$X(61877)$	1

The optimization-star candidates contribute

$$F_{\mathrm{IVS}} = X(1), \qquad F_{\mathrm{EVS}} = F_{\mathrm{CVS}} = X(3).$$

DGS, ERS and NFIS have no accepted ETC foot in this audit. The common EVS/CVS foot is geometrically natural: both apices stand above the circumcenter, but their heights and defining optimization principles are different.

8.4 Ordinary traces

The ordinary family examines T_{ij} for every unordered pair of distinct stars. Its complete status partition is

status	number of pairs
finite real trace matching an ETC center	1,591
finite real trace with no ETC match	4,502
finite complex trace, not certified	8,355
no finite trace: joining line parallel to ABC	430
coincident apices	0
total	14,878

The 1,591 matched occurrences represent 371 distinct ETC centers. Among the 6,093 finite real ordinary traces, the match rate is therefore

$$\frac{1{,}591}{6{,}093} \approx 26.1\%.$$

Table 8.2: Most frequent ETC centers produced by ordinary traces.

center	frequency	center	frequency
$X(2)$	111	$X(5066)$	21
$X(3)$	61	$X(8703)$	20
$X(4)$	33	$X(547)$	19
$X(20)$	33	$X(546)$	18
$X(140)$	32	$X(1125)$	18
$X(12100)$	28	$X(3534)$	18
$X(5)$	26	$X(15691)$	17
$X(381)$	25	$X(548)$	15
$X(3845)$	25	$X(549)$	15
$X(13624)$	25	$X(15690)$	15
$X(376)$	23	$X(18483)$	15
$X(550)$	22	$X(50802)$	15

The centroid $X(2)$ is the dominant ordinary trace, occurring for 111 different pairs. The high multiplicities of $X(2)$, $X(3)$, $X(4)$ and $X(20)$ show that the low-index sky contains a dense network of lines through the classical Euler-line centers.

The six optimization-star candidates add 16 matched ordinary traces: 15 occurrences of $X(3)$ and one occurrence of $X(36)$. In particular,

$$\mathrm{Tr}(\mathrm{IVS}, \mathrm{CVS}) = X(36), \qquad \mathrm{Tr}(\mathrm{EVS}, \mathrm{CVS}) = X(3).$$

The second identity follows immediately because EVS and CVS have the same circumcentral foot and different heights.

8.5 Cross-conjugate traces

Cross-conjugate traces have a particularly simple geometric form. Write

$$D_i = F_i + h_i\mathbf{n}, \qquad \overline{D_j} = F_j - h_j\mathbf{n}.$$

Solving for the intersection with the base plane gives

$$\boxed{T_{i\bar{j}} = \frac{h_jF_i + h_iF_j}{h_i + h_j},} \tag{8.1}$$

provided $h_i + h_j \neq 0$. Consequently,

$$T_{i\bar{j}} = T_{j\bar{i}}, \qquad T_{i\bar{i}} = F_i.$$

Both identities were also verified numerically for all catalogue entries. Only $i < j$ is counted; the 173 diagonal cases are omitted because they reproduce the foot experiment exactly.

cross-conjugate status	number of pairs
finite real trace matching an ETC center	1,343
finite real trace with no ETC match	5,131
finite complex trace, not certified	8,404
undefined trace	0
total	14,878

The 1,343 matched occurrences represent 297 distinct ETC centers. Of these, 144 also occur in the ordinary family and 153 are new. Therefore the union of the two trace families contains

$$371 + 297 - 144 = 524$$

distinct ETC centers.

Table 8.3: Most frequent cross-conjugate ETC traces.

center	frequency	Euler?	center	frequency	Euler?
$X(2)$	87	yes	$X(1125)$	25	no
$X(3)$	59	yes	$X(547)$	22	yes
$X(140)$	44	yes	$X(5)$	20	yes
$X(12100)$	36	yes	$X(14891)$	19	yes
$X(549)$	35	yes	$X(34200)$	18	yes
$X(13624)$	28	no	$X(8703)$	17	yes
$X(3530)$	16	yes	$X(50828)$	15	no
$X(10124)$	14	yes	$X(3524)$	13	yes
$X(11812)$	13	yes	$X(548)$	11	yes
$X(11539)$	11	yes	$X(15699)$	11	yes

Equation (8.1) explains why this construction is productive: it makes invariant star heights into coefficients of a natural affine combination of two triangle centers.

8.6 The exceptional concentration on the Euler line

For an ETC triple $(x : y : z)$, the corresponding homogeneous barycentrics are $(ax : by : cz)$. Euler-line membership was tested projectively by

$$\det \begin{pmatrix} ax & by & cz \\ 1 & 1 & 1 \\ O_A & O_B & O_C \end{pmatrix} = 0, \tag{8.2}$$

where $(O_A : O_B : O_C)$ are the barycentrics of the circumcenter. This test also handles the point at infinity $X(30)$.

Table 8.4: Euler-line concentration in the two trace families.

trace family	distinct ETC centers	distinct on Euler line	matched occurrences on Euler line
ordinary	371	260	1,220 of 1,591
cross-conjugate	297	261	1,156 of 1,343
union	524	383	—

Thus 87.9% of the distinct cross-conjugate centers and 86.1% of their matched occurrences lie on the Euler line. In the combined distinct set,

$$\frac{383}{524} \approx 73.1\%$$

are Euler-line centers. This concentration is not mysterious: whenever both F_i and F_j lie on the Euler line, the weighted affine combination in (8.1) lies there as well. Special height ratios can also place the trace on the line even when this sufficient condition is not visibly present in the original definitions.

Applied to all 72,486 ETC triples, the projective test (8.2) finds 7,033 entries numerically on the Euler line for the 6–9–13 triangle. This large list is a numerical candidate census, not a proof that every entry satisfies a universal symbolic Euler-line identity. A second generic table or symbolic substitution into the Euler-line equation is required for certification.

8.7 Complex traces and the corrected argument audit

The complex cases must not be silently discarded, but neither should they be promoted to ETC identities from a phase-only coincidence. The corrected audit uses the ETC's absolute first-argument convention and then checks the remaining two cyclic arguments.

There are 53 complex star feet. Exactly one matches the first-argument search and the complete cyclic argument triple: the foot of ranked star 8 matches the 6–9–13 argument triple for $X(61083)$,

$$(1.649399424050078,\ 1.785348893246411,\ -0.624913472418126).$$

However, this candidate fails the independent acute 13–20–21 control, so it is not accepted as a universal foot identity.

Among the 8,355 complex ordinary traces, twelve incidences match a first ETC argument; all point initially to $X(5374)$. Only one survives both cyclic checks:

$$\mathrm{Tr}(S_4, S_9) \sim X(5374),$$

where

$$S_4 = \mathrm{TSZ}[3], \qquad S_9 = \mathrm{TSY}[1, A, B, C, \mathrm{TSZ}[3]].$$

Its argument triple is

$$(-0.462575660392042,\ -0.462575660392042,\ 1.108220666402855).$$

This is the strongest surviving complex-trace candidate, but it remains numerical until verified on another generic triangle or symbolically.

Among the 8,404 complex cross-conjugate traces, none matches even the first ETC argument at tolerance 10^{-9}. The earlier phase-difference screen had returned eight provisional ordinary candidates involving $X(20034)$, $X(5374)$, $X(62254)$ and $X(62255)$. The absolute ETC convention eliminates all but the single $X(5374)$ candidate above. Accordingly, the thousands of nonreal outputs should be called *complex trace points*, not thousands of identified complex ETC centers.

8.8 ETC power of a star

Foot frequency measures how often a center occurs below stars; trace frequency measures how often it occurs between stars. A complementary statistic measures how strongly an individual star participates in the production of ETC centers.

For a star S, let $\mathcal{I}(S)$ be the multiset of matched incidences from both ordinary and cross-conjugate traces involving S. If an incidence produces the same ETC center as F_S, it is removed for S only. Thus a trace may count for one participant but not for the other.

Definition 8.2 (ETC powers)**.** Define

$$\begin{aligned}
\text{ETC-P1}(S) &= \#\{X(n) : X(n) \text{ occurs in an eligible incidence involving } S\},\\
\text{ETC-P2}(S) &= \#\mathcal{I}(S),
\end{aligned}$$

where ETC-P1 discards multiplicity and ETC-P2 retains it.

There are

$$2(1{,}591 + 1{,}343) = 5{,}868$$

raw participant incidences. Removing 640 own-foot incidences leaves

$$\sum_S \text{ETC-P2}(S) = 5{,}228.$$

Of the 173 stars, 137 have positive ETC power.

Table 8.5: The twenty-five strongest stars, ordered by ETC-P2 and then ETC-P1.

power rank	catalogue rank	index	independent definitions	ETC-P1	ETC-P2	foot in ETC
1	3	1	1	88	123	$X(4)$
2	4	1	13	84	122	$X(3)$
3	1	10/13	5	79	114	$X(5)$
4	82	5	1	90	113	$X(2)$
5	5	5/4	4	83	112	$X(631)$
6	98	5	1	82	107	$X(2)$
7	2	1	1	76	105	$X(20)$
8	10	5/2	2	76	105	$X(5)$
9	11	5/2	2	72	104	$X(3)$
10	14	5/2	2	75	102	$X(2)$
11	107	5	1	80	99	$X(3)$
12	86	5	1	76	98	$X(8703)$
13	6	10/7	2	58	97	$X(140)$
14	36	3	1	58	96	$X(3628)$
15	105	5	1	75	94	$X(8703)$
16	100	5	1	66	93	$X(546)$
17	22	5/2	2	62	93	$X(5)$
18	15	5/2	2	61	91	$X(140)$
19	7	5/3	3	65	90	$X(3091)$
20	83	5	1	75	89	$X(2)$
21	133	5	1	62	88	$X(5)$
22	16	5/2	2	60	87	$X(140)$
23	20	5/2	2	65	85	$X(5066)$
24	129	5	1	65	83	$X(2)$
25	12	5/2	2	60	83	$X(548)$

The maximum ETC-P2 is 123, attained by rank 3, the Orthostar. The maximum ETC-P1 is 90, attained by rank 82. Thus the Orthostar has the largest incidence multiplicity, whereas rank 82 has the greatest diversity of ETC outputs. The primitive CS1, rank 4, is nearly as powerful as the Orthostar and is supported by thirteen independent definitions.

Table 8.6: ETC powers of the six optimization-star candidates.

star	index	definitions	ETC-P1	ETC-P2	foot in ETC
IVS	3/2	1	2	2	$X(1)$
DGS	5/3	1	0	0	no
ERS	7/4	1	0	0	no
EVS	2	1	0	0	$X(3)$
NFIS	2	1	0	0	no
CVS	9/4	1	2	2	$X(3)$

EVS has zero power under this definition because all its matched trace incidences produce $X(3)$, its own foot, and are therefore deliberately removed. Zero power does not mean geometric insignificance; it means that the star produces no *other* ETC center in the present trace universe.

8.9 Repeated centers not found in the ETC

The matched audit answers which ETC centers are reproduced. A complementary question is whether the nominally unmatched feet and traces repeatedly produce the *same* new center. This requires a stricter equivalence test than agreement on the original 6–9–13 triangle.

The present audit combines feet, ordinary traces and cross-conjugate traces. First, the complete directed cyclic trilinear triple is checked against all 72,486 ETC entries at tolerance 10^{-9}. Each surviving finite real point is then evaluated on the three scalene triangles

$$(6, 9, 13), \qquad (13, 20, 21), \qquad (7, 9, 11).$$

Two occurrences are placed in the same class only when their normalized barycentrics coincide on all three triangles. This removes special-triangle coincidences. Of the 29,929 possible foot and trace occurrences, 9,676 are ETC-unmatched, finite and real on all three controls. They contain 702 repeated generic classes and 2,405 occurrences belonging to such classes. The symbols $U_1, U_2, \ldots$ below are local audit labels, not ETC numbers.

The main structural result is unexpectedly simple. Let

$$s = \frac{a+b+c}{2}, \qquad \Phi(a, b, c) = a\left(\frac{1}{s-b} + \frac{1}{s-c} - \frac{1}{s-a}\right).$$

Every one of the twelve most frequent unmatched classes has barycentrics

$$\big(f(a, b, c) : f(b, c, a) : f(c, a, b)\big), \qquad f(a, b, c) = A + B\frac{a}{s} + C\Phi(a, b, c), \tag{8.3}$$

with small primitive integers (A, B, C). These identities were derived from the exact foot functions and the two trace formulas, then verified cyclically; they are not numerical interpolations.

This three-term function has a direct classical interpretation. Write $G = X(2)$, $I = X(1)$ and $L = X(20)$. The normalized first coordinate of L is

$$L_a = -1 + \frac{a}{2s} + \frac{1}{2}\Phi(a, b, c).$$

Since the cyclic sums of 1, a/s and Φ are 3, 2 and 6, put

$$D = 3A + 2B + 6C.$$

Then the point defined by (8.3) is exactly

$$\frac{3(A+2C)}{D}\,G+\frac{2(B-C)}{D}\,I+\frac{2C}{D}\,X(20). \tag{8.4}$$

Thus the leading unmatched centers form a rational affine family generated by three classical centers.

The simplest individual candidate is U_8. Its function reduces to

$$f(a,b,c)=7(a+b+c)+3a,$$

and hence

$$U_8=(7p+3a:7p+3b:7p+3c)=\frac{7}{8}G+\frac{1}{8}I, \qquad p=a+b+c.$$

Its trilinears are obtained by dividing the three barycentrics by a,b,c.

These twelve centers should be presented to the ETC team as one coherent rational affine family, with complete trace provenance. The recommended first tranche is U_8 for its linear function; U_1 and U_2 for their maximal frequency; and U_4, U_5 because all of their 25 and 24 reproductions are cross-conjugate traces, suggesting a particularly clean trace theorem. U_3 and U_6 are equally short algebraically but are affine extrapolations because their $X(20)$ coefficients are negative. Table 8.7 gives the complete leading list.

Table 8.7: Most frequent generic centers absent from the ETC audit. Ordinary and cross denote ordinary and cross-conjugate trace multiplicity.

class	total	foot	ordinary	cross	(A,B,C)	affine description
U_1	27	4	14	9	$(4,-5,-3)$	$\frac{3}{8}G+\frac{1}{4}I+\frac{3}{8}X(20)$
U_2	27	0	9	18	$(16,15,3)$	$\frac{11}{16}G+\frac{1}{4}I+\frac{1}{16}X(20)$
U_3	26	0	14	12	$(20,3,-3)$	$\frac{7}{8}G+\frac{1}{4}I-\frac{1}{8}X(20)$
U_4	25	0	0	25	$(4,15,9)$	$\frac{11}{16}G+\frac{1}{8}I+\frac{3}{16}X(20)$
U_5	24	0	0	24	$(32,21,9)$	$\frac{25}{32}G+\frac{1}{8}I+\frac{3}{32}X(20)$
U_6	20	3	7	10	$(32,9,-3)$	$\frac{13}{16}G+\frac{1}{4}I-\frac{1}{16}X(20)$
U_7	19	0	0	19	$(2,2,1)$	$\frac{3}{4}G+\frac{1}{8}I+\frac{1}{8}X(20)$
U_8	18	0	0	18	$(14,3,0)$	$\frac{7}{8}G+\frac{1}{8}I$
U_9	18	0	7	11	$(2,-6,-3)$	$\frac{1}{2}G+\frac{1}{4}I+\frac{1}{4}X(20)$
U_{10}	17	0	0	17	$(16,-39,-27)$	$\frac{19}{32}G+\frac{1}{8}I+\frac{9}{32}X(20)$
U_{11}	17	0	0	17	$(0,11,7)$	$\frac{21}{32}G+\frac{1}{8}I+\frac{7}{32}X(20)$
U_{12}	16	3	6	7	$(16,-27,-15)$	$\frac{7}{16}G+\frac{1}{4}I+\frac{5}{16}X(20)$

8.10 Interpretation and reproducibility

The final audit supports five numerical conclusions within this dated data set.

1. The foot map numerically recovers a nontrivial classical layer: 77 entries land on 25 ETC centers.
2. Pair traces are substantially richer: the two families together numerically recover 524 distinct ETC centers, 153 of which appear only after conjugation.
3. The Euler line is the dominant planar carrier of the low-index sky: 383 of the 524 recovered trace centers lie on it numerically.
4. ETC-P1 and ETC-P2 distinguish diversity from multiplicity and reveal highly connected stars that are not necessarily the lowest in the original cost ranking.
5. The most frequent classes unmatched in the snapshot are not algebraically wild: the leading twelve form a small rational affine family generated by G, I and $X(20)$.

The complete frequency, pair-provenance, Euler-line and power tables accompany the report as machine-readable files. The principal files are:

- `trace_frequency.csv` and `conjugate_trace_frequency.csv`;
- `matched_trace_pairs.csv` and `matched_conjugate_trace_pairs.csv`;
- `recovered_trace_centers_on_euler_line.csv`;
- `star_etc_power_ranking.csv`.
- `repeated_unmatched_center_classes.csv`;
- `repeated_unmatched_center_occurrences.csv`;
- `repeated_unmatched_center_functions.csv`.

The corresponding Wolfram Language audits are:

```
TriangleSkyCascadeETCCoverage.wl
TriangleSkyConjugateTraceEulerAudit.wl
TriangleSkyETCPowerAudit.wl
TriangleSkyUnmatchedCenterAudit.wl
TriangleSkyUnmatchedFunctionFit.wl
```

The most valuable next step is theorem-level consolidation: prove directly why the repeated classes close inside the affine G–I–$X(20)$ family, submit the leading members to the ETC team with their complete provenance, and characterize the height ratios that force (8.1) onto the Euler line.

Chapter 9

Centers unmatched in the dated ETC audit

The scope of this table is precise: it contains every unmatched candidate that occurs in the thirty catalogue cards or in the apex/incenter/centroid projections discussed for EVS, CVS, ERS, DGS and NFIS. Known centers such as $X(1)$ and $X(3)$ are excluded. "Unmatched" always means that no numerical fingerprint survived the audited July 2026 snapshot; it does not assert mathematical absence from the ETC or establish novelty.

Center	audit status	abs. trilin. 6–9–13	abs. trilin. 13–20–21
Foot of ranked star 8	rejected by acute control	-0.205378+2.607461i : -0.556875+2.555568i : 4.120983-2.972683i	3.150566 : 4.372660 : 5.885212
Foot of ranked star 9	no complex numerical match	4.583215-1.334908i : 3.769486-1.097901i : -1.084310+1.376196i	8.058618 : 4.198434 : 3.012823
Foot of ranked star 24	no numerical match	1.356355 : 0.701752 : 2.528826	5.461538 : 4.325000 : 4.500000
Foot of ranked star 30	no complex numerical match	0.599004+2.531270i : 0.315935+2.472117i : 3.145477-2.879744i	3.319782 : 4.392393 : 5.761666
ERS apex foot	no numerical match	3.639754 : 2.633938 : 0.137282	7.362021 : 4.129682 : 3.509528
DGS apex foot	no numerical match	0.429024 : 1.888444 : 2.135269	2.522545 : 5.106496 : 5.575095
NFIS apex foot	no numerical match	0.366455 : 0.510456 : 3.118139	2.238974 : 4.983644 : 5.867641
Foot of the tetrahedral incenter of the EVS tetrahedron	no numerical match	2.832315 : 2.551521 : 0.567004	5.957756 : 4.478672 : 4.046463
Foot of the tetrahedral incenter of the CVS tetrahedron	no numerical match	2.435083 : 2.264990 : 0.948710	5.884511 : 4.490048 : 4.080971
Foot of the tetrahedral incenter of the ERS tetrahedron	no numerical match	2.076479 : 1.859410 : 1.395006	5.505237 : 4.492243 : 4.313670
Foot of the tetrahedral centroid of the ERS tetrahedron	no numerical match	2.881965 : 1.973169 : 0.944487	6.686659 : 4.182420 : 3.877382
Foot of the tetrahedral incenter of DGS	no numerical match	1.158586 : 1.765667 : 1.883547	3.916028 : 4.814460 : 4.990592
Foot of the tetrahedral centroid of DGS	no numerical match	2.079283 : 1.786795 : 1.443983	5.476790 : 4.426624 : 4.393774
Foot of the tetrahedral incenter of NFIS	no numerical match	0.908112 : 0.972974 : 2.547938	3.787225 : 4.767654 : 5.114905
Foot of the tetrahedral centroid of NFIS	no numerical match	2.063640 : 1.442298 : 1.689701	5.405897 : 4.395911 : 4.466910

9.1 Barycentric center functions

The following formulas are normalized barycentric functions. Long radical functions are intentionally supplied verbatim so the catalogue remains reproducible.

Foot of ranked star 8

Audit: RejectedByAcuteControl.

```
{(-2*a^2*(b^2 + c^2)*Sqrt[a^4 - (b^2 - c^2)^2] + a^4*(-Sqrt[-((a - b - c)*(a + b - c)*(a - b + c)*(a +
 b + c))] + Sqrt[a^4 - (b^2 - c^2)^2]) + (b - c)^2*(b + c)^2*(Sqrt[-((a - b - c)*(a + b - c)*(a - b + c)
*(a + b + c))] + Sqrt[a^4 - (b^2 - c^2)^2]))/((a - b - c)*(a + b - c)*(a - b + c)*(a + b + c)*(Sqrt[-(
a^2 - b^2)^2 + c^4] + Sqrt[b^4 - (a^2 - c^2)^2] + Sqrt[a^4 - (b^2 - c^2)^2] + 2*Sqrt[b^2*c^2 - (-a^2 +
 b^2 + c^2)^2/4])), (a^4*(Sqrt[-((a - b - c)*(a + b - c)*(a - b + c)*(a + b + c))] + Sqrt[b^4 - (a^2 -
 c^2)^2]) + (b - c)*(b + c)*(b^2*(-Sqrt[-((a - b - c)*(a + b - c)*(a - b + c)*(a + b + c))] + Sqrt[b^4 -
 (a^2 - c^2)^2]) - c^2*(Sqrt[-((a - b - c)*(a + b - c)*(a - b + c)*(a + b + c))] + Sqrt[b^4 - (a^2 -
 c^2)^2])) - 2*a^2*(b^2*Sqrt[b^4 - (a^2 - c^2)^2] + c^2*(Sqrt[-((a - b - c)*(a + b - c)*(a - b + c)*(a +
 b + c))] + Sqrt[b^4 - (a^2 - c^2)^2])))/((a - b - c)*(a + b - c)*(a - b + c)*(a + b + c)*(Sqrt[-(a^2 -
 b^2)^2 + c^4] + Sqrt[b^4 - (a^2 - c^2)^2] + Sqrt[a^4 - (b^2 - c^2)^2] + 2*Sqrt[b^2*c^2 - (-a^2 + b^2 +
 c^2)^2/4])), (a^4*(Sqrt[-((a - b - c)*(a + b - c)*(a - b + c)*(a + b + c))] + Sqrt[-(a^2 - b^2)^2 +
 c^4]) - 2*a^2*(c^2*Sqrt[-(a^2 - b^2)^2 + c^4] + b^2*(Sqrt[-((a - b - c)*(a + b - c)*(a - b + c)*(a +
 b + c))] + Sqrt[-(a^2 - b^2)^2 + c^4])) + (b - c)*(b + c)*(c^2*(Sqrt[-((a - b - c)*(a + b - c)*(a - b +
 c)*(a + b + c))] - Sqrt[-(a^2 - b^2)^2 + c^4]) + b^2*(Sqrt[-((a - b - c)*(a + b - c)*(a - b + c)*(a +
 b + c))] + Sqrt[-(a^2 - b^2)^2 + c^4])))/((a - b - c)*(a + b - c)*(a - b + c)*(a + b + c)*(Sqrt[-(a^2 -
 b^2)^2 + c^4] + Sqrt[b^4 - (a^2 - c^2)^2] + Sqrt[a^4 - (b^2 - c^2)^2] + 2*Sqrt[b^2*c^2 - (-a^2 + b^2 +
 c^2)^2/4]))}
```

Foot of ranked star 9

Audit (DATABASE AUDIT): No complex numerical match found in the audited ETC snapshot.

```
{(a*(Sqrt[2]*a^4*Sqrt[-a^2 + b^2 + c^2] + Sqrt[2]*(b^2 - c^2)^2*Sqrt[-a^2 + b^2 + c^2] - 2*Sqrt[2]*a^2*(
b^2 + c^2)*Sqrt[-a^2 + b^2 + c^2] + 2*a^3*Sqrt[-a^4 - (b^2 - c^2)^2 + 2*a^2*(b^2 + c^2)] - 2*a*(b^2 +
 c^2)*Sqrt[-a^4 - (b^2 - c^2)^2 + 2*a^2*(b^2 + c^2)]))/((a^4 + (b^2 - c^2)^2 - 2*a^2*(b^2 + c^2))*(
Sqrt[2]*c*Sqrt[a^2 + b^2 - c^2] + Sqrt[2]*b*Sqrt[a^2 - b^2 + c^2] + Sqrt[2]*a*Sqrt[-a^2 + b^2 + c^2] +
 4*Sqrt[b^2*c^2 - (-a^2 + b^2 + c^2)^2/4])), (b*(Sqrt[2]*a^4*Sqrt[a^2 - b^2 + c^2] - 2*a^2*(Sqrt[2]*b^2*
Sqrt[a^2 - b^2 + c^2] + Sqrt[2]*c^2*Sqrt[a^2 - b^2 + c^2] + b*Sqrt[-a^4 - (b^2 - c^2)^2 + 2*a^2*(b^2 +
 c^2)]) + (b^2 - c^2)*(Sqrt[2]*b^2*Sqrt[a^2 - b^2 + c^2] - Sqrt[2]*c^2*Sqrt[a^2 - b^2 + c^2] + 2*b*
Sqrt[-a^4 - (b^2 - c^2)^2 + 2*a^2*(b^2 + c^2)])))/((a^4 + (b^2 - c^2)^2 - 2*a^2*(b^2 + c^2))*(Sqrt[2]*c*
Sqrt[a^2 + b^2 - c^2] + Sqrt[2]*b*Sqrt[a^2 - b^2 + c^2] + Sqrt[2]*a*Sqrt[-a^2 + b^2 + c^2] + 4*Sqrt[b^2*
c^2 - (-a^2 + b^2 + c^2)^2/4])), (c*(Sqrt[2]*a^4*Sqrt[a^2 + b^2 - c^2] - 2*a^2*(Sqrt[2]*b^2*Sqrt[a^2 +
 b^2 - c^2] + c*(Sqrt[2]*c*Sqrt[a^2 + b^2 - c^2] + Sqrt[-a^4 - (b^2 - c^2)^2 + 2*a^2*(b^2 + c^2)])) + (
b^2 - c^2)*(Sqrt[2]*b^2*Sqrt[a^2 + b^2 - c^2] - c*(Sqrt[2]*c*Sqrt[a^2 + b^2 - c^2] + 2*Sqrt[-a^4 - (
b^2 - c^2)^2 + 2*a^2*(b^2 + c^2)]))))/((a^4 + (b^2 - c^2)^2 - 2*a^2*(b^2 + c^2))*(Sqrt[2]*c*Sqrt[a^2 +
 b^2 - c^2] + Sqrt[2]*b*Sqrt[a^2 - b^2 + c^2] + Sqrt[2]*a*Sqrt[-a^2 + b^2 + c^2] + 4*Sqrt[b^2*c^2 - (-
a^2 + b^2 + c^2)^2/4]))}
```

Foot of ranked star 24

Audit (DATABASE AUDIT): No numerical match found in the audited ETC snapshot.

```
{1/3 + (a*(-(a + b - c)^(-1) - (a - b + c)^(-1) + (-a + b + c)^(-1) + 3/(a + b + c)))/16, 1/3 + (b*((a -
 b - c)^(-1) - (a + b - c)^(-1) + (a - b + c)^(-1) + 3/(a + b + c)))/16, (16 + (3*(a + b))/(a + b - c) +
 (3*(a - b))/(a - b + c) - (3*(a - b))/(-a + b + c) - (9*(a + b))/(a + b + c))/48}
```

Foot of ranked star 30

Audit (DATABASE AUDIT): No complex numerical match found in the audited ETC snapshot.

```
{(a^4 - b^4 + 2*b^2*c^2 - c^4 + 2*Sqrt[a^4 - b^4 + 2*b^2*c^2 - c^4]*Sqrt[b^2*c^2 - (-a^2 + b^2 + c^2)^2/
4] + Sqrt[2]*Sqrt[-a^4 + b^4 + 2*a^2*c^2 - c^4]*Sqrt[((a^4 - b^4 + 2*b^2*c^2 - c^4)*(-a^4 + 2*a^2*b^2 -
 b^4 + 2*a^2*c^2 + 2*b^2*c^2 - c^4 + 2*Sqrt[a^4 - b^4 + 2*b^2*c^2 - c^4]*Sqrt[b^2*c^2 - (-a^2 + b^2 +
 c^2)^2/4]))/(Sqrt[-a^4 + b^4 + 2*a^2*c^2 - c^4] + Sqrt[a^4 - b^4 + 2*b^2*c^2 - c^4] + Sqrt[-a^4 + 2*
a^2*b^2 - b^4 + c^4] + 2*Sqrt[b^2*c^2 - (-a^2 + b^2 + c^2)^2/4])^2] + Sqrt[2]*Sqrt[a^4 - b^4 + 2*b^2*
c^2 - c^4]*Sqrt[((a^4 - b^4 + 2*b^2*c^2 - c^4)*(-a^4 + 2*a^2*b^2 - b^4 + 2*a^2*c^2 + 2*b^2*c^2 - c^4 +
 2*Sqrt[a^4 - b^4 + 2*b^2*c^2 - c^4]*Sqrt[b^2*c^2 - (-a^2 + b^2 + c^2)^2/4]))/(Sqrt[-a^4 + b^4 + 2*a^2*
c^2 - c^4] + Sqrt[a^4 - b^4 + 2*b^2*c^2 - c^4] + Sqrt[-a^4 + 2*a^2*b^2 - b^4 + c^4] + 2*Sqrt[b^2*c^2 - (
-a^2 + b^2 + c^2)^2/4])^2] + Sqrt[2]*Sqrt[-a^4 + 2*a^2*b^2 - b^4 + c^4]*Sqrt[((a^4 - b^4 + 2*b^2*c^2 -
 c^4)*(-a^4 + 2*a^2*b^2 - b^4 + 2*a^2*c^2 + 2*b^2*c^2 - c^4 + 2*Sqrt[a^4 - b^4 + 2*b^2*c^2 - c^4]*
Sqrt[b^2*c^2 - (-a^2 + b^2 + c^2)^2/4]))/(Sqrt[-a^4 + b^4 + 2*a^2*c^2 - c^4] + Sqrt[a^4 - b^4 + 2*b^2*
c^2 - c^4] + Sqrt[-a^4 + 2*a^2*b^2 - b^4 + c^4] + 2*Sqrt[b^2*c^2 - (-a^2 + b^2 + c^2)^2/4])^2] + 2*
Sqrt[2]*Sqrt[b^2*c^2 - (-a^2 + b^2 + c^2)^2/4]*Sqrt[((a^4 - b^4 + 2*b^2*c^2 - c^4)*(-a^4 + 2*a^2*b^2 -
 b^4 + 2*a^2*c^2 + 2*b^2*c^2 - c^4 + 2*Sqrt[a^4 - b^4 + 2*b^2*c^2 - c^4]*Sqrt[b^2*c^2 - (-a^2 + b^2 +
 c^2)^2/4]))/(Sqrt[-a^4 + b^4 + 2*a^2*c^2 - c^4] + Sqrt[a^4 - b^4 + 2*b^2*c^2 - c^4] + Sqrt[-a^4 + 2*
a^2*b^2 - b^4 + c^4] + 2*Sqrt[b^2*c^2 - (-a^2 + b^2 + c^2)^2/4])^2])/((Sqrt[-a^4 + b^4 + 2*a^2*c^2 -
 c^4] + Sqrt[a^4 - b^4 + 2*b^2*c^2 - c^4] + Sqrt[-a^4 + 2*a^2*b^2 - b^4 + c^4] + 2*Sqrt[b^2*c^2 - (-
a^2 + b^2 + c^2)^2/4])*(2*Sqrt[b^2*c^2 - (-a^2 + b^2 + c^2)^2/4] + Sqrt[2]*Sqrt[-(((a^4 - b^4 - 2*a^2*
c^2 + c^4)*(-a^4 + 2*a^2*b^2 - b^4 + 2*a^2*c^2 + 2*b^2*c^2 - c^4 + 2*Sqrt[-a^4 + b^4 + 2*a^2*c^2 - c^4]*
Sqrt[b^2*c^2 - (-a^2 + b^2 + c^2)^2/4]))/(Sqrt[-a^4 + b^4 + 2*a^2*c^2 - c^4] + Sqrt[a^4 - b^4 + 2*b^2*
c^2 - c^4] + Sqrt[-a^4 + 2*a^2*b^2 - b^4 + c^4] + 2*Sqrt[b^2*c^2 - (-a^2 + b^2 + c^2)^2/4])^2)] +
 Sqrt[2]*Sqrt[((a^4 - b^4 + 2*b^2*c^2 - c^4)*(-a^4 + 2*a^2*b^2 - b^4 + 2*a^2*c^2 + 2*b^2*c^2 - c^4 + 2*
Sqrt[a^4 - b^4 + 2*b^2*c^2 - c^4]*Sqrt[b^2*c^2 - (-a^2 + b^2 + c^2)^2/4]))/(Sqrt[-a^4 + b^4 + 2*a^2*
c^2 - c^4] + Sqrt[a^4 - b^4 + 2*b^2*c^2 - c^4] + Sqrt[-a^4 + 2*a^2*b^2 - b^4 + c^4] + 2*Sqrt[b^2*c^2 - (
-a^2 + b^2 + c^2)^2/4])^2] + Sqrt[2]*Sqrt[-(((a^4 - 2*a^2*b^2 + b^4 - c^4)*(-a^4 + 2*a^2*b^2 - b^4 + 2*
a^2*c^2 + 2*b^2*c^2 - c^4 + 2*Sqrt[-a^4 + 2*a^2*b^2 - b^4 + c^4]*Sqrt[b^2*c^2 - (-a^2 + b^2 + c^2)^2/4])
)/(Sqrt[-a^4 + b^4 + 2*a^2*c^2 - c^4] + Sqrt[a^4 - b^4 + 2*b^2*c^2 - c^4] + Sqrt[-a^4 + 2*a^2*b^2 -
```

```
 b^4 + c^4] + 2*Sqrt[b^2*c^2 - (-a^2 + b^2 + c^2)^2/4])^2)])), (-a^4 + b^4 + 2*a^2*c^2 - c^4 + 2*Sqrt[-
a^4 + b^4 + 2*a^2*c^2 - c^4]*Sqrt[b^2*c^2 - (-a^2 + b^2 + c^2)^2/4] + Sqrt[2]*Sqrt[-a^4 + b^4 + 2*a^2*
c^2 - c^4]*Sqrt[-(((a^4 - b^4 - 2*a^2*c^2 + c^4)*(-a^4 + 2*a^2*b^2 - b^4 + 2*a^2*c^2 + 2*b^2*c^2 - c^4 +
 2*Sqrt[-a^4 + b^4 + 2*a^2*c^2 - c^4]*Sqrt[b^2*c^2 - (-a^2 + b^2 + c^2)^2/4]))/(Sqrt[-a^4 + b^4 + 2*a^2*
c^2 - c^4] + Sqrt[a^4 - b^4 + 2*b^2*c^2 - c^4] + Sqrt[-a^4 + 2*a^2*b^2 - b^4 + c^4] + 2*Sqrt[b^2*c^2 - (
-a^2 + b^2 + c^2)^2/4])^2)] + Sqrt[2]*Sqrt[a^4 - b^4 + 2*b^2*c^2 - c^4]*Sqrt[-(((a^4 - b^4 - 2*a^2*c^2 +
 c^4)*(-a^4 + 2*a^2*b^2 - b^4 + 2*a^2*c^2 + 2*b^2*c^2 - c^4 + 2*Sqrt[-a^4 + b^4 + 2*a^2*c^2 - c^4]*
Sqrt[b^2*c^2 - (-a^2 + b^2 + c^2)^2/4]))/(Sqrt[-a^4 + b^4 + 2*a^2*c^2 - c^4] + Sqrt[a^4 - b^4 + 2*b^2*
c^2 - c^4] + Sqrt[-a^4 + 2*a^2*b^2 - b^4 + c^4] + 2*Sqrt[b^2*c^2 - (-a^2 + b^2 + c^2)^2/4])^2)] +
 Sqrt[2]*Sqrt[-a^4 + 2*a^2*b^2 - b^4 + c^4]*Sqrt[-(((a^4 - b^4 - 2*a^2*c^2 + c^4)*(-a^4 + 2*a^2*b^2 -
 b^4 + 2*a^2*c^2 + 2*b^2*c^2 - c^4 + 2*Sqrt[-a^4 + b^4 + 2*a^2*c^2 - c^4]*Sqrt[b^2*c^2 - (-a^2 + b^2 +
 c^2)^2/4]))/(Sqrt[-a^4 + b^4 + 2*a^2*c^2 - c^4] + Sqrt[a^4 - b^4 + 2*b^2*c^2 - c^4] + Sqrt[-a^4 + 2*
a^2*b^2 - b^4 + c^4] + 2*Sqrt[b^2*c^2 - (-a^2 + b^2 + c^2)^2/4])^2)] + 2*Sqrt[2]*Sqrt[b^2*c^2 - (-a^2 +
 b^2 + c^2)^2/4]*Sqrt[-(((a^4 - b^4 - 2*a^2*c^2 + c^4)*(-a^4 + 2*a^2*b^2 - b^4 + 2*a^2*c^2 + 2*b^2*c^2 -
 c^4 + 2*Sqrt[-a^4 + b^4 + 2*a^2*c^2 - c^4]*Sqrt[b^2*c^2 - (-a^2 + b^2 + c^2)^2/4]))/(Sqrt[-a^4 + b^4 +
 2*a^2*c^2 - c^4] + Sqrt[a^4 - b^4 + 2*b^2*c^2 - c^4] + Sqrt[-a^4 + 2*a^2*b^2 - b^4 + c^4] + 2*Sqrt[b^2*
c^2 - (-a^2 + b^2 + c^2)^2/4])^2)])/((Sqrt[-a^4 + b^4 + 2*a^2*c^2 - c^4] + Sqrt[a^4 - b^4 + 2*b^2*c^2 -
 c^4] + Sqrt[-a^4 + 2*a^2*b^2 - b^4 + c^4] + 2*Sqrt[b^2*c^2 - (-a^2 + b^2 + c^2)^2/4])*(2*Sqrt[b^2*c^2 -
 (-a^2 + b^2 + c^2)^2/4] + Sqrt[2]*Sqrt[-(((a^4 - b^4 - 2*a^2*c^2 + c^4)*(-a^4 + 2*a^2*b^2 - b^4 + 2*
a^2*c^2 + 2*b^2*c^2 - c^4 + 2*Sqrt[-a^4 + b^4 + 2*a^2*c^2 - c^4]*Sqrt[b^2*c^2 - (-a^2 + b^2 + c^2)^2/4])
)/(Sqrt[-a^4 + b^4 + 2*a^2*c^2 - c^4] + Sqrt[a^4 - b^4 + 2*b^2*c^2 - c^4] + Sqrt[-a^4 + 2*a^2*b^2 -
 b^4 + c^4] + 2*Sqrt[b^2*c^2 - (-a^2 + b^2 + c^2)^2/4])^2)] + Sqrt[2]*Sqrt[((a^4 - b^4 + 2*b^2*c^2 -
 c^4)*(-a^4 + 2*a^2*b^2 - b^4 + 2*a^2*c^2 + 2*b^2*c^2 - c^4 + 2*Sqrt[a^4 - b^4 + 2*b^2*c^2 - c^4]*
Sqrt[b^2*c^2 - (-a^2 + b^2 + c^2)^2/4]))/(Sqrt[-a^4 + b^4 + 2*a^2*c^2 - c^4] + Sqrt[a^4 - b^4 + 2*b^2*
c^2 - c^4] + Sqrt[-a^4 + 2*a^2*b^2 - b^4 + c^4] + 2*Sqrt[b^2*c^2 - (-a^2 + b^2 + c^2)^2/4])^2] +
 Sqrt[2]*Sqrt[-(((a^4 - 2*a^2*b^2 + b^4 - c^4)*(-a^4 + 2*a^2*b^2 - b^4 + 2*a^2*c^2 + 2*b^2*c^2 - c^4 +
 2*Sqrt[-a^4 + 2*a^2*b^2 - b^4 + c^4]*Sqrt[b^2*c^2 - (-a^2 + b^2 + c^2)^2/4]))/(Sqrt[-a^4 + b^4 + 2*a^2*
c^2 - c^4] + Sqrt[a^4 - b^4 + 2*b^2*c^2 - c^4] + Sqrt[-a^4 + 2*a^2*b^2 - b^4 + c^4] + 2*Sqrt[b^2*c^2 - (
-a^2 + b^2 + c^2)^2/4])^2)])), (-a^4 + 2*a^2*b^2 - b^4 + c^4 + 2*Sqrt[-a^4 + 2*a^2*b^2 - b^4 + c^4]*
Sqrt[b^2*c^2 - (-a^2 + b^2 + c^2)^2/4] + Sqrt[2]*Sqrt[-a^4 + b^4 + 2*a^2*c^2 - c^4]*Sqrt[-(((a^4 - 2*
a^2*b^2 + b^4 - c^4)*(-a^4 + 2*a^2*b^2 - b^4 + 2*a^2*c^2 + 2*b^2*c^2 - c^4 + 2*Sqrt[-a^4 + 2*a^2*b^2 -
 b^4 + c^4]*Sqrt[b^2*c^2 - (-a^2 + b^2 + c^2)^2/4]))/(Sqrt[-a^4 + b^4 + 2*a^2*c^2 - c^4] + Sqrt[a^4 -
 b^4 + 2*b^2*c^2 - c^4] + Sqrt[-a^4 + 2*a^2*b^2 - b^4 + c^4] + 2*Sqrt[b^2*c^2 - (-a^2 + b^2 + c^2)^2/4])
^2)] + Sqrt[2]*Sqrt[a^4 - b^4 + 2*b^2*c^2 - c^4]*Sqrt[-(((a^4 - 2*a^2*b^2 + b^4 - c^4)*(-a^4 + 2*a^2*
b^2 - b^4 + 2*a^2*c^2 + 2*b^2*c^2 - c^4 + 2*Sqrt[-a^4 + 2*a^2*b^2 - b^4 + c^4]*Sqrt[b^2*c^2 - (-a^2 +
 b^2 + c^2)^2/4]))/(Sqrt[-a^4 + b^4 + 2*a^2*c^2 - c^4] + Sqrt[a^4 - b^4 + 2*b^2*c^2 - c^4] + Sqrt[-a^4 +
 2*a^2*b^2 - b^4 + c^4] + 2*Sqrt[b^2*c^2 - (-a^2 + b^2 + c^2)^2/4])^2)] + Sqrt[2]*Sqrt[-a^4 + 2*a^2*
b^2 - b^4 + c^4]*Sqrt[-(((a^4 - 2*a^2*b^2 + b^4 - c^4)*(-a^4 + 2*a^2*b^2 - b^4 + 2*a^2*c^2 + 2*b^2*c^2 -
 c^4 + 2*Sqrt[-a^4 + 2*a^2*b^2 - b^4 + c^4]*Sqrt[b^2*c^2 - (-a^2 + b^2 + c^2)^2/4]))/(Sqrt[-a^4 + b^4 +
 2*a^2*c^2 - c^4] + Sqrt[a^4 - b^4 + 2*b^2*c^2 - c^4] + Sqrt[-a^4 + 2*a^2*b^2 - b^4 + c^4] + 2*Sqrt[b^2*
c^2 - (-a^2 + b^2 + c^2)^2/4])^2)] + 2*Sqrt[2]*Sqrt[b^2*c^2 - (-a^2 + b^2 + c^2)^2/4]*Sqrt[-(((a^4 - 2*
a^2*b^2 + b^4 - c^4)*(-a^4 + 2*a^2*b^2 - b^4 + 2*a^2*c^2 + 2*b^2*c^2 - c^4 + 2*Sqrt[-a^4 + 2*a^2*b^2 -
 b^4 + c^4]*Sqrt[b^2*c^2 - (-a^2 + b^2 + c^2)^2/4]))/(Sqrt[-a^4 + b^4 + 2*a^2*c^2 - c^4] + Sqrt[a^4 -
 b^4 + 2*b^2*c^2 - c^4] + Sqrt[-a^4 + 2*a^2*b^2 - b^4 + c^4] + 2*Sqrt[b^2*c^2 - (-a^2 + b^2 + c^2)^2/4])
^2)])/((Sqrt[-a^4 + b^4 + 2*a^2*c^2 - c^4] + Sqrt[a^4 - b^4 + 2*b^2*c^2 - c^4] + Sqrt[-a^4 + 2*a^2*b^2 -
 b^4 + c^4] + 2*Sqrt[b^2*c^2 - (-a^2 + b^2 + c^2)^2/4])*(2*Sqrt[b^2*c^2 - (-a^2 + b^2 + c^2)^2/4] +
 Sqrt[2]*Sqrt[-(((a^4 - b^4 - 2*a^2*c^2 + c^4)*(-a^4 + 2*a^2*b^2 - b^4 + 2*a^2*c^2 + 2*b^2*c^2 - c^4 +
 2*Sqrt[-a^4 + b^4 + 2*a^2*c^2 - c^4]*Sqrt[b^2*c^2 - (-a^2 + b^2 + c^2)^2/4]))/(Sqrt[-a^4 + b^4 + 2*a^2*
c^2 - c^4] + Sqrt[a^4 - b^4 + 2*b^2*c^2 - c^4] + Sqrt[-a^4 + 2*a^2*b^2 - b^4 + c^4] + 2*Sqrt[b^2*c^2 - (
-a^2 + b^2 + c^2)^2/4])^2)] + Sqrt[2]*Sqrt[((a^4 - b^4 + 2*b^2*c^2 - c^4)*(-a^4 + 2*a^2*b^2 - b^4 + 2*
a^2*c^2 + 2*b^2*c^2 - c^4 + 2*Sqrt[a^4 - b^4 + 2*b^2*c^2 - c^4]*Sqrt[b^2*c^2 - (-a^2 + b^2 + c^2)^2/4]))
/(Sqrt[-a^4 + b^4 + 2*a^2*c^2 - c^4] + Sqrt[a^4 - b^4 + 2*b^2*c^2 - c^4] + Sqrt[-a^4 + 2*a^2*b^2 - b^4 +
 c^4] + 2*Sqrt[b^2*c^2 - (-a^2 + b^2 + c^2)^2/4])^2] + Sqrt[2]*Sqrt[-(((a^4 - 2*a^2*b^2 + b^4 - c^4)*(-
a^4 + 2*a^2*b^2 - b^4 + 2*a^2*c^2 + 2*b^2*c^2 - c^4 + 2*Sqrt[-a^4 + 2*a^2*b^2 - b^4 + c^4]*Sqrt[b^2*
c^2 - (-a^2 + b^2 + c^2)^2/4]))/(Sqrt[-a^4 + b^4 + 2*a^2*c^2 - c^4] + Sqrt[a^4 - b^4 + 2*b^2*c^2 -
 c^4] + Sqrt[-a^4 + 2*a^2*b^2 - b^4 + c^4] + 2*Sqrt[b^2*c^2 - (-a^2 + b^2 + c^2)^2/4])^2)]))}
```

ERS apex foot

Audit (DATABASE AUDIT): No numerical match found in the audited ETC snapshot.

```
\lambda_{ERS}(a,b,c)=\operatorname{argmin}_{\alpha+\beta+\gamma=1,\ h>0} R_T/r_T
```

DGS apex foot

Audit (DATABASE AUDIT): No numerical match found in the audited ETC snapshot.

```
\operatorname*{argmin}\sum_e(\cos\theta_e-1/3)^2
```

NFIS apex foot

Audit (DATABASE AUDIT): No numerical match found in the audited ETC snapshot.

```
\operatorname*{argmin}\|\sum_i n_i n_i^{\mathsf T}-(4/3)I\|_F^2
```

Foot of the tetrahedral incenter of the EVS tetrahedron

Audit (DATABASE AUDIT): No numerical match found in the audited ETC snapshot.

```
\iota_i=(F_i+\Delta\lambda_i)/(\Delta+F_a+F_b+F_c),\quad \lambda=\lambda_{EVS}
```

Foot of the tetrahedral incenter of the CVS tetrahedron

Audit (DATABASE AUDIT): No numerical match found in the audited ETC snapshot.

```
\iota_i=(F_i+\Delta\lambda_i)/(\Delta+F_a+F_b+F_c),\quad \lambda=\lambda_{CVS}
```

Foot of the tetrahedral incenter of the ERS tetrahedron

Audit (DATABASE AUDIT): No numerical match found in the audited ETC snapshot.

```
\iota_i=(F_i+\Delta\lambda_i)/(\Delta+F_a+F_b+F_c),\quad \lambda=\lambda_{ERS}
```

Foot of the tetrahedral centroid of the ERS tetrahedron

Audit (DATABASE AUDIT): No numerical match found in the audited ETC snapshot.

```
g_i=(1+\lambda_i)/4,\quad \lambda=\lambda_{ERS}
```

Foot of the tetrahedral incenter of DGS

Audit (DATABASE AUDIT): No numerical match found in the audited ETC snapshot.

```
\iota_i=(F_i+\Delta\lambda_i)/S,\quad \lambda=\lambda_{DGS}
```

Foot of the tetrahedral centroid of DGS

Audit (DATABASE AUDIT): No numerical match found in the audited ETC snapshot.

```
g_i=(1+\lambda_i)/4,\quad \lambda=\lambda_{DGS}
```

Foot of the tetrahedral incenter of NFIS

Audit (DATABASE AUDIT): No numerical match found in the audited ETC snapshot.

```
\iota_i=(F_i+\Delta\lambda_i)/S,\quad \lambda=\lambda_{NFIS}
```

Foot of the tetrahedral centroid of NFIS

Audit (DATABASE AUDIT): No numerical match found in the audited ETC snapshot.

```
g_i=(1+\lambda_i)/4,\quad \lambda=\lambda_{NFIS}
```

Chapter 10

Triangle Hyperstars: the sky in four dimensions

The ordinary Triangle Sky completes a fixed triangle by one point in three-dimensional space. There is a natural next level: complete the same triangle by two points in four-dimensional space. The result is a 4-simplex, so its metric geometry brings ten edges, five tetrahedral facets, ten dihedral angles, and the higher-dimensional analogues of the centroid, incenter, circumcenter and Monge point into the theory. The two added points will be called a pair of *twin hyperstars*.

This chapter is a higher-dimensional research extension rather than part of the thirty-star ranking. Its OHS and CPOH identities are exact results with stated domains; the broader optimization programme and unclassified projected centers remain exploratory. The claim-status legend at the beginning of the report applies throughout.

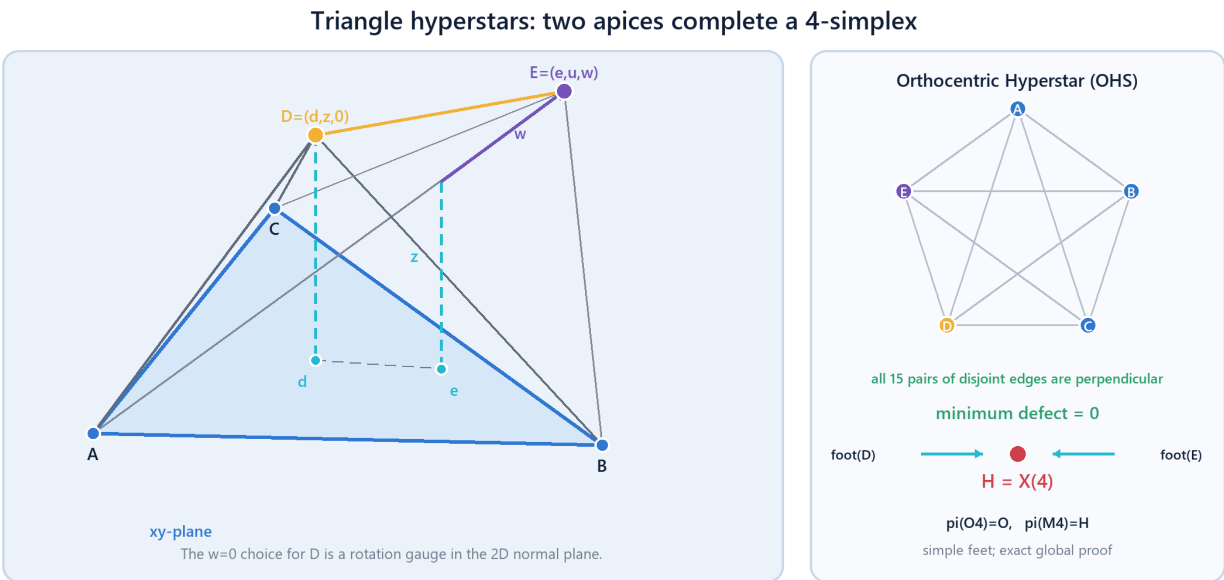

Figure 10.1: A two-dimensional shadow of a triangle-hyperstar completion. The purple direction represents the second normal coordinate, which cannot be drawn faithfully in three dimensions. The right panel previews the exact Orthocentric Hyperstar introduced in section 10.5.

10.1 Definition, coordinates and the normal-plane gauge

Embed the reference triangle as

$$A = (A_x, A_y, 0, 0), \qquad B = (B_x, B_y, 0, 0), \qquad C = (C_x, C_y, 0, 0)$$

in $\mathbb{R}^4$, and let

$$D = (d_x, d_y, z, 0), \qquad E = (e_x, e_y, u, w).$$

The vertical projection is

$$\pi(x, y, z, w) = (x, y),$$

so $d = \pi(D)$ and $e = \pi(E)$ are the two feet.

The form of D is not a geometric restriction. The plane orthogonal to ABC is two-dimensional. A rotation in that normal plane puts the nonzero normal component of D on the first normal axis, giving $(z, 0)$; a reflection and an orientation choice then permit $z > 0$ and $w > 0$. Thus

$$(z, 0), \quad (u, w)$$

are simply Gram–Schmidt coordinates for the two normal components. The conditions $z > 0$ and $w > 0$ fix a convenient gauge.

Definition 10.1 (Twin triangle hyperstar)**.** A *twin triangle hyperstar rule* assigns to every nondegenerate triangle an ordered pair (D, E) as above, or an unordered pair when no natural ordering exists, such that:

1. $ABCDE$ is a nondegenerate 4-simplex;
2. the rule is equivariant under similarities of the reference plane and under permutations of A, B, C;
3. every multivalued optimization is supplied with a permutation-compatible canonical branch rule.

The feet d, e are then triangle centers individually when the branches remain ordered, or a permutation-invariant pair of centers when the branches may exchange.

The equivariance clause is essential. Merely finding two numerical minimizers for one labelled triangle does *not* prove that their projections are triangle centers. Uniqueness, or an explicit canonical selection from the minimizer set, is the higher-dimensional version of the variance-zero certificate used in the Stars Cascade.

Proposition 10.2 (The volume separates)**.** *Let Δ be the area of ABC. Then*

$$V_4(ABCDE) = \frac{\Delta\,|zw|}{12}. \tag{10.1}$$

Consequently $ABCDE$ is nondegenerate exactly when $zw \neq 0$.

Proof. The determinant of the four edge vectors based at A is block triangular after the first two rows are separated from the two normal rows. Its planar 2×2 determinant has absolute value 2Δ, while the normal 2×2 determinant is zw. Dividing $|2\Delta zw|$ by $4! = 24$ proves (10.1). ☐

This simple formula is useful computationally. The horizontal feet d, e and the shear coordinate u do not affect the 4-volume. A similarity-covariant volume normalization therefore has the form

$$V_4 = V_0 := \eta\Delta^2, \qquad \eta > 0, \tag{10.2}$$

because both sides have degree four in length.

10.2 Simplex centers and their planar descendants

Write the five vertices as $P_0 = A, P_1 = B, P_2 = C, P_3 = D, P_4 = E$. The standard simplex centers extend several familiar triangle constructions [20, 21]:

$$G_4 = \frac{1}{5}\sum_{i=0}^{4} P_i, \tag{10.3}$$

$$I_4 = \frac{\sum_{i=0}^{4} F_i P_i}{\sum_{i=0}^{4} F_i}, \tag{10.4}$$

where F_i is the three-dimensional volume of the tetrahedral facet opposite P_i. The circumcenter O_4 is the solution of

$$2O_4 \cdot (P_i - P_0) = \|P_i\|^2 - \|P_0\|^2, \qquad i = 1, \ldots, 4. \tag{10.5}$$

A general simplex need not possess concurrent altitudes. Its always-defined Monge point M_4 is the common point of the ten hyperplanes that are perpendicular to an edge and pass through the centroid of the other three vertices. In dimension four,

$$M_4 = \frac{5G_4 - 2O_4}{3}. \tag{10.6}$$

Indeed, take O_4 as the origin, so all $\|P_i\|$ are equal. Subtracting the centroid of the three vertices complementary to an edge P_iP_j from the right side of (10.6) leaves $(P_i + P_j)/3$, which is perpendicular to $P_i - P_j$.

Theorem 10.3 (Uniqueness–equivariance projection principle)**.** *Suppose a system of geometric constraints on $ABCDE$ is intrinsic, similarity covariant and invariant under every permutation of A, B, C. Suppose further that it determines a unique congruence class of completions relative to the fixed base, modulo isometries of the two-dimensional normal plane and, if necessary, exchange of D and E. Then $\{d, e\} = \{\pi(D), \pi(E)\}$ is an invariant twin-center-system. If the two branches have a permutation-equivariant ordering, each of d, e is a triangle center separately. If $Y(ABCDE)$ is any canonical simplex-center construction equivariant under Euclidean similarities and vertex relabelling, then $\pi(Y)$ is a triangle center. In particular, this applies to G_4, I_4, O_4 and M_4.*

Proof. Apply a planar similarity or a permutation of A, B, C to a completed simplex. By covariance and symmetry its image satisfies the constraints for the transformed triangle. Uniqueness forces that image to be the selected completion, up to a normal-plane isometry and possibly $D \leftrightarrow E$. Normal-plane isometries do not change horizontal projections, while an exchange merely exchanges d, e. Therefore the unordered pair $\{d, e\}$ is invariant; an equivariant ordering makes its members individual centers. The simplex-center construction commutes with the induced transformation of $ABCDE$, and orthogonal projection commutes with its planar part. The composition is consequently a similarity- and permutation-equivariant point rule on triangles. □

Two descendants are especially transparent. For *every* nondegenerate completion,

$$\pi(G_4) = \frac{A + B + C + d + e}{5}, \tag{10.7}$$

$$\pi(O_4) = O = X(3). \tag{10.8}$$

The second identity needs no optimization: equality of the distances from O_4 to A, B, C forces the horizontal component of O_4 to be the circumcenter of ABC. The incenter descendant follows directly from (10.4):

$$\pi(I_4) = \frac{F_A A + F_B B + F_C C + F_D d + F_E e}{F_A + F_B + F_C + F_D + F_E}. \tag{10.9}$$

It is a genuine center function, although its radicals can be substantially more complicated than those of d and e.

10.3 Natural optimization families

There are ten edges and five tetrahedral facets. Let $\ell_{ij} = \|P_i - P_j\|$, let R_4, r_4 be the circumradius and inradius, let F_i be the facet volumes, and let n_i be outward unit facet normals. The following are natural first candidates.

Table 10.1: Optimization-defined triangle hyperstars. Polynomial or dimensionless normalizations are preferable to raw dimensional objectives.

Name	Objective	Geometric meaning and warning
Hyper-Edge Variance	$\mathrm{Var}\{\ell_{ij}^2 : i < j\}$	Polynomial best approximation to a regular 4-simplex. Fix $V_4 = \eta\Delta^2$ to exclude flattening and to select a scale.
Hyper-Euler Ratio	R_4/r_4	In dimension four, $R_4 \geq 4r_4$. A fixed scalene face normally prevents equality; the problem seeks the closest admissible shape.
Centroid–circumcenter	$\|G_4 - O_4\|^2/R_4^2$	Zero means a well-distributed edge-length structure, not necessarily a regular 4-simplex.
Centroid–incenter	$\|G_4 - I_4\|^2/R_4^2$	Zero is equivalent to equal tetrahedral facet volumes (an equiareal simplex).
Facet variance	$\mathrm{Var}(F_0, \ldots, F_4)/\overline{F}^2$	A direct and numerically stable version of the preceding equiareal condition.
Normal-frame isotropy	$\left\|\sum_i n_i n_i^{\mathsf{T}} - \frac{5}{4}I_4\right\|_F^2$	The five facet normals should form a unit-norm tight frame in $\mathbb{R}^4$.
Dihedral regularity	$\sum_{i<j}(\cos\theta_{ij} - \frac{1}{4})^2$	The regular 4-simplex has ten equal internal dihedral angles with cosine 1/4. This is the four-dimensional analogue of DGS.

The refined simplex Euler inequality is

$$R_4^2 \geq 16r_4^2 + \|O_4 - G_4\|^2, \tag{10.10}$$

with equality only for the regular simplex [22]. This connects the Euler-ratio and centroid–circumcenter objectives, but it does not make them identical away from equality.

There is another important caution. In four dimensions $G_4 = O_4$ does not force regularity. It characterizes a "well-distributed edge lengths" condition; likewise $G_4 = I_4$ characterizes equiareal facets, and $O_4 = I_4$ characterizes equiradial facets [20]. Nonregular 4-simplices can even exhibit several center coincidences. Thus center-distance objectives are mathematically interesting, but their minimizers can be families and require a secondary selector.

10.4 Two exact controls with simple feet

Before attacking the global objectives numerically, two exact controls are useful. The first is deliberately elementary:

$$\mathcal{C}_O(D, E) = \mathrm{Var}(AD^2, BD^2, CD^2) + \mathrm{Var}(AE^2, BE^2, CE^2). \tag{10.11}$$

Its minimum is zero, and equality forces

$$d = e = O = X(3),$$

because the vertical terms cancel from every difference such as $AD^2 - BD^2$. This gives a very short barycentric center function, but the objective distinguishes the base vertices from the two new vertices and therefore has less intrinsic 4-simplex meaning.

The second control treats all five vertices uniformly and is considerably deeper.

10.5 The Orthocentric Hyperstar

Let $\mathcal{P}$ be the set of the 15 unordered pairs of disjoint edges of the complete graph on A, B, C, D, E. Define the angular orthocentric defect

$$\mathcal{O}_\angle(D,E) = \sum_{\{ij,kl\}\in\mathcal{P}} \left(\frac{(P_i - P_j)\cdot(P_k - P_l)}{\ell_{ij}\ell_{kl}}\right)^2. \tag{10.12}$$

It is dimensionless, nonnegative, invariant under every relabelling of the five vertices, and vanishes exactly when every pair of disjoint edges is perpendicular. For symbolic elimination one may instead use the polynomial defect

$$\mathcal{O}_2(D,E) = \sum_{\{ij,kl\}\in\mathcal{P}} ((P_i - P_j)\cdot(P_k - P_l))^2. \tag{10.13}$$

Definition 10.4 (Orthocentric Hyperstar family (OHS))**.** Fix $\eta > 0$. First minimize $\mathcal{O}_\angle$ subject to $V_4 = \eta\Delta^2$ and the gauge $z, w > 0$. Among all primary minimizers, minimize the normal energy

$$\mathcal{N} = z^2 + u^2 + w^2. \tag{10.14}$$

The resulting ordered pair (D, E) is the *Orthocentric Hyperstar* OHS_η. Thus OHS is a one-parameter invariant family until a universal value of η is adopted. The regular calibration in (10.42) gives the particularly natural choice $\eta_0 = \sqrt{5}/18$.

Theorem 10.5 (Exact feet and invariant normal coordinates)**.** *For every nondegenerate triangle, the OHS primary minimum is zero and both feet are the orthocenter:*

$$d = e = H = X(4). \tag{10.15}$$

Put

$$q = (H-A)\cdot(H-B) = (H-B)\cdot(H-C) = (H-C)\cdot(H-A) = 4R^2 - \frac{a^2+b^2+c^2}{2} \tag{10.16}$$

and $c_0 = 12\eta\Delta$. *The secondary minimizer is unique in the gauge* $z, w > 0$ *and is*

$$z = (q^2 + c_0^2)^{1/4}, \qquad u = -\frac{q}{z}, \qquad w = \frac{c_0}{z}. \tag{10.17}$$

Hence OHS has an exact, similarity-covariant algebraic structure rather than merely a numerical one.

Proof. Suppose first that the defect is zero. The disjoint-edge conditions

$$AB \perp CD, \qquad AC \perp BD, \qquad BC \perp AD$$

project to the three altitude equations for d, so $d = H$. Replacing D by E gives $e = H$. Thus every zero-defect completion must have the feet in (10.15).

The three expressions used to define q are equal: for example, the difference of the first two is $(H - B)\cdot(C - A) = 0$. To obtain the last expression in (10.16), place the triangle circumcenter at the origin. The three vertex vectors have squared norm R^2, $H = A + B + C$, and $A \cdot B = R^2 - c^2/2$, with the cyclic analogues. Expanding any one of the three products gives the stated symmetric formula.

Conversely, set

$$D = (H, z, 0), \qquad E = (H, u, w).$$

Because H is the triangle orthocenter, all disjoint-edge products containing a base edge vanish automatically. Each of the remaining six products equals $q + zu$. Therefore all 15 products vanish exactly when

$$zu = -q. \tag{10.18}$$

This is always solvable with $z \neq 0$ and $w \neq 0$, including the right-triangle case $q = 0$. Hence the primary minimum is exactly zero.

The volume condition and positive gauge give $zw = c_0$. Equations (10.18) and $zw = c_0$ imply

$$u = -q/z, \qquad w = c_0/z.$$

Thus

$$\mathcal{N} = z^2 + \frac{q^2 + c_0^2}{z^2} \geq 2\sqrt{q^2 + c_0^2},$$

with equality at the unique positive solution $z^4 = q^2 + c_0^2$. This proves (10.17). □

The barycentric function of the two OHS feet is exceptionally short:

$$H = (\tan A : \tan B : \tan C) = \left(\frac{1}{b^2 + c^2 - a^2} : \frac{1}{c^2 + a^2 - b^2} : \frac{1}{a^2 + b^2 - c^2}\right). \tag{10.19}$$

The formula is interpreted projectively at a right triangle. It is already the ETC center $X(4)$, so the OHS succeeds at the stated goal: a nontrivial intrinsic four-dimensional optimization reproduces an elementary classical center.

Why this candidate is preferable

The circumfoot control (10.11) gives the even simpler center $X(3)$, but it builds the answer from two separate three-distance variances. OHS uses all 15 disjoint-edge relations of the full 4-simplex, has a zero lower bound attained for every triangle, supplies a complete exact proof, and gives a canonical closed-form vertical branch. It therefore has more geometric content while retaining simple barycentrics.

10.6 The descendants of OHS

The OHS completion is orthocentric in the standard simplex sense [21]. Several projected simplex centers now simplify without calculation of a 4×4 inverse.

Table 10.2: Planar descendants of the OHS 4-simplex.

Simplex point	Projected point	Consequence
Twin apices D, E	H and H	Both feet are $X(4)$.
Circumcenter O_4	O	Always $X(3)$, for every hyperstar completion.
Centroid G_4	$(3G + 2H)/5$	A simple Euler-line center with normalized barycentrics $(1 + 2h_A : 1 + 2h_B : 1 + 2h_C)$, where (h_A, h_B, h_C) are normalized orthocenter barycentrics.
Monge point M_4	H	Since $H = 3G - 2O$, equations (10.6) and (10.7) give $\pi(M_4) = H$.
Incenter I_4	Equation (10.9) with $d = e = H$	A canonical triangle center; its facet-volume function is the main symbolic elimination problem left by OHS.

For the centroid descendant, let

$$T = \tan A + \tan B + \tan C.$$

One convenient homogeneous barycentric form is

$$\pi(G_4) = (T + 2\tan A : T + 2\tan B : T + 2\tan C). \tag{10.20}$$

This is an explicit example of the hyperstar mechanism creating a second triangle center from an already simple pair of feet. Its exact ETC status should be checked by the same two-triangle symbolic-and-numerical audit used elsewhere in this report; no identifier is asserted here without that audit.

10.7 The exact incenter foot of OHS

The incenter descendant can also be written explicitly. Define the cyclic quantities

$$\sigma_A = \frac{b^2+c^2-a^2}{2}, \qquad \sigma_B = \frac{c^2+a^2-b^2}{2}, \qquad \sigma_C = \frac{a^2+b^2-c^2}{2}, \tag{10.21}$$

and

$$\Sigma = \frac{1}{\sigma_A} + \frac{1}{\sigma_B} + \frac{1}{\sigma_C}, \qquad \widehat{h}_A = \frac{1/\sigma_A}{\Sigma}, \tag{10.22}$$

with cyclic definitions for $\widehat{h}_B, \widehat{h}_C$. These are the normalized barycentrics of H. Put

$$k = z^2 + q = \sqrt{q^2 + (12\eta\Delta)^2} + q. \tag{10.23}$$

Proposition 10.6 (Facet volumes of OHS_η)**.** *The five tetrahedral facet volumes are*

$$F_A = \frac{1}{6}\sqrt{k(a^2k + 2\sigma_B\sigma_C)}, \qquad F_B = \frac{1}{6}\sqrt{k(b^2k + 2\sigma_C\sigma_A)}, \tag{10.24}$$

$$F_C = \frac{1}{6}\sqrt{k(c^2k + 2\sigma_A\sigma_B)}, \qquad F_D = F_E = \frac{\Delta z}{3}. \tag{10.25}$$

Proof. The secondary OHS equation implies

$$u^2 + w^2 = \frac{q^2 + (12\eta\Delta)^2}{z^2} = z^2.$$

The facets $ABCD$ and $ABCE$ are tetrahedra on base ABC with respective normal heights z and $\sqrt{u^2+w^2} = z$, proving (10.25). For the facet $BCDE$, use D as origin. The Gram matrix of $B-D, C-D, E-D$ is

$$\begin{pmatrix} k+\sigma_B & k & k \\ k & k+\sigma_C & k \\ k & k & 2k \end{pmatrix}.$$

Its determinant is $k(a^2k + 2\sigma_B\sigma_C)$. Dividing its square root by $3! = 6$ gives F_A; the other formulas follow cyclically. □

Theorem 10.7 (OHS incenter foot)**.** *The vertical projection $J_\eta = \pi(I_4)$ of the 4-simplex incenter has barycentrics*

$$J_\eta = (\Lambda_A : \Lambda_B : \Lambda_C), \qquad \Lambda_A = F_A + \frac{2\Delta z}{3}\widehat{h}_A, \tag{10.26}$$

with cyclic formulas for Λ_B, Λ_C. Equivalently, after multiplication by the common factor 6,

$$\Lambda_A \sim \sqrt{k(a^2k + 2\sigma_B\sigma_C)} + \frac{4\Delta z}{\sigma_A\Sigma}. \tag{10.27}$$

The absolute trilinears are $\Lambda_A/a : \Lambda_B/b : \Lambda_C/c$.

Proof. The simplex incenter is the facet-volume-weighted mean of the five vertices. Since $d = e = H$ and $F_D = F_E = \Delta z/3$, projecting that weighted mean gives (10.26). □

At a right triangle, formulas containing $1/\sigma_i$ are read by their continuous projective limit, since H then equals the right-angle vertex. The important point is structural: the OHS incenter foot is a one-parameter family of exact algebraic triangle centers, because η is part of the OHS definition.

For the regular calibration $\eta_0 = \sqrt{5}/18$, the two report controls give:

Table 10.3: Incenter feet of $\mathrm{OHS}_{\sqrt{5}/18}$.

Triangle	normalized barycentrics	normalized absolute trilinears
6–9–13	0.004076 : 0.004202 : 0.991722	1.455015 : 1 : 163.396725
13–20–21	0.177577 : 0.352869 : 0.469554	1 : 1.291634 : 1.636899

10.8 The center-proximity orthocentric hyperstar

There is a second natural way to select one member of the orthocentric family: require orthocentricity and minimize the distance from the simplex orthocenter to its centroid or circumcenter. Provisionally call the result the *Center-Proximity Orthocentric Hyperstar* (CPOH).

For an orthocentric 4-simplex its orthocenter K_4 is its Monge point, so (10.6) gives

$$K_4 - G_4 = \frac{2}{3}(G_4 - O_4), \qquad K_4 - O_4 = \frac{5}{3}(G_4 - O_4). \tag{10.28}$$

Consequently minimizing any one of

$$\|K_4 - G_4\|, \qquad \|K_4 - O_4\|, \qquad \|G_4 - O_4\|$$

produces exactly the same completion.

Place the horizontal origin at the triangle orthocenter H and write $\mathbf{o} = O - H$. Every orthocentric completion is

$$D = (\mathbf{0}, z, 0), \qquad E = (\mathbf{0}, u, w), \qquad zu = -q, \qquad z, w > 0. \tag{10.29}$$

A direct solution of the circumcenter equations, followed by (10.6), gives

$$G_4 = \left(\frac{2\mathbf{o}}{5}, \frac{z+u}{5}, \frac{w}{5}\right), \tag{10.30}$$

$$K_4 = \left(0, u, \frac{u(z-u)}{w}\right). \tag{10.31}$$

Therefore

$$25\|K_4 - G_4\|^2 = 4OH^2 + (4u - z)^2 + \frac{(5u(z-u) - w^2)^2}{w^2}. \tag{10.32}$$

Theorem 10.8 (Exact CPOH completion)**.** *For every nonright triangle,* (10.32) *has a unique nondegenerate minimum in the gauge* $z, w > 0$*.*

1. *If* ABC *is acute, then* $q < 0$ *and*

$$z = 2\sqrt{-q}, \qquad u = \frac{\sqrt{-q}}{2}, \qquad w = \frac{\sqrt{15(-q)}}{2}. \tag{10.33}$$

2. *If* ABC *is obtuse, then* $q > 0$ *and*

$$z = \sqrt{6q}, \qquad u = -\sqrt{\frac{q}{6}}, \qquad w = \sqrt{\frac{35q}{6}}. \tag{10.34}$$

For a right triangle $q = 0$*, the infimum is approached as* $z, w \to 0$ *but is not attained by a nondegenerate* 4*-simplex.*

Proof. For $q < 0$ one has $u > 0$. Both variable squares in (10.32) vanish uniquely when $z = 4u$ and $w^2 = 5u(z-u) = 15u^2$. Combining this with $zu = -q$ gives (10.33).

For $q > 0$, put $z = \sqrt{q}\,t$ and $u = -\sqrt{q}/t$. For fixed t, the last term in (10.32) is minimized by $w^2 = -5u(z-u)$. The remaining variable part is

$$q\left(t^2 + 28 + \frac{36}{t^2}\right),$$

whose unique minimum occurs at $t^2 = 6$. This gives (10.34). When $q = 0$, orthocentricity gives $u = 0$ and the variable part becomes $z^2 + w^2$, whose infimum lies on the degenerate boundary. □

The comparison with OHS is now exact. Both CPOH solutions satisfy

$$u^2 + w^2 = z^2, \tag{10.35}$$

which is precisely the secondary energy-balance equation of OHS. However CPOH selects the triangle-dependent volume

$$c_0 = zw = \begin{cases} \sqrt{15}(-q), & q < 0, \\ \sqrt{35}\, q, & q > 0, \end{cases} \qquad \eta_{\text{CPOH}} = \frac{c_0}{12\Delta}. \tag{10.36}$$

Thus, for every nonright triangle, CPOH is a member of the energy-balanced OHS family, but it is generally *not* the same as OHS_{η_0} with one universal fixed η_0. They coincide for an equilateral triangle, where $\eta_{\text{CPOH}} = \sqrt{5}/18$, and more generally whenever the chosen fixed OHS volume happens to equal (10.36). The CPOH incenter foot follows from (10.27) by substituting $k = -3q$ in the acute case and $k = 7q$ in the obtuse case.

10.8.1 The CPOH centroid and incenter feet

The projected centroid does not depend on the normal coordinates once both apex feet are H:

$$C_{\text{CPOH}} = \pi(G_4) = \frac{3G + 2H}{5}. \tag{10.37}$$

Using (10.21), one exact barycentric form is

$$C_{\text{CPOH}} = (\Gamma_A : \Gamma_B : \Gamma_C), \qquad \Gamma_A = 3\sigma_B\sigma_C + \sigma_C\sigma_A + \sigma_A\sigma_B. \tag{10.38}$$

Since

$$4\Gamma_A = a^4 + 2a^2(b^2 + c^2) - 3(b^2 - c^2)^2, \tag{10.39}$$

with cyclic analogues, this is exactly $X(3091)$ in the ETC [2]. The ETC also records $X(3091)$ as an Euler-line center with Shinagawa coefficients $(1, 2)$.

For the incenter foot, the common factors containing $\sqrt{|q|}$ can be removed from (10.27). Thus

$$J_{\text{CPOH}} = (\Xi_A : \Xi_B : \Xi_C), \tag{10.40}$$

where, cyclically,

$$\Xi_A = \begin{cases} \sqrt{3(-3a^2q + 2\sigma_B\sigma_C)} + 8\Delta\widehat{h}_A, & q < 0, \\ \sqrt{7(7a^2q + 2\sigma_B\sigma_C)} + 4\sqrt{6}\,\Delta\widehat{h}_A, & q > 0. \end{cases} \tag{10.41}$$

This is an invariant piecewise algebraic triangle-center function on the acute and obtuse domains. CPOH itself has no nondegenerate right-triangle value.

Table 10.4: CPOH projected centers and ETC audit.

Projection	Triangle	normalized barycentrics	ETC status
$\pi(G_4)$	every triangle	$(3G + 2H)/5$	$X(3091)$, exact
$\pi(I_4)$	6–9–13	$0.087490 : 0.117781 : 0.794729$	no numerical match in snapshot
$\pi(I_4)$	13–20–21	$0.171308 : 0.351093 : 0.477599$	acute control value

For 6–9–13, the normalized absolute trilinears of the incenter foot are

$$1.114225 : 1 : 4.671357.$$

Its directed-distance triple was compared with all 72,486 entries in the audited July 2026 ETC search snapshot. The nearest row was $X(15306)$, but its Euclidean triple error was approximately 1.45×10^{-2}, far above the 10^{-9} matching tolerance. Hence no numerical match was found for the CPOH incenter foot in that ETC snapshot; this does not prove mathematical absence from the ETC.

10.9 Equilateral calibration

Let the base be equilateral with side s. Then

$$\Delta = \frac{\sqrt{3}}{4}s^2, \qquad q = -\frac{s^2}{6}.$$

A regular 4-simplex of side s has volume $\sqrt{5}s^4/96$, so choosing

$$\eta = \frac{\sqrt{5}}{18} \tag{10.42}$$

makes $V_0 = \eta\Delta^2$ equal to that regular volume. Formula (10.17) then produces a regular 4-simplex completion. Thus the OHS does not merely imitate regularity: on the maximally symmetric base it recovers the regular object exactly, while on a scalene base it gives the canonical orthocentric substitute allowed by the fixed face.

10.10 A Hyperstars Cascade

The original cascade can now be extended in two stages:

$$ABC \longmapsto (D, E) \longmapsto \{G_4, I_4, O_4, M_4, \ldots\} \xrightarrow{\pi} \text{triangle centers.}$$

The same admissibility principles remain necessary:

1. use homogeneous, similarity-covariant constraints;
2. make the admissible domain closed or coercive, normally by $V_4 = \eta\Delta^2$ and $z, w > 0$;
3. certify permutation equivariance of the selected branch;
4. distinguish independent geometric meanings from algebraic rewritings;
5. retain exact center functions whenever elimination is possible, and audit numerical candidates on both an acute and an obtuse control triangle.

Hyperstar costs should initially be kept in a separate ledger from ordinary star indices, since two free apices and a simplex-center operation represent a genuine increase in construction depth. A reasonable provisional cost is 7/4 for the circumfoot control and 9/4 for OHS: both lie in the report's permitted interval $(1, 3)$, while the latter receives the larger cost for its global all-edge constraint and secondary branch selection. A projected simplex-center operation should then add its usual operation cost rather than being counted as a new independent optimization.

10.11 Recommended computational programme

The next calculations should proceed in the following order.

1. Implement the polynomial defect (10.13) and use theorem 10.5 as an exact unit test for the full 4-simplex code.
2. Audit the exact OHS incenter family (10.27) against the ETC and search for distinguished values of η at which the radicals simplify.
3. Solve the edge-variance, Euler-ratio, normal-isotropy and dihedral objectives under the same volume gauge, using many starting points and a permutation audit.
4. Compare the two feet and the four projected simplex centers with the ETC using the corrected complex matching protocol, including first-coordinate arguments.

5. Search for coincidences among the planar descendants. Such coincidences are higher-dimensional independent definitions and should reduce the effective hyperstar index just as they do in the ordinary Stars Cascade.

The central conceptual payoff is that a triangle can govern not only a family of tetrahedral apices but an entire hierarchy of higher-dimensional simplex geometry. OHS shows that this hierarchy need not become algebraically opaque: a fully intrinsic 4-dimensional optimization can collapse to the elementary center $X(4)$ and still carry new invariant normal coordinates and new center descendants.

Chapter 11

Reproducibility and limitations

11.1 What is exact

The exact rational scores and printed symbolic functions are transcribed from the audited workbook/JSON. The structural theorem in theorem 4.1 and the stated OHS/CPOH theorems are mathematical results proved in the text. Closed forms for EVS, CVS and IVS are exact consequences of their reduced stationary equations. By contrast, the claimed independence counts remain classification judgments until every equivalence class has a proof dependency record, and ETC identifiers remain database fingerprints unless a symbolic projective identity is supplied.

11.2 What is computational evidence

The ERS, DGS and NFIS feet, their projected tetrahedral centers, the Euler-line census, and ETC match/non-match decisions are numerical. They are strong discovery evidence, not uniqueness proofs or timeless database statements. EVS, CVS and IVS also still require a complete global optimization argument, even though their reduced stationary solutions are exact. An optimization-defined star should ultimately have: (i) a specified admissible domain, (ii) an existence and boundary/coercivity proof, (iii) a global-minimum proof, (iv) uniqueness up to base reflection, (v) a symbolic permutation certificate, and ideally (vi) an algebraic elimination polynomial for its foot and height.

11.3 Build and data provenance

The public source release is intended to contain the main LaTeX file, both included chapter files, all six figures, the Mathematica figure specifications, generation sources, the audited JSON catalogue, the ETC audit scripts and the CSV tables named in Chapter 8. The accompanying `build.ps1` performs a one-command Tectonic build from the release directory. The release README records the report version, page count after compilation, required engine, generated/source distinction, and the dated ETC snapshot policy. A release checksum manifest should be regenerated whenever any source, figure, table or PDF changes.

The local workbook and JSON export are project inputs, not scholarly citations. The public report should be cited by author, title, version and date; an archival URL or DOI can be added when one is assigned.

11.4 Figure provenance

The figures are original for this report. The companion file `TriangleSkyReportFigures.wl` gives Mathematica `Graphics3D` and `Graphics` specifications for the mathematical scenes, including the hyperstar projection schematic. The distributed PNGs were rendered from the same stated coordinates and audited numerical data by the companion source renderers. This is a provenance statement, not a claim that every PNG is a direct Mathematica export.

11.5 Suggested next theorems

1. Prove global uniqueness and obtain elimination equations for ERS, DGS and NFIS.
2. Characterize exactly when each cascade height is real and relate each boundary to acute/obtuse or stronger side inequalities.
3. Explain the exceptional multiple definitions of CS1 and ranks 1, 5 and 7 by synthetic tetrahedral theorems.
4. Determine whether unmatched feet define genuinely new center functions under the ETC center-function axioms, including their branch domains.
5. Compare DGS and NFIS infinitesimally near the regular tetrahedron by Hessian and Gram-matrix analysis.
6. Audit the exact OHS incenter family, analyze the right-triangle boundary of CPOH, and solve the remaining hyperstar objectives under the common 4-volume gauge.

Chapter 12

Conclusions and open problems

12.1 Established contributions

This report establishes a precise foot–height language for lifting triangle centers to mirror pairs of tetrahedral apices, separates real Euclidean stars from their algebraic complexifications, and proves a certified closure theorem for permutation-compatible constructions. It also gives exact orthocentric hyperstar results, including the repeated appearance of $X(4)$, and organizes a reproducible set of symbolic catalogue records.

12.2 Computational findings

Within the stated July 2026 ETC snapshot, the low-index cascade produces a substantial numerical network of known center fingerprints through feet, ordinary traces and cross-conjugate traces. The Euler line is an especially frequent carrier. Several repeated unmatched classes have short affine descriptions in familiar centers. These are discovery results: each proposed new center still requires a generic center-function proof and a renewed database audit before submission.

12.3 Open mathematical questions

The most immediate tasks are to prove global existence and uniqueness for the optimization-star candidates, characterize every real domain and branch boundary, and replace numerical ETC identifications by symbolic projective identities where feasible. A second task is to formalize independence through proof-dependency graphs and to test whether the leading ranks remain stable under reasonable alternative cost schedules. A third is to determine which hyperstar optimizations admit unique, permutation-equivariant twin completions and simple projected center functions.

The Triangle Sky should therefore be read neither as a finished classification nor as a list of unsupported experiments. It is a versioned research programme with a proved core, exact symbolic records, numerical discovery layers and explicitly marked conjectural frontiers.

Bibliography

[1] C. Kimberling, "Triangle centers and central triangles," *Congressus Numerantium* 129 (1998), 1–295.

[2] C. Kimberling, *Encyclopedia of Triangle Centers*, University of Evansville, continuously updated, https://faculty.evansville.edu/ck6/encyclopedia/.

[3] H. S. M. Coxeter and S. L. Greitzer, *Geometry Revisited*, Mathematical Association of America, 1967.

[4] H. S. M. Coxeter, *Regular Polytopes*, 3rd ed., Dover, 1973.

[5] D. M. Y. Sommerville, *An Introduction to the Geometry of* n *Dimensions*, Dover, 1958.

[6] Z. A. Melzak, "Companion to the problem of the tetrahedron," *Canadian Mathematical Bulletin* 9 (1966), 515–520, https://doi.org/10.4153/CMB-1966-080-0.

[7] M. Pollicott and M. Sewell, "An isoperimetric problem for tetrahedra," Warwick manuscript, https://warwick.ac.uk/fac/sci/maths/people/staff/mark_pollicott/p3/kneading.pdf.

[8] A. Drozdov and A. Osborne, "A generalization of the Grace–Danielsson inequality," arXiv:1404.0525 (2014), https://arxiv.org/abs/1404.0525.

[9] J. Fricke, "A proof of the Grace–Danielsson inequality," arXiv:1805.08435 (2018), https://arxiv.org/abs/1805.08435.

[10] J. J. Benedetto and M. Fickus, "Finite normalized tight frames," *Advances in Computational Mathematics* 18 (2003), 357–385, https://doi.org/10.1023/A:1021323312367.

[11] D. G. Mixon, T. Needham, C. Shonkwiler and S. Villar, "Three proofs of the Benedetto–Fickus theorem," arXiv:2112.02916 (2021), https://arxiv.org/abs/2112.02916.

[12] G.-P. Paillé, N. Ray, P. Poulin, A. Sheffer and B. Lévy, "Dihedral angle-based maps of tetrahedral meshes," *ACM Transactions on Graphics* 34:4 (2015), Art. 54, https://doi.org/10.1145/2766900.

[13] H. Si, *TetGen: A Quality Tetrahedral Mesh Generator and Three-Dimensional Delaunay Triangulator*, v1.5 manual, WIAS Berlin, 2015, https://wias-berlin.de/software/tetgen/1.5/doc/manual/manual.html.

[14] J. R. Shewchuk, "What is a good linear finite element? Interpolation, conditioning, anisotropy, and quality measures," unpublished preprint, 2002.

[15] P. M. Knupp, "Algebraic mesh quality metrics," *SIAM Journal on Scientific Computing* 23 (2001), 193–218.

[16] D. A. Field, "Qualitative measures for initial meshes," *International Journal for Numerical Methods in Engineering* 47 (2000), 887–906.

[17] H. Edelsbrunner, *Geometry and Topology for Mesh Generation*, Cambridge University Press, 2001.

[18] J. H. Conway and R. K. Guy, *The Book of Numbers*, Springer, 1996.

[19] O. Christensen, *An Introduction to Frames and Riesz Bases*, 2nd ed., Birkhäuser, 2016.

[20] A. L. Edmonds, M. Hajja and H. Martini, "Coincidences of simplex centers and related facial structures," arXiv:math/0411093 (2004), https://arxiv.org/abs/math/0411093.

[21] A. L. Edmonds, M. Hajja and H. Martini, "Orthocentric simplices and their centers," arXiv:math/0508080 (2005), https://arxiv.org/abs/math/0508080.

[22] S. Yang and S. Cheng, "Inequalities for inscribed simplex and applications," *Journal of Inequalities in Pure and Applied Mathematics* 7:5 (2006), Article 165, https://www.maths.tcd.ie/EMIS/journals/JIPAM/images/019_05_JIPAM/019_05_www.pdf.

[23] J. Nocedal and S. J. Wright, *Numerical Optimization*, 2nd ed., Springer, 2006.